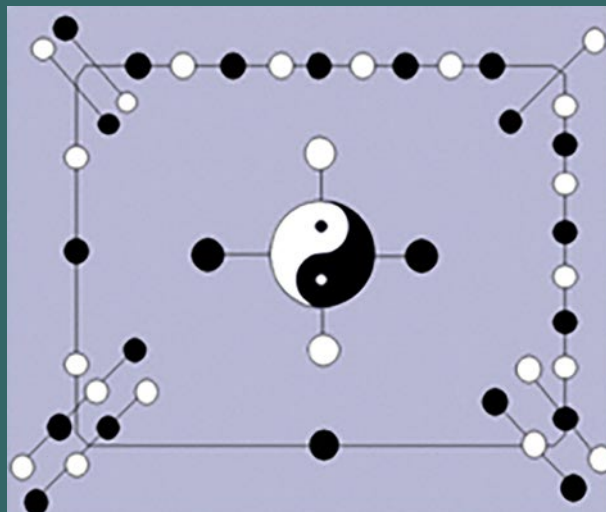




ISSN 1937 - 1055

VOLUME 4, 2025

INTERNATIONAL JOURNAL OF
MATHEMATICAL COMBINATORICS



EDITED BY

THE MADIS OF CHINESE ACADEMY OF SCIENCES AND
ACADEMY OF MATHEMATICAL COMBINATORICS & APPLICATIONS, USA

December, 2025

Vol.4, 2025

ISSN 1937-1055

International Journal of
Mathematical Combinatorics
(www.mathcombin.com)

Edited By

The Madis of Chinese Academy of Sciences and
Academy of Mathematical Combinatorics & Applications, USA

December, 2025

Aims and Scope: The *mathematical combinatorics* is a subject that applying combinatorial notion to all mathematics and all sciences for understanding the reality of things in the universe, motivated by *CC Conjecture* of Dr.L.F. MAO on mathematical sciences. The **International J.Mathematical Combinatorics** (*ISSN 1937-1055*) is a fully refereed international journal, sponsored by the *MADIS of Chinese Academy of Sciences* and published in USA quarterly, which publishes original research papers and survey articles in all aspects of mathematical combinatorics, Smarandache multi-spaces, Smarandache geometries, non-Euclidean geometry, topology and their applications to other sciences. Topics in detail to be covered are:

Mathematical combinatorics;
Smarandache multi-spaces and Smarandache geometries with applications to other sciences;
Topological graphs; Algebraic graphs; Random graphs; Combinatorial maps; Graph and map enumeration; Combinatorial designs; Combinatorial enumeration;
Differential Geometry; Geometry on manifolds; Low Dimensional Topology; Differential Topology; Topology of Manifolds;
Geometrical aspects of Mathematical Physics and Relations with Manifold Topology;
Mathematical theory on gravitational fields and parallel universes;
Applications of Combinatorics to mathematics and theoretical physics.
Generally, papers on applications of combinatorics to other mathematics and other sciences are welcome by this journal.

It is also available from the below international databases:

Serials Group/Editorial Department of EBSCO Publishing
10 Estes St. Ipswich, MA 01938-2106, USA
Tel.: (978) 356-6500, Ext. 2262 Fax: (978) 356-9371
<http://www.ebsco.com/home/printsubs/priceproj.asp>

and

Gale Directory of Publications and Broadcast Media, Gale, a part of Cengage Learning
27500 Drake Rd. Farmington Hills, MI 48331-3535, USA
Tel.: (248) 699-4253, ext. 1326; 1-800-347-GALE Fax: (248) 699-8075
<http://www.gale.com>

Indexing and Reviews: Mathematical Reviews (USA), Zentralblatt Math (Germany), Index EuroPub (UK), Referativnyi Zhurnal (Russia), Matematika (Russia), EBSCO (USA), Google Scholar, Baidu Scholar, Directory of Open Access (DoAJ), International Scientific Indexing (ISI, impact factor 2.012), Institute for Scientific Information (PA, USA), Library of Congress Subject Headings (USA), CNKI(China).

Subscription A subscription can be ordered by an email directly to

Linfan Mao

The Editor-in-Chief of *International Journal of Mathematical Combinatorics*
Chinese Academy of Mathematics and System Science Beijing, 100190, P.R.China, and also the
President of Academy of Mathematical Combinatorics & Applications (AMCA), Colorado, USA
Email: maolinfan@163.com

Price: US\$48.00

Editorial Board (5th)

Editor-in-Chief

Linfan MAO

Chinese Academy of Mathematics and System
Science, P.R.China and
Academy of Mathematical Combinatorics &
Applications, Colorado, USA
Email: maolinfan@163.com

Deputy Editor-in-Chief

Han Ren

East China Normal University, P.R.China
Email: hren@math.ecnu.edu.cn

Editors

Arindam Bhattacharyya

Jadavpur University, India
Email: bhattachar1968@yahoo.co.in

Said Broumi

Hassan II University Mohammedia
Hay El Baraka Ben M'sik Casablanca
B.P.7951 Morocco

Junliang Cai

Beijing Normal University, P.R.China
Email: caijunliang@bnu.edu.cn

Yanxun Chang

Beijing Jiaotong University, P.R.China
Email: yxchang@center.njtu.edu.cn

Jingan Cui

Beijing University of Civil Engineering and
Architecture, P.R.China
Email: cuijingan@bucea.edu.cn

Shaofei Du

Capital Normal University, P.R.China
Email: dushf@mail.cnu.edu.cn

Xiaodong Hu

Chinese Academy of Mathematics and System
Science, P.R.China
Email: xdhu@amss.ac.cn

Yuanqiu Huang

Hunan Normal University, P.R.China
Email: hyqq@public.cs.hn.cn

H.Iseri

Mansfield University, USA
Email: hiseri@mnsfld.edu

Xueliang Li

Nankai University, P.R.China
Email: lxl@nankai.edu.cn

Guodong Liu

Huizhou University
Email: lgd@hzu.edu.cn

W.B.Vasantha Kandasamy

Indian Institute of Technology, India
Email: vasantha@iitm.ac.in

Ion Patrascu

Fratii Buzesti National College
Craiova Romania

P.S.K.Reddy

JSS Science and Technology University,
Mysuru-570 006, India
Email: pskreddy@jssstuniv.in

Ovidiu-Ilie Sandru

Politehnica University of Bucharest
Romania

Mingyao Xu

Peking University, P.R.China
Email: xumy@math.pku.edu.cn

Guiying Yan

Chinese Academy of Mathematics and System
Science, P.R.China
Email: yanguiying@yahoo.com

Y. Zhang

Department of Computer Science
Georgia State University, Atlanta, USA

Famous Words:

No matter how abstract any branch of mathematics, one day will be applied in this real world.

By *N.I.Lobachevsky*, a Russian mathematician.

On the Application of Separable $R_0R_1R_2 \cdots R_a$ -Cyclic DNA Codes to DNA Computing

Yasemin Cengellenmis

(Department of Mathematics, Trakya University, Edirne, Turkey)

Abdullah Dertli*

(Department of Mathematics, Ondokuz Mayıs University, Samsun, Turkey)

E-mail: ycengellenmis@gmail.com, abduallah.dertli@gmail.com

Abstract: In this paper, the $R_0R_1R_2 \cdots R_a$ -cyclic codes of block length $(\alpha_0, \dots, \alpha_a)$ are studied, where $R_i = F_4[u_1, \dots, u_i] / \langle u_j^2 - u_j, u_j u_s - u_s u_j \rangle$, $j, s = 1, 2, \dots, i$, $j \neq s$ for $i = 1, 2, \dots, a$ and $R_0 = F_4$. Their generator polynomials are given. The structures of the separable $R_0R_1R_2 \cdots R_a$ -cyclic codes are determined. A necessary and sufficient conditions of the separable $R_0R_1R_2 \cdots R_a$ cyclic codes to be reversible and reversible complement are determined. By introducing a map, the separable $R_0R_1R_2 \cdots R_a$ -cyclic DNA codes are mapped to DNA codes with some examples.

Key Words: $R_0R_1R_2 \cdots R_a$ -cyclic code, separable $R_0R_1R_2 \cdots R_a$ cyclic code, generator polynomial, Gray map, DNA code.

AMS(2010): 94B15.

§1. Introduction

It is well known that DNA contains a genetic program for the biological development of life and has two strands which are linked by Watson-Crick pairing so that every A is linked with a T and every C with a G, and vice versa, where A,T,C,G are the four bases of a DNA sequence.

DNA computing started in 1994 when Adleman showed how to solve a computationally difficult problem (traveling salesman problem, a well-known NP-complete problem) by manipulations of DNA molecules in [2]. A DNA code C of length n is a subset of $S_{D_4}^n$, where $S_{D_4} = \{A, T, C, G\}$ is the DNA alphabet. Moreover a DNA code satisfies some constraints such as the Hamming constraint for minimum distance, the reverse-complement constraint, the reverse constraint, and the fixed GC content.

Designing the DNA codes for DNA computing has been a major topic of research since the beginning of the century. The authors used a lot of methods to obtain them. One of the methods is to use skew cyclic codes over some finite rings. In [4], they introduced the $F_4(F_4 + vF_4)$ -skew cyclic codes, where $v^2 = v$. A characterization of the $F_4(F_4 + vF_4)$ -skew

¹ Received March 16, 2024. Accepted November 16, 2025

² *Corresponding author

cyclic codes, which are reversible complements, has been obtained.

The other method is to use the cyclic DNA codes. In [7], they introduced the F_4RS -cyclic codes, where $R = F_4 + uF_4$, $u^2 = u$, $S = F_4 + uF_4 + vF_4$ with $u^2 = u$, $v^2 = v$, $uv = vu = 0$ in order to construct the DNA code. They gave a one-to-one correspondence between DNA codons of the alphabet

$$\{A, C, T, G\}^2, \{A, C, T, G\}^3,$$

by using the Gray maps from R to F_4^2 and S to F_4^3 , respectively. By using the structures of separable codes, they studied cyclic DNA codes. They constructed DNA codes from them.

Motivated by the work in [7], we decided to study separable $R_0R_1R_2 \cdots R_a$ -cyclic DNA codes to construct DNA codes.

This paper is organized as follows. Section 2 gives some basic knowledge and in Section 3, the structures of linear codes over R_i , for $i = 1, 2, \dots, a$ and the Gray maps are presented. Section 4 gives the structures of $R_0R_1R_2 \cdots R_a$ -cyclic codes, and a necessary and sufficient conditions of $R_0R_1R_2 \cdots R_a$ -cyclic to be separable are determined. Section 5 determines a necessary and sufficient condition of cyclic codes over R_i to be reversible and reversible complement for $i = 2, 3, \dots, a$, obtain a necessary and sufficient condition of separable $R_0R_1R_2 \cdots R_a$ -cyclic to be reversible and reversible complement. It is obtained the DNA codes by using a map and these type codes with some examples.

§2. Preliminaries

Let $R_0 = F_4 = \{0, 1, w, w^2 = w + 1\}$. A family of the finite rings $R_i = F_4[u_1, \dots, u_i] / \langle u_j^2 - u_j, u_j u_s - u_s u_j \rangle$, where $j, s = 1, 2, \dots, i$ and $j \neq s$ for $i = 1, 2, \dots, a$ is studied in [5]. If $i = 1$, then $R_1 = F_4 + u_1 F_4$, where $u_1^2 = u_1$. If $i = 2$, the $R_2 = F_4 + u_1 F_4 + u_2 F_4 + u_1 u_2 F_4$, where $u_1^2 = u_1, u_2^2 = u_2, u_1 u_2 = u_2 u_1$. The rings in this family contain the commutative ring with 4^{2^i} elements and the characteristic 2, where $i = 1, 2, \dots, a$.

Let $B \subseteq \{1, 2, \dots, i\}$ and $u_B = \prod_{j \in B} u_j$, where $i = 1, 2, \dots, a$. In particular $u_\emptyset = 1$. Each element of R_i is of the form $\sum_{B \in P_i} \alpha_B u_B$, where $\alpha_B \in F_4, P_i$ is the power set of the set $\{1, 2, \dots, i\}$ for $i = 1, \dots, a$. For $A, B \subseteq \{1, 2, \dots, i\}$, we have that $u_A u_B = u_{A \cup B}$ which gives that

$$\sum_{B \in P_i} \alpha_B u_B \cdot \sum_{C \in P_i} \beta_C u_C = \sum_{D \in P_i} \left(\sum_{B \cup C = D} \alpha_B \beta_C \right) u_D$$

for integers $i = 1, \dots, a$.

The finite rings of the family are also written as recursively

$$R_i = R_{i-1} + u_i R_{i-1},$$

where $i = 1, 2, \dots, a$.

The set $R_0 R_1 R_2 \cdots R_a = \{(r_0, \dots, r_a) | r_i \in R_i, i = 0, \dots, a\}$ forms an R_a module under the componentwise addition and the following multiplication. For any elements $z \in R_a, r =$

$(r_0, \dots, r_a) \in R_0R_1R_2 \cdots R_a$, the multiplication is defined as

$$\begin{aligned} \bullet & : R_a \times R_0R_1R_2 \cdots R_a \longrightarrow R_0R_1R_2 \cdots R_a \\ (z, r) & \mapsto z \bullet r = (\rho_0(z)r_0, \dots, \rho_{a-1}(z)r_{a-1}, zr_a), \end{aligned}$$

where

$$\begin{aligned} \rho_i & : R_a \longrightarrow R_i \\ \sum_{B \in P_a} \alpha_B u_B & \mapsto \sum_{B \in P_i} \alpha_B u_B \end{aligned}$$

ring homomorphisms for $i = 0, \dots, a-1$ and

$$\begin{aligned} \rho_0 & : R_a \longrightarrow R_0 \\ \sum_{B \in P_a} \alpha_B u_B & \mapsto \alpha_0. \end{aligned}$$

This multiplication can be extended componentwise on $R_{\alpha_0\alpha_1 \cdots \alpha_a} = R_0^{\alpha_0} \times R_1^{\alpha_1} \times \cdots \times R_a^{\alpha_a}$ as for any $z \in R_a$ and $\mathbf{r} = (\mathbf{r}_0, \mathbf{r}_1, \dots, \mathbf{r}_a) \in R_{\alpha_0\alpha_1 \cdots \alpha_a}$, where $\mathbf{r}_i = (r_0^i, r_1^i, \dots, r_{\alpha_i-1}^i) \in R_i^{\alpha_i}$ for $i = 0, 1, \dots, a$,

$$\begin{aligned} \bullet & : R_a \times R_{\alpha_0\alpha_1 \cdots \alpha_a} \longrightarrow R_{\alpha_0\alpha_1 \cdots \alpha_a} \\ (z, \mathbf{r}) & \mapsto z \bullet \mathbf{r} = (\rho_0(z)\mathbf{r}_0, \rho_1(z)\mathbf{r}_1, \dots, \rho_{a-1}(z)\mathbf{r}_{a-1}, z\mathbf{r}_a) \end{aligned}$$

So $R_{\alpha_0\alpha_1 \cdots \alpha_a}$ is an R_a -module. A non empty subset C of $R_{\alpha_0\alpha_1 \cdots \alpha_a}$ is called an $R_0R_1R_2 \cdots R_a$ -linear code of block length $(\alpha_0, \dots, \alpha_a)$ if C is an R_a -submodule of $R_{\alpha_0\alpha_1 \cdots \alpha_a}$.

Definition 2.1 An $R_0R_1R_2 \cdots R_a$ -linear code C of block length $(\alpha_0, \dots, \alpha_a)$ is called an $R_0R_1R_2 \cdots R_a$ -cyclic code if its cyclic shift $\sigma(\mathbf{r}) = (\sigma(\mathbf{r}_0), \sigma(\mathbf{r}_1), \dots, \sigma(\mathbf{r}_a)) \in C$, for any $\mathbf{r} = (\mathbf{r}_0, \mathbf{r}_1, \dots, \mathbf{r}_a) \in C$.

Definition 2.2 Let $\mathbf{r} = (r_0^0, r_1^0, \dots, r_{\alpha_0-1}^0, r_0^1, r_1^1, \dots, r_{\alpha_1-1}^1, \dots, r_0^a, r_1^a, \dots, r_{\alpha_a-1}^a)$ and $\mathbf{r}' = ((r_0^0)', (r_1^0)', \dots, (r_{\alpha_0-1}^0)', (r_0^1)', (r_1^1)', \dots, (r_{\alpha_1-1}^1)', \dots, (r_0^a)', (r_1^a)', \dots, (r_{\alpha_a-1}^a)')$ be two elements of $R_{\alpha_0\alpha_1 \cdots \alpha_a}$. Then, the inner product is defined as

$$\begin{aligned} \mathbf{r} \cdot \mathbf{r}' & = u_1 u_2 \cdots u_a \sum_{j_0=0}^{\alpha_0-1} r_{j_0}^0 (r_{j_0}^0)' + u_2 u_3 \cdots u_a \sum_{j_1=0}^{\alpha_1-1} r_{j_1}^1 (r_{j_1}^1)' \\ & \quad + \cdots + u_a \sum_{j_{a-1}=0}^{\alpha_{a-1}-1} r_{j_{a-1}}^{a-1} (r_{j_{a-1}}^{a-1})' + \sum_{j_a=0}^{\alpha_a-1} r_{j_a}^a (r_{j_a}^a)' \end{aligned}$$

Theorem 2.3 Let C be an $R_0R_1R_2 \cdots R_a$ -cyclic code of block length $(\alpha_0, \dots, \alpha_a)$. Then, its dual C^\perp is also an $R_0R_1R_2 \cdots R_a$ -cyclic code.

Proof For any $\mathbf{r}' = (\mathbf{r}'_0, \mathbf{r}'_1, \dots, \mathbf{r}'_a) \in C^\perp$, we have to show that $\sigma(\mathbf{r}') \in C^\perp$. For this, take $\mathbf{r} = (\mathbf{r}_0, \mathbf{r}_1, \dots, \mathbf{r}_a) \in C$, where C is a $R_0R_1R_2 \cdots R_a$ -cyclic code of block length $(\alpha_0, \dots, \alpha_a)$, then we have

$$\begin{aligned} \mathbf{r}\sigma(\mathbf{r}') &= u_1u_2 \cdots u_a \sum \mathbf{r}_0\sigma(\mathbf{r}'_0) + u_2u_3 \cdots u_a \sum \mathbf{r}_1\sigma(\mathbf{r}'_1) \\ &\quad + \cdots + u_a \sum \mathbf{r}_{a-1}\sigma(\mathbf{r}'_{a-1}) + \sum \mathbf{r}_a\sigma(\mathbf{r}'_a). \end{aligned}$$

Since C is an $R_0R_1R_2 \cdots R_a$ -cyclic, if we take $\text{lcm}(\alpha_0, \dots, \alpha_a) = d$, then we have $\sigma^{d-1}(\mathbf{r}) = (\sigma^{d-1}(\mathbf{r}_0), \dots, \sigma^{d-1}(\mathbf{r}_a)) \in C$, for any $\mathbf{r} \in C$. By taking the inner product of $\sigma^{d-1}(\mathbf{r}) \in C$ and $\mathbf{r}' \in C^\perp$, we get

$$\begin{aligned} \sigma^{d-1}(\mathbf{r})\mathbf{r}' &= u_1u_2 \cdots u_a \sum \sigma^{d-1}(\mathbf{r}'_0)\mathbf{r}'_0 + u_2u_3 \cdots u_a \sum \sigma^{d-1}(\mathbf{r}'_1)\mathbf{r}'_1 \\ &\quad + \cdots + u_a \sum \sigma^{d-1}(\mathbf{r}'_{a-1})\mathbf{r}'_{a-1} + \sum \sigma^{d-1}(\mathbf{r}'_a)\mathbf{r}'_a. \end{aligned}$$

By comparing the coefficients, we have

$$\sigma^{d-1}(\mathbf{r}'_i)\mathbf{r}'_i = \mathbf{r}_i\sigma(\mathbf{r}'_i),$$

where $i = 0, 1, \dots, a$. Hence $\mathbf{r}\sigma(\mathbf{r}') = 0$, which shows that $\sigma(\mathbf{r}') \in C^\perp$. \square

With the map $\Upsilon_{\alpha_0\alpha_1 \cdots \alpha_a}$ from $R_{\alpha_0\alpha_1 \cdots \alpha_a}$ to

$$\Omega_{\alpha_0 \cdots \alpha_a} = R_0[x]/\langle x^{\alpha_0} - 1 \rangle \times \cdots \times R_a[x]/\langle x^{\alpha_a} - 1 \rangle,$$

and to any element $\mathbf{r} = (r_0^0, r_1^0, \dots, r_{\alpha_0-1}^0, r_0^1, r_1^1, \dots, r_{\alpha_1-1}^1, \dots, r_0^a, r_1^a, \dots, r_{\alpha_a-1}^a) \in R_{\alpha_0\alpha_1 \cdots \alpha_a}$ corresponds to the element $\mathbf{r}(x) = (r_0^0 + r_1^0x + \cdots + r_{\alpha_0-1}^0x^{\alpha_0-1}, r_0^1 + r_1^1x + \cdots + r_{\alpha_1-1}^1x^{\alpha_1-1}, \dots, r_0^a + r_1^ax + \cdots + r_{\alpha_a-1}^ax^{\alpha_a-1}) = (r_0(x), r_1(x), \dots, r_a(x)) \in \Omega_{\alpha_0 \cdots \alpha_a}$.

The multiplication of any element $f(x) = f_0 + f_1x + \cdots + f_sx^s \in R_a[x]$ with the element $\mathbf{r}(x) = (r_0(x), \dots, r_a(x)) \in \Omega_{\alpha_0 \cdots \alpha_a}$ is defined as

$$f(x) \star (r_0(x), \dots, r_a(x)) = (\rho_0(f(x))r_0(x), \dots, \rho_{a-1}(f(x))r_{a-1}(x), f(x)r_a(x))$$

where $\rho_i(f(x)) = \rho_i(f_0) + \rho_i(f_1)x + \cdots + \rho_i(f_s)x^s$ for $i = 0, \dots, a-1$. So the set $\Omega_{\alpha_0, \dots, \alpha_a}$ forms an $R_a[x]$ -module with respect to usual addition and multiplication \star . For any $\mathbf{r}(x) \in \Omega_{\alpha_0 \cdots \alpha_a}$, the vector $x \star \mathbf{r}(x)$ is a cyclic shift of the corresponding vector of $\mathbf{r}(x)$.

Theorem 2.4 *A linear code C is called an $R_0R_1R_2 \cdots R_a$ -cyclic code of block length $(\alpha_0, \dots, \alpha_a)$ if and only if $\Upsilon_{\alpha_0\alpha_1 \cdots \alpha_a}(C)$ is an $R_a[x]$ -submodule of $\Omega_{\alpha_0 \cdots \alpha_a}$.*

§3. Linear Codes Over R_i

In [6], an idempotent decomposition of the finite ring $B_i = F_{p^r}[u_1, \dots, u_i]/\langle u_j^2 - u_j, u_ju_s - u_su_j \rangle$ for $j, s = 1, \dots, i$ was given. By taking $p = 2, r = 2$, a idempotent decomposition of R_i

is written as follows, where $i = 1, \dots, a$.

$$e_{u_\emptyset} = e_1 = 1 + \sum_{B \in P_i} u_B$$

and the number of e_{u_\emptyset} is $\binom{i}{0}$,

$$e_{u_{k_1}} = u_{k_1} + \sum_{k_1 \in B \in P_i, |B| \geq 2} u_B$$

for $k_1 = 1, 2, \dots, i$ and the number of $e_{u_{k_1}}$ is $\binom{i}{1}$.

$$e_{u_{k_1 u_{k_2}}} = \frac{u_{k_1} u_{k_2}}{k_1 < k_2} + \sum_{k_1, k_2 \in B \in P_i, |B| \geq 3} u_B$$

for $k_1, k_2 = 1, 2, \dots, i$ and the number of $e_{u_{k_1 u_{k_2}}}$ is $\binom{i}{2}$,

$$e_{u_{k_1 u_{k_2} u_{k_3}}} = \frac{u_{k_1} u_{k_2} u_{k_3}}{k_1 < k_2 < k_3} + \sum_{k_1, k_2, k_3 \in B \in P_i, |B| \geq 4} u_B$$

for $k_1, k_2, k_3 = 1, 2, \dots, i$ and the number of $e_{u_{k_1 u_{k_2} u_{k_3}}}$ is $\binom{i}{3}$

..... ,

$$e_{u_1 u_2 \cdots u_i} = u_1 u_2 \cdots u_i$$

and the number of $e_{u_1 u_2 \cdots u_i}$ is $\binom{i}{i}$, where $B \subseteq \{1, 2, \dots, i\}$ and P_i is the power set of $\{1, 2, \dots, i\}, i = 1, 2, \dots, a$.

Then, we have

$$\sum_{B \in P_i} e_{u_B} = 1, (e_{u_B})^2 = e_{u_B} \text{ and } e_{u_B} e_{u_A} = 0$$

if $A \neq B$ for any $A, B \subseteq \{1, 2, \dots, i\}$. Hence,

$$R_i = \bigoplus_{B \in P_i} R_i e_{u_B} \cong \bigoplus_{B \in P_i} F_4 e_{u_B}$$

for $i = 1, \dots, a$. So every element r_i of R_i can be uniquely expressed as

$$r_i = \sum_{B \in P_i} r_{i, u_B} e_{u_B},$$

$$|C_{\alpha_i}| = \prod_{B \in P_i} |C_{\alpha_i, u_B}| \quad \text{and} \quad d_G(C_{\alpha_i}) = \min\{d_H(C_{\alpha_i, u_B})\}$$

for $i = 1, \dots, a$. In [5], the map on R_i was defined as

$$\begin{aligned} \phi_i & : R_i \longrightarrow R_{i-1}^2 \\ x_{i-1} + u_i y_{i-1} & \longmapsto (x_{i-1}, x_{i-1} + y_{i-1}) \end{aligned}$$

where $i = 2, \dots, a$ and

$$\begin{aligned} \phi_1 & : R_1 \longrightarrow R_0^2 \\ x_0 + u_1 y_0 & \longmapsto (x_0, x_0 + y_0) \end{aligned}$$

So, the Gray map is defined as follows

$$\begin{aligned} \phi = \phi_1 \phi_2 \cdots \phi_i & : R_i \longrightarrow R_0^{2^i} \\ x_{i-1} + u_i y_{i-1} & \longmapsto \phi(x_{i-1} + u_i y_{i-1}) \end{aligned}$$

where $i = 1, \dots, a$.

If we take the element of R_i as $\sum_{B \in P_i} r_{i, u_B} e_{u_B}$, the Gray map defined also as

$$\begin{aligned} \psi_i & : R_i \longrightarrow R_0^{2^i} \\ \sum_{B \in P_i} r_{i, u_B} e_{u_B} & \longmapsto (r_{i, u_B})_{B \in P_i} \end{aligned}$$

where $i = 1, \dots, a$.

Example 3.2 Let $a = 2$. The Gray map on R_2 is defined as

$$\begin{aligned} \psi_2 & : R_2 \longrightarrow R_0^4 \\ \sum_{B \in P_2} r_{2, u_B} e_{u_B} & \longmapsto (r_{2,1}, r_{2, u_1}, r_{2, u_2}, r_{2, u_1 u_2}) \end{aligned}$$

This can be extended from $R_i^{\alpha_i}$ to $R_0^{2^i \alpha_i}$ as

$$\begin{aligned} \psi_i & : R_i^{\alpha_i} \longrightarrow R_0^{2^i \alpha_i} \\ \mathbf{r}_i = (r_0^i, r_1^i, \dots, r_{\alpha_i-1}^i) & \longmapsto (r_{j, i, u_B})_{B \in P_i} \end{aligned}$$

where $(r_0^i, r_1^i, \dots, r_{\alpha_i-1}^i) \in R_i^{\alpha_i}$ and $r_j^i = \sum_{B \in P_i} r_{j, i, u_B} e_{u_B}$, for $j = 0, \dots, \alpha_i - 1, i = 1, \dots, a$.

We define the Gray weight $wt_G(r_j^i)$ of an element $r_j^i \in R_i$ is defined as

$$wt_G(r_j^i) = wt_H(\psi_i(r_j^i)),$$

where w_{t_H} denotes the Hamming weight over F_4 , $j = 0, \dots, \alpha_i - 1, i = 1, \dots, a$. For any $\mathbf{r}_i, \mathbf{r}'_i \in R_i^{\alpha_i}$, the Gray distance between $\mathbf{r}_i, \mathbf{r}'_i$ is defined as

$$d_G(\mathbf{r}_i, \mathbf{r}'_i) = w_H(\psi_i(\mathbf{r}_i - \mathbf{r}'_i)).$$

It can be easily seen that the Gray map is a F_4 -linear and distance preserving map from $R_i^{\alpha_i}$ (Gray distance) to $F_4^{2^i \alpha_i}$ (Hamming distance) where $i = 1, \dots, a$.

Notice that a linear code over F_4 of length α_0 is a subspace of $F_4^{\alpha_0}$ and a linear code over R_i of length α_i is a R_i -submodule of $R_i^{\alpha_i}$ for $i = 1, 2, \dots, a$.

For any element $(r_0, \dots, r_a) = (r_0, r_{1,1}(1+u_1) + r_{1,u_1}(u_1), r_{2,1}(1+u_1+u_2+u_1u_2) + r_{2,u_1}(u_1+u_1u_2) + r_{2,u_2}(u_2+u_1u_2) + r_{2,u_1u_2}(u_1u_2), \dots, \sum_{B \in P_a} r_{a,u_B} e_{u_B}) \in R_0 R_1 R_2 \dots R_a$, we define a Gray map from $R_0 R_1 R_2 \dots R_a$ to $F_4^{2^{a+1}-1}$ as

$$\begin{aligned} \varphi & : R_0 R_1 R_2 \dots R_a \longrightarrow F_4^{2^{a+1}-1} \\ (r_0, \dots, r_a) & \longmapsto \varphi(r_0, \dots, r_a) = (r_0, \psi_1(r_1), \dots, \psi_a(r_a)) = \epsilon, \end{aligned}$$

where

$$\epsilon = (r_0, r_{1,1}, r_{1,u_1}, r_{2,1}, r_{2,u_1}, r_{2,u_2}, r_{2,u_1u_2}, \dots, r_{a,1}, r_{a,u_1}, \dots, r_{a,u_a}, r_{a,u_1u_2}, \dots, r_{a,u_1u_2, \dots, u_a}).$$

It is seen that the map φ is a F_4 -linear, which can be extended on $R_{\alpha_0 \alpha_1 \dots \alpha_a}$ as follow

$$\varphi : R_{\alpha_0 \alpha_1 \dots \alpha_a} \longrightarrow F_4^{\sum_{i=0}^a 2^i \alpha_i}$$

$$(\mathbf{r}_0, \dots, \mathbf{r}_a) = (r_0^0, \dots, r_{\alpha_0-1}^0, r_0^1, \dots, r_{\alpha_1-1}^1, \dots, r_0^a, \dots, r_{\alpha_a-1}^a) \mapsto \epsilon$$

with $\epsilon = (r_0^0, \dots, r_{\alpha_0-1}^0, r_{0,1,1}, r_{0,1,u_1}, r_{1,1,1}, r_{1,1,u_1}, \dots, (r_{j,a,u_B})_{B \in P_a}, (r_0^i, \dots, r_{\alpha_i-1}^i) \in R_i^{\alpha_i}$ and

$$r_j^i = \sum_{B \in P_i} r_{j,i,u_B} e_{u_B},$$

for $j = 0, \dots, \alpha_i - 1, i = 1, \dots, a$.

The Gray weight of any element $(\mathbf{r}_0, \dots, \mathbf{r}_a) \in R_{\alpha_0 \alpha_1 \dots \alpha_a}$ is defined as $w_G((\mathbf{r}_0, \dots, \mathbf{r}_a)) = w_H(\mathbf{r}_0) + w_G(\mathbf{r}_1) + \dots + w_G(\mathbf{r}_a)$ where w_H represents the Hamming weight over F_4 . Moreover, it can be defined Gray distance between any two elements $\mathbf{r}, \hat{\mathbf{r}} \in R_{\alpha_0 \alpha_1 \dots \alpha_a}$ as

$$d_G(\mathbf{r}, \hat{\mathbf{r}}) = w_G(\mathbf{r} - \hat{\mathbf{r}})$$

Proposition 3.3 *A Gray map φ is F_4 -linear and distance preserving map from $R_{\alpha_0 \alpha_1 \dots \alpha_a}$ (Gray distance) to $F_4^{\sum_{i=0}^a 2^i \alpha_i}$ (Hamming distance).*

Proof Let $\mathbf{r} = (\mathbf{r}_0, \dots, \mathbf{r}_a), \mathbf{r}' = (\mathbf{r}'_0, \dots, \mathbf{r}'_a) \in R_{\alpha_0 \dots \alpha_a}$, where $\mathbf{r}_0 = (r_0, \dots, r_{\alpha_0-1}), \mathbf{r}_0 =$

Theorem 4.1([8]) *Let C_{α_0} be a cyclic code of length α_0 over F_4 . Then there exists a unique monic polynomial $f(x) \in F_4[x]/\langle x^{\alpha_0} - 1 \rangle$ such that $\zeta_0(C_{\alpha_0}) = \langle f(x) \rangle$ and $f(x)$ divides $x^{\alpha_0} - 1$. Moreover C_{α_0} has 4^{k_1} codewords, where $k_1 = \alpha_0 - \deg f(x)$ and the set $\{f(x), xf(x), \dots, x^{k_1-1}f(x)\}$ forms a basis of C_{α_0} .*

In [3], the structures and properties of cyclic codes over R_1 are given. Similarly, we have the following results for cyclic codes over R_i for $i = 2, 3, \dots, a$.

Theorem 4.2 *Let $C_{\alpha_i} = \bigoplus_{B \in P_i} C_{\alpha_i, u_B} e_{u_B}$ be a linear code of length α_i over R_i for $i = 2, \dots, a$. Then,*

1) C_{α_i} is a cyclic code of length α_i over R_i if and only if C_{α_i, u_B} are cyclic codes of length α_i over R_0 , for $i = 2, \dots, a$;

2) If C_{α_i} is a cyclic code of length α_i over R_i , then its dual

$$C_{\alpha_i}^\perp = \bigoplus_{B \in P_i} C_{\alpha_i, u_B}^\perp e_{u_B}$$

is also cyclic code over R_i , $B \in P_i$, for $i = 2, \dots, a$;

3) If C_{α_i} is a cyclic code of length α_i over R_i , then $\zeta_i(C_{\alpha_i}) = \langle c_i(x) \rangle$, where

$$c_i(x) = \sum (c_{i, u_B}(x)) e_{u_B}$$

with $c_i(x) | x^{\alpha_i} - 1$ and $\zeta_0(C_{\alpha_i, u_B}) = \langle c_{i, u_B}(x) \rangle$, $B \in P_i$, for $i = 2, \dots, a$. Moreover

$$|C_{\alpha_i}| = 4^{2^i \alpha_i - \sum \deg(c_{i, u_B}(x))}.$$

From [4], the following theorem can be given as follows:

Theorem 4.3 *Let C be an R_0R_1 -cyclic code of block length (α_0, α_1) . Then, $\Upsilon_{\alpha_0\alpha_1}(C) = \langle (f_{0,0}(x), 0), (f_{0,1}(x), f_{1,0}(x)) \rangle$ where $f_{0,0}(x) | x^{\alpha_0} - 1$, $f_{1,0}(x) = (1 + u_1)f_{1,0,1}(x) + u_1f_{1,0,u_1}(x)$, $f_{1,0}(x) | x^{\alpha_1} - 1$ and $f_{0,1}(x) \in R_0[x]$.*

Theorem 4.4 *Let C be an $R_0R_1R_2$ -cyclic code of block length $(\alpha_0, \alpha_1, \alpha_2)$. Then $\Upsilon_{\alpha_0\alpha_1\alpha_2}(C) = \langle (f_{0,0}(x), 0, 0), (f_{0,1}(x), f_{1,0}(x), 0), (f_{0,2}(x), f_{1,1}(x), f_{2,0}(x)) \rangle$, where $f_{0,0}(x) | x^{\alpha_0} - 1$, $f_{1,0}(x) = (1 + u_1)f_{1,0,1}(x) + u_1f_{1,0,u_1}(x)$, $f_{1,0}(x) | x^{\alpha_1} - 1$, $f_{2,0}(x) = (1 + u_1 + u_2 + u_1u_2)f_{2,0,1}(x) + (u_1 + u_1u_2)f_{2,0,u_1}(x) + (u_2 + u_1u_2)f_{2,0,u_2}(x) + (u_1u_2)f_{2,0,u_1u_2}(x)$ with $f_{2,0}(x) | x^{\alpha_2} - 1$ and $f_{0,1}(x), f_{0,2}(x) \in R_0[x]$, $f_{1,1}(x) \in R_1[x]$.*

Proof By defining a homomorphism $\Xi_{\alpha_0\alpha_1\alpha_2}$ between $\Upsilon_{\alpha_0\alpha_1\alpha_2}(C)$ and $R_2[x]/\langle x^{\alpha_2} - 1 \rangle$ by $\Xi_{\alpha_0\alpha_1\alpha_2}(r_0(x), r_1(x), r_2(x)) = r_2(x)$, we can obtain $\Xi_{\alpha_0\alpha_1\alpha_2}(\Upsilon_{\alpha_0\alpha_1\alpha_2}(C)) = \langle f_{2,0}(x) \rangle$, where

$$\begin{aligned} f_{2,0}(x) &= (1 + u_1 + u_2 + u_1u_2)f_{2,0,1}(x) + (u_1 + u_1u_2)f_{2,0,u_1}(x) + (u_2 + u_1u_2)f_{2,0,u_2}(x) \\ &\quad + (u_1u_2)f_{2,0,u_1u_2}(x) \end{aligned}$$

and

$$Ker\Xi_{\alpha_0\alpha_1\alpha_2} = \{(r_0(x), r_1(x), 0) \in \Omega_{\alpha_0\alpha_1\alpha_2} | (r_0(x), r_1(x), r_2(x)) \in \Upsilon_{\alpha_0\alpha_1\alpha_2}(C)\}.$$

By defining R_1 -submodule $I_1 = \{(r_0(x), r_1(x)) \in \Omega_{\alpha_0\alpha_1} | (r_0(x), r_1(x), 0) \in Ker\Xi_{\alpha_0\alpha_1\alpha_2}\}$ and by using Theorem 5 in [7], we can say that I_1 has the generator polynomials of the form $\langle (f_{0,0}(x), 0), (f_{0,1}(x), f_{1,0}(x)) \rangle$ where $f_{0,0}(x)|x^{\alpha_0} - 1$, $f_{1,0}(x) = (1 + u_1)f_{1,0,1}(x) + u_1f_{1,0,u_1}(x)$ with $f_{1,0}(x)|x^{\alpha_1} - 1$ and $f_{0,1}(x) \in R_0[x]$. Since we have $(r_0(x), r_1(x)) \in I_1$, for any $(r_0(x), r_1(x), 0) \in Ker\Xi_{\alpha_0\alpha_1\alpha_2}$, then there exist some $m_t(x) \in R_t[x]$ for $t = 0, 1$ such that

$$(r_0(x), r_1(x)) = m_0(x) * (f_{0,0}(x), 0) + m_1(x) * (f_{0,1}(x), f_{1,0}(x)).$$

Therefore

$$(r_0(x), r_1(x), 0) = m_0(x) * (f_{0,0}(x), 0, 0) + m_1(x) * (f_{0,1}(x), f_{1,0}(x), 0)$$

and we have

$$Ker\Xi_{\alpha_0\alpha_1\alpha_2} = \langle (f_{0,0}(x), 0, 0), (f_{0,1}(x), f_{1,0}(x), 0) \rangle.$$

From first isomorphism theorem, we have

$$\Upsilon_{\alpha_0\alpha_1\alpha_2}(C)/Ker\Xi_{\alpha_0\alpha_1\alpha_2} \cong \Xi_{\alpha_0\alpha_1\alpha_2}(\Upsilon_{\alpha_0\alpha_1\alpha_2}(C)) = \langle f_{2,0}(x) \rangle.$$

and let $(f_{0,2}(x), f_{1,1}(x), f_{2,0}(x)) \in \Upsilon_{\alpha_0\alpha_1\alpha_2}(C)$ with

$$\Xi_{\alpha_0\alpha_1\alpha_2}(f_{0,2}(x), f_{1,1}(x), f_{2,0}(x)) = f_{2,0}(x).$$

So, an $R_0R_1R_2$ -cyclic code is generated by elements of form $(f_{0,0}(x), 0, 0)$, $(f_{0,1}(x), f_{1,0}(x), 0)$ and $(f_{0,2}(x), f_{1,1}(x), f_{2,0}(x))$. \square

Theorem 4.5 *Let C be an $R_0R_1R_2R_3$ -cyclic code of block length $(\alpha_0, \alpha_1, \alpha_2, \alpha_3)$. Then,*

$$\Upsilon_{\alpha_0\alpha_1\alpha_2\alpha_3}(C) = \langle A_1, A_2, A_3, A_4 \rangle,$$

where

$$\begin{aligned} A_1 &= (f_{0,0}(x), 0, 0, 0), \\ A_2 &= (f_{0,1}(x), f_{1,0}(x), 0, 0), \\ A_3 &= (f_{0,2}(x), f_{1,1}(x), f_{2,0}(x), 0), \\ A_4 &= (f_{0,3}(x), f_{1,2}(x), f_{2,1}(x), f_{3,0}(x)) \end{aligned}$$

and $f_{0,0}(x)|x^{\alpha_0} - 1$, $f_{1,0}(x) = (1 + u_1)f_{1,0,1}(x) + u_1f_{1,0,u_1}(x)$, $f_{1,0}(x)|x^{\alpha_1} - 1$, $f_{2,0}(x) = (1 + u_1 + u_2 + u_1u_2)f_{2,0,1}(x) + (u_1 + u_1u_2)f_{2,0,u_1}(x) + (u_2 + u_1u_2)f_{2,0,u_2}(x) + (u_1u_2)f_{2,0,u_1u_2}(x)$, $f_{2,0}(x)|x^{\alpha_2} - 1$, $f_{3,0}(x) = (1 + u_1 + u_2 + u_3 + u_1u_2 + u_1u_3 + u_2u_3 + u_1u_2u_3)f_{3,0,1}(x) + (u_1 + u_1u_2 + u_1u_3 + u_1u_2u_3)f_{3,0,u_1}(x) + (u_2 + u_1u_2 + u_2u_3 + u_1u_2u_3)f_{3,0,u_2}(x) + (u_3 + u_1u_3 +$

$u_2u_3 + u_1u_2u_3)f_{3,0,u_3}(x) + (u_1u_2 + u_1u_2u_3)f_{3,0,u_1u_2}(x) + (u_1u_3 + u_1u_2u_3)f_{3,0,u_1u_3}(x) + (u_2u_3 + u_1u_2u_3)f_{3,0,u_2u_3}(x) + u_1u_2u_3f_{3,0,u_1u_2u_3}(x)$ with

$$f_{0,1}(x), f_{0,2}(x), f_{0,3}(x) \in R_0[x], f_{1,1}(x), f_{1,2}(x) \in R_1[x], f_{2,1}(x) \in R_2[x].$$

Proof Similarly, to proof of the Theorem 4.4, by defining a homomorphism $\Xi_{\alpha_0\alpha_1\alpha_2\alpha_3}$ between $\Upsilon_{\alpha_0\alpha_1\alpha_2\alpha_3}(C)$ and $R_3[x]/\langle x^{\alpha_3} - 1 \rangle$ by $\Xi_{\alpha_0\alpha_1\alpha_2\alpha_3}(r_0(x), r_1(x), r_2(x), r_3(x)) = r_3(x)$, by defining R_2 -submodule I_2 , the desired result is obtained. \square

From all the above discussion, by using the same process an induction on a , we get the following corollary.

Corollary 4.6 *Let C be an $R_0R_1R_2 \cdots R_i$ -cyclic code of block length $(\alpha_0, \alpha_1, \alpha_2, \dots, \alpha_i)$. Then,*

$$\begin{aligned} \Upsilon_{\alpha_0\alpha_1 \cdots \alpha_i}(C) = & \langle (f_{0,0}(x), 0, 0, 0, \cdots, 0), (f_{0,1}(x), f_{1,0}(x), 0, 0, \cdots, 0), (f_{0,2}(x), \\ & f_{1,1}(x), f_{2,0}(x), 0, \cdots, 0), (f_{0,3}(x), f_{1,2}(x), f_{2,1}(x), f_{3,0}(x), 0, \cdots, 0), \\ & \cdots, (f_{0,i}(x), f_{1,i-1}(x), f_{2,i-2}(x), f_{3,i-3}(x), \cdots, f_{i,0}(x)) \rangle, \end{aligned}$$

where $f_{i,0}(x)|x^{\alpha_i} - 1$ for $i = 0, 1, \dots, a$,

$$f_{i,0}(x) = \sum_{B \in P_i} f_{i,0,u_B}(x)e_{u_B}$$

for $i = 1, \dots, a$ and $f_{i,1}(x), f_{i,2}(x), \dots, f_{i,(a-i)}(x) \in R_i[x]$ for $i = 0, 1, 2, \dots, a - 1$.

In [7], some lemmas and theorems about the R_0R_1S cyclic codes and the separable codes were given, where $S = F_4 + uF_4 + vF_4$ and $u^2 = u, v^2 = v, uv = vu = 0$. Similarly, we get the following lemmas and theorems.

Lemma 4.7 *Let*

$$\begin{aligned} \Upsilon_{\alpha_0\alpha_1 \cdots \alpha_a}(C) = & \langle (f_{0,0}(x), 0, 0, 0, \cdots, 0), (f_{0,1}(x), f_{1,0}(x), 0, 0, \cdots, 0), (f_{0,2}(x), \\ & f_{1,1}(x), f_{2,0}(x), 0, \cdots, 0), (f_{0,3}(x), f_{1,2}(x), f_{2,1}(x), f_{3,0}(x), 0, \cdots, 0), \\ & \cdots, (f_{0,a}(x), f_{1,a-1}(x), f_{2,a-2}(x), f_{3,a-3}(x), \cdots, f_{a,0}(x)) \rangle \end{aligned}$$

be an $R_0R_1R_2 \cdots R_a$ -cyclic code. Then, we assume that $\deg f_{i,j}(x) < \deg f_{i,0}(x)$ for $i = 0, \dots, a - 1, j = 1, 2, \dots, a - i$.

An $R_0R_1R_2 \cdots R_a$ -linear code C of length $(\alpha_0, \alpha_1, \alpha_2, \dots, \alpha_i)$ is called a separable code if $C = C'_{\alpha_0} \times \cdots \times C'_{\alpha_a}$, while considering C'_{α_i} as punctured codes over C by deleting the coordinates outside the α_i components, for $i = 0, \dots, a$.

Lemma 4.8 *Let $\Upsilon_{\alpha_0\alpha_1 \cdots \alpha_a}(C) = \langle (f_{0,0}(x), 0, 0, 0, \cdots, 0), (f_{0,1}(x), f_{1,0}(x), 0, 0, \cdots, 0), (f_{0,2}(x),$*

α_i over R_i , for $i = 0, 1, \dots, a$, respectively. Conversely, let C_{α_i} be cyclic codes of length α_i over R_i , for $i = 0, 1, \dots, a$, respectively and $\mathbf{r}_{\alpha_i} \in C_{\alpha_i}$ where $i = 0, 1, \dots, a$. By using the fact that C_{α_i} are cyclic, then $\sigma(\mathbf{r}_i) \in C_{\alpha_i}$ for $i = 0, 1, \dots, a$. Take $\mathbf{r} = (\mathbf{r}_0, \mathbf{r}_1, \dots, \mathbf{r}_a) \in C$. So $\sigma(\mathbf{r}) = (\sigma(\mathbf{r}_0), \sigma(\mathbf{r}_1), \dots, \sigma(\mathbf{r}_a)) \in C$. \square

Theorem 4.12 Let $C = C_{\alpha_0} \times \dots \times C_{\alpha_a}$ be a separable $R_0R_1R_2 \dots R_a$ -cyclic of block length $(\alpha_0, \dots, \alpha_a)$, where $\zeta_0(C_{\alpha_0}) = \langle f_{0,0}(x) \rangle, \dots, \zeta_a(C_{\alpha_a}) = \langle f_{a,0}(x) \rangle$. Then, $\Upsilon_{\alpha_0\alpha_1 \dots \alpha_a}(C) = \langle f_{0,0}(x) \rangle \times \dots \times \langle f_{a,0}(x) \rangle$.

Example 4.13 Let a be 3. Let $f_{0,0}(x) = x^2 + (w+1)x + w$. Then $\zeta_0(C_{\alpha_0}) = \langle f_{0,0}(x) \rangle$ is a cyclic code over R_0 with length $\alpha_0 = 3$ and $|C_{\alpha_0}| = 4, d = 3$.

Let $f_{1,0,1}(x) = f_{1,0,u_1}(x) = x^2 + (w+1)x + 1$. Then $\zeta_0(C_{\alpha_{1,1}}) = \zeta_0(C_{\alpha_{1,u_1}}) = \langle f_{1,0,1}(x) \rangle$ are cyclic codes over R_0 with length 5 and $|C_{\alpha_{1,1}}| = 4^3, d = 3$. Therefore, $\zeta_1(C_{\alpha_1}) = \langle f_{1,0}(x) \rangle$ is a cyclic code over R_1 with length $\alpha_1 = 5$ with cardinality $4^{10-4} = 4^6, d = 3$.

Let $f_{2,0,1}(x) = f_{2,0,u_1}(x) = x^3 + x + 1, f_{2,0,u_2}(x) = f_{2,0,u_1u_2}(x) = x^3 + x^2 + 1$. Then $\zeta_0(C_{\alpha_{2,1}}) = \zeta_0(C_{\alpha_{2,u_1}}) = \langle f_{2,0,1}(x) \rangle, \zeta_0(C_{\alpha_{2,u_2}}) = \zeta_0(C_{\alpha_{2,u_1u_2}}) = \langle f_{2,0,u_2}(x) \rangle$ are cyclic codes over R_0 with length 7 and $|C_{\alpha_{2,1}}| = |C_{\alpha_{2,u_2}}| = 4^4, d = 3$. Therefore, $\zeta_2(C_{\alpha_2}) = \langle f_{2,0}(x) \rangle$ is a cyclic code over R_2 with length $\alpha_2 = 7$ with cardinality $4^{28-12} = 4^{16}, d = 3$.

Let $f_{3,0,1}(x) = f_{3,0,u_1}(x) = f_{3,0,u_2}(x) = f_{3,0,u_3}(x) = x^6 + wx^4 + wx^3 + x^2 + (w+1)x + 1, f_{3,0,u_1u_2}(x) = f_{3,0,u_1u_3}(x) = f_{3,0,u_2u_3}(x) = f_{3,0,u_1u_2u_3}(x) = x^6 + (w+1)x^5 + x^4 + wx^3 + wx^2 + 1$. Then $\zeta_0(C_{\alpha_{3,1}}) = \zeta_0(C_{\alpha_{3,u_1}}) = \zeta_0(C_{\alpha_{3,u_2}}) = \zeta_0(C_{\alpha_{3,u_3}}) = \langle f_{3,0,1}(x) \rangle, \zeta_0(C_{\alpha_{3,u_1u_2}}) = \zeta_0(C_{\alpha_{3,u_1u_3}}) = \zeta_0(C_{\alpha_{3,u_2u_3}}) = \zeta_0(C_{\alpha_{3,u_1u_2u_3}}) = \langle f_{3,0,u_1u_2}(x) \rangle$ are cyclic codes over R_0 with length 35 and $|C_{\alpha_{3,1}}| = |C_{\alpha_{3,u_1u_2}}| = 4^{29}, d = 3$. Therefore, $\zeta_3(C_{\alpha_3}) = \langle f_{3,0}(x) \rangle$ is a cyclic code over R_3 with length $\alpha_3 = 35$ with cardinality $4^{280-48} = 4^{232}, d = 3$.

Hence, $\Upsilon_{\alpha_0\alpha_1 \dots \alpha_a}(C) = \langle f_{0,0}(x) \rangle \times \langle f_{1,0}(x) \rangle \times \langle f_{2,0}(x) \rangle \times \langle f_{3,0}(x) \rangle$ is a separable $R_0R_1R_2R_3$ -cyclic code of block length $(3, 5, 7, 35)$. Moreover, $|C| = 4^{255}, d = 3$.

§5. DNA Codes

In this section, some basic definitions and details about cyclic DNA codes over R_0 and R_1 in literature will be given. Later the necessary and sufficient conditions cyclic codes over R_i for $i = 1, \dots, a$ and separable $R_0R_1R_2 \dots R_a$ cyclic codes to be reversible and reversible complement will be discussed.

It is well known that DNA has two strands that are linked that Watson-Crick pairing, every A is linked with a T and every C is linked with a G , and vice versa, where A, T, C , and G are four bases of DNA sequences. i.e. one writes $\overline{A} = T, \overline{T} = A, \overline{C} = G$ and $\overline{G} = C$. The \overline{A} denotes complement of A .

Let M be a finite commutative ring and \mathbf{C} be a linear code of length n over M . Let $\mathbf{a} = (a_1, \dots, a_n)$ be a codeword in \mathbf{C} . The reverse of \mathbf{a} is $\mathbf{a}^R = (a_n, a_{n-1}, \dots, a_1)$. The complement of \mathbf{a} is $\mathbf{a}^C = (\overline{a_1}, \overline{a_2}, \dots, \overline{a_n})$. The reverse complement of \mathbf{a} is $\mathbf{a}^{RC} = (\overline{a_n}, \overline{a_{n-1}}, \dots, \overline{a_1})$, where $\overline{a_i}$ denotes complement of a_i , for $i = 1, \dots, n$.

Definition 5.1 Let \mathbf{C} be a linear code of length n over M . Then \mathbf{C} is called reversible if

$\mathbf{a}^R \in \mathbf{C}$, for any $\mathbf{a} \in \mathbf{C}$, \mathbf{C} is called complement if $\mathbf{a}^C \in \mathbf{C}$, for any $\mathbf{a} \in \mathbf{C}$ and \mathbf{C} is called reversible complement if $\mathbf{a}^{RC} \in \mathbf{C}$, for any $\mathbf{a} \in \mathbf{C}$.

Definition 5.2 Let \mathbf{C} be a linear code of length n over M . Then \mathbf{C} is said to be cyclic DNA codes if \mathbf{C} is a cyclic and reversible complement.

Definition 5.3 For any polynomial $s(x) = s_0 + s_1x + \cdots + s_tx^t \in M[x]$ with $s_t \neq 0$, the reciprocal polynomial of $s(x)$ is defined as

$$s^*(x) = x^t s(1/x)$$

If $s^*(x) = s(x)$, then $s(x)$ is called self reciprocal.

Lemma 5.4([9]) Let $\zeta_0(C_{\alpha_0}) = \langle f(x) \rangle$ be a cyclic code of length α_0 over $R_0 = F_4$. Then C_{α_0} is reversible if and only if $f(x)$ is self reciprocal.

In [1], they studied cyclic DNA code over $R_0 = F_4$ and used the bijection map between the set of DNA alphabet $S_{D_4} = \{A, T, C, G\}$ and $R_0 = F_4 = \{0, 1, w, w^2\}$, with $0 \mapsto A, 1 \mapsto T, w \mapsto C, w + 1 \mapsto G$.

Lemma 5.5([1]) Let $\zeta_0(C_{\alpha_0}) = \langle f(x) \rangle$ be a cyclic code of length α_0 over $R_0 = F_4$. Then C_{α_0} is a complement if and only if $f(x)$ is not divisible by $x - 1$.

Theorem 5.6([7]) Let $\zeta_0(C_{\alpha_0}) = \langle f(x) \rangle$ be a cyclic code of length α_0 over $R_0 = F_4$. Then, C_{α_0} is reversible complement if and only if $f(x)$ is self reciprocal and $f(x)$ is not divisible by $x - 1$.

In [7], they extended the map from R_1 to $S_{D_4}^2$, by using the Gray map ψ_1 as follows:

$r_1 \in R_1$	Gray Images $\psi_1(r_1)$	Codon $\gamma_1(r_1)$
0	(0, 0)	AA
u_1	(0, 1)	AT
u_1w	(0, w)	AC
u_1w^2	(0, w^2)	AG
1	(1, 1)	TT
$1 + u_1$	(1, 0)	TA
$1 + u_1w$	(1, w)	TC
$1 + u_1w^2$	(1, w^2)	TG
w	(w, w)	CC
$u_1w + w$	($w, 0$)	CA
$u_1w^2 + w$	($w, 1$)	CT
$u_1 + w$	(w, w^2)	CG

$w^2 + u_1w^2$	$(w^2, 0)$	GA
$w^2 + u_1$	(w^2, w)	GC
$w^2 + u_1w$	$(w^2, 1)$	GT
w^2	(w^2, w^2)	GG

Definition 5.7([7]) *Let C_{α_1} be a linear code of length α_1 over R_1 and $\mathbf{r}_1 = (r_0, \dots, r_{\alpha_1-1}) \in C_{\alpha_1}$. By using the table, the map Λ_1 is defined as follows*

$$\Lambda_1 : C_{\alpha_1} \longrightarrow S_{D_4}^{2\alpha_1}$$

$$\mathbf{r}_1 = (r_0, \dots, r_{\alpha_1-1}) \mapsto \Lambda_1(\mathbf{r}_1) = (\gamma_1(r_0), \dots, \gamma_1(r_{\alpha_1-1})).$$

Theorem 5.8([7]) *Let $C_{\alpha_1} = C_{\alpha_1,1}e_1 + C_{\alpha_1,u_1}e_{u_1}$ be a cyclic code of length α_1 over R_1 . Then, C_{α_1} is reversible over R_1 if and only if $C_{\alpha_1,1}, C_{\alpha_1,u_1}$ are reversible over F_4 .*

Lemma 5.9([7]) *For any $r_1 \in R_1$, $\bar{r}_1 + \bar{0} = r_1$.*

Theorem 5.10([7]) *Let $C_{\alpha_1} = C_{\alpha_1,1}e_1 + C_{\alpha_1,u_1}e_{u_1}$ be a cyclic code of length α_1 over R_1 . Then, C_{α_1} is reversible complement over R_1 if and only if C_{α_1} is reversible and $(\bar{0}, \dots, \bar{0}) \in C_{\alpha_1}$.*

Theorem 5.11 *Let C_{α_1} be a cyclic DNA code of length α_1 over the ring R_1 and minimum Hamming distance d . Then, $\Lambda_1(C_{\alpha_1})$ is a DNA code of length $2\alpha_1$ over the alphabet $\{A, T, G, C\}$ with minimum Hamming distance at least d .*

Similarly, we define a bijection map between R_2 to $S_{D_4}^4$ as follows, by considering the Gray images of elements of R_2 .

$r_2 \in R_2$	Gray Images $\psi_2(r_2)$	Codon $\gamma_2(r_2)$
0	$(0, 0, 0, 0)$	AAAA
u_1	$(0, 1, 0, 1)$	TATA
$1 + w$	(w^2, w^2, w^2, w^2)	GGGG
1	$(1, 1, 1, 1)$	TTTT
w	(w, w, w, w)	CCCC
...

Definition 5.12 *Let C_{α_2} be a linear code of length α_2 over R_2 and $\mathbf{r}_2 = (r_0, \dots, r_{\alpha_2-1}) \in C_{\alpha_2}$. By using the table, the map Λ_2 is defined as follows*

$$\Lambda_2 : C_{\alpha_2} \longrightarrow S_{D_4}^{4\alpha_2}$$

$$\mathbf{r}_2 = (r_0, \dots, r_{\alpha_2-1}) \mapsto \Lambda_2(\mathbf{r}_2) = (\gamma_2(r_0), \dots, \gamma_2(r_{\alpha_2-1})).$$

Theorem 5.13 *Let $C_{\alpha_2} = C_{\alpha_2,1}e_1 + C_{\alpha_2,u_1}e_{u_1} + C_{\alpha_2,u_2}e_{u_2} + C_{\alpha_2,u_1u_2}e_{u_1u_2}$ be a cyclic code of*

length α_2 over R_2 . Then C_{α_2} is reversible over R_2 if and only if $C_{\alpha_2,1}, C_{\alpha_2,u_1}, C_{\alpha_2,u_2}, C_{\alpha_2,u_1u_2}$ are reversible over F_4 .

Lemma 5.14 For any $r_2 \in R_2$, $\overline{r_2} + \overline{0} = r_2$.

Theorem 5.15 Let $C_{\alpha_2} = C_{\alpha_2,1}e_1 + C_{\alpha_2,u_1}e_{u_1} + C_{\alpha_2,u_2}e_{u_2} + C_{\alpha_2,u_1u_2}e_{u_1u_2}$ be a cyclic code of length α_2 over R_2 . Then C_{α_2} is reversible complement over R_2 if and only if C_{α_2} are reversible over R_2 and $(\overline{0}, \dots, \overline{0}) \in C_{\alpha_2}$.

Theorem 5.16 Let C_{α_2} be a cyclic DNA code of length α_2 over the ring R_2 and minimum Hamming distance d . Then, $\Lambda_2(C_{\alpha_2})$ is a DNA code of length $4\alpha_2$ over the alphabet $\{A, T, G, C\}$ with minimum Hamming distance at least d .

Similarly, we define a bijection map between R_i to $S_{D_4}^{2^i}$ as follows, by considering the Gray images of elements of R_i for $i = 3, \dots, a$.

$r_i \in R_i$	Gray Images $\psi_i(r_i)$	Codon $\gamma_i(r_i)$
0	$(0, 0, 0, \dots, 0)$	$AAA \cdots A$
$1 + w$	$(w^2, w^2, w^2, \dots, w^2)$	$GGG \cdots G$
1	$(1, 1, 1, \dots, 1)$	$TTT \cdots T$
w	(w, w, w, \dots, w)	$CCC \cdots C$
\dots	\dots	\dots

Definition 5.17 Let C_{α_i} be a linear code of length α_i over R_i and $\mathbf{r}_i = (r_0, \dots, r_{\alpha_i-1}) \in C_{\alpha_i}$ for $i = 3, \dots, a$. By using the table, the map Λ_i is defined as follows

$$\Lambda_i : C_{\alpha_i} \longrightarrow S_{D_4}^{2^i \alpha_i}$$

$$\mathbf{r}_i = (r_0, \dots, r_{\alpha_i-1}) \mapsto \Lambda_i(\mathbf{r}_i) = (\gamma_i(r_0), \dots, \gamma_i(r_{\alpha_i-1}))$$

Theorem 5.18 Let $C_{\alpha_i} = \bigoplus_{B \in P_i} C_{\alpha_i, u_B} e_{u_B}$ be a cyclic code of length α_i over R_i for $i = 3, \dots, a$. Then C_{α_i} is reversible over R_i if and only if C_{α_i, u_B} are reversible over $R_0 = F_4$, where all $B \in P_i$ for $i = 3, \dots, a$.

Proof It is proven as proof of Theorem 10 in [7]. □

From Lemma 5.9 and Lemma 5.14, the following lemma can be obtained.

Lemma 5.19 The following conditions hold.

- i) For any $r_i \in R_i$, $\overline{r_i} = \overline{(x_{i-1} + u_i y_{i-1})} = \overline{(x_{i-1})} + u_i y_{i-1}$, where $x_{i-1}, y_{i-1} \in R_{i-1}, i = 3, 2, \dots, a$;
- ii) For any $r_i \in R_i$, $\overline{r_i} + \overline{0} = r_i$ for $i = 3, \dots, a$.

Theorem 5.20 Let $C_{\alpha_i} = \bigoplus_{B \in P_i} C_{\alpha_i, u_B} e_{u_B}$ be a cyclic code of length α_i over R_i , for $i = 3, \dots, a$. Then, C_{α_i} is reversible complement over R_i if and only if C_{α_i} are reversible over R_i

and $(\bar{0}, \dots, \bar{0}) \in C_{\alpha_i}$, where all $B \in P_i$ for $i = 3, \dots, a$.

Proof It is proven as proof of Theorem 11 in [7]. \square

Theorem 5.21 Let C_{α_i} be a cyclic DNA code of length α_i over the ring R_i and minimum Hamming distance d . Then, $\Lambda_i(C_{\alpha_i})$ is a DNA code of length $2^i \alpha_i$ over the alphabet $\{A, T, G, C\}$ with minimum Hamming distance at least d , for $i = 3, \dots, a$.

Example 5.22 Let $R_1 = F_4 + u_1 F_4$,

$$\begin{aligned} x^{11} - 1 &= (x+1)(x^5 + wx^4 + x^3 + x^2 + (w+1)x + 1) \\ &\quad (x^5 + (w+1)x^4 + x^3 + x^2 + wx + 1) \\ &= h_1(x)h_2(x)h_3(x) \in F_4[x] \end{aligned}$$

and let $f_{1,0,1}(x) = f_{1,0,u_1}(x) = h_2(x)h_3(x)$. Then $\zeta_0(C_{\alpha_{1,1}}) = \zeta_0(C_{\alpha_{1,u_1}}) = \langle f_{1,0,1}(x) \rangle$ are cyclic codes over R_0 with length 11 and $|C_{\alpha_{1,1}}| = 4, d = 11$. Hence, $\zeta_1(C_{\alpha_1}) = \langle f_{1,0}(x) \rangle$ is a cyclic code over R_1 with length 11 with $d = 11$. As $f_{1,0,1}(x)$ and $f_{1,0,u_1}(x)$ are self-reciprocal polynomials, by Lemma 5.24, $C_{\alpha_{1,1}}, C_{\alpha_{1,u_1}}$ are reversible over R_0 . Therefore, C_{α_1} is reversible over R_1 . Also, C_{α_1} has $4^{22-20} = 16$ codewords. As C_{α_1} is reversible and $(\bar{0}, \bar{0}, \dots, \bar{0}) \in C_{\alpha_1}$, then C_{α_1} is a reversible complement code over R_1 . Moreover, C_{α_1} is a cyclic DNA code and the image of the C_{α_1} under the map Δ is a DNA code of length 22, size 16 and minimum distance $d = 11$. The DNA codewords are given in the following

A
A C A C A C A C A C A C A C A C A C A C A C A C
A G A G A G A G A G A G A G A G A G A G A G A G
A T A T A T A T A T A T A T A T A T A T A T A T
C A C A C A C A C A C A C A C A C A C A C A C A
C G C G C G C G C G C G C G C G C G C G C G C G
C
C T C T C T C T C T C T C T C T C T C T C T C T

T C T C T C T C T C T C T C T C T C T C T C T
T
T A T A T A T A T A T A T A T A T A T A T A T A
T G T G T G T G T G T G T G T G T G T G T G T G
G T G T G T G T G T G T G T G T G T G T G T G T
G A G A G A G A G A G A G A G A G A G A G A G A
G C G C G C G C G C G C G C G C G C G C G C G C
G G

Example 5.23 Let $R_2 = F_4 + u_1 F_4 + u_2 F_4 + u_1 u_2 F_4, \alpha_2 = 41$ and $f_{2,0,1}(x) = f_{2,0,u_1}(x) = f_{2,0,u_2}(x) = f_{2,0,u_1 u_2}(x) = x^{20} + wx^{19} + wx^{17} + (w+1)x^{16} + x^{13} + (w+1)x^{12} + x^{11} + (w+1)x^{10} + x^9 + (w+1)x^8 + x^7 + (w+1)x^4 + wx^3 + wx + 1$. Then $\zeta_0(C_{\alpha_3, u_1 u_2}) = \zeta_0(C_{\alpha_3, u_1 u_3}) = \zeta_0(C_{\alpha_3, u_2 u_3}) = \zeta_0(C_{\alpha_3, u_1 u_2 u_3})$ are cyclic codes over R_0 with length 41 and $|C_{\alpha_{1,1}}| = 4^{21}, d =$

11. Hence, $\zeta_2(C_{\alpha_2}) = \langle f_{2,0}(x) \rangle$ is a cyclic code over R_2 with length 41 with $d = 11$. As $f_{2,0,1}(x), f_{2,0,u_1}(x), f_{2,0,u_2}(x)$ and $f_{2,0,u_1u_2}(x)$ are self-reciprocal polynomials, by Lemma 5.24, $C_{\alpha_3, u_1 u_2}, C_{\alpha_3, u_1 u_3}, C_{\alpha_3, u_2 u_3}, C_{\alpha_3, u_1 u_2 u_3}$ are reversible codes over R_0 . Therefore, C_{α_2} is a reversible code over R_2 . Also, C_{α_2} has $4^{164-80} = 4^{84}$ codewords. As C_{α_2} is a reversible code and $(\bar{0}, \bar{0}, \dots, \bar{0}) \in C_{\alpha_2}$, C_{α_2} is a reversible complement code over R_2 . Moreover, C_{α_2} is a cyclic DNA code and the image of the C_{α_2} under the map Δ is a DNA code of length 164, size 4^{84} and minimum distance $d = 11$.

Definition 5.24 Let D be an $R_0R_1R_2 \cdots R_a$ -linear code of block length $(\alpha_0, \dots, \alpha_a)$. Then D is said to be reversible, if $\mathbf{r}^R = (\mathbf{r}_0^R, \dots, \mathbf{r}_a^R) \in D$, for any $\mathbf{r} = (\mathbf{r}_0, \dots, \mathbf{r}_a) \in D$, where $\mathbf{r}_i = (r_0^i, r_1^i, \dots, r_{\alpha_i-1}^i) \in R_i^{\alpha_i}$ for $i = 0, 1, \dots, a$.

Definition 5.25 Let D be an $R_0R_1R_2 \cdots R_a$ linear code of block length $(\alpha_0, \dots, \alpha_a)$. Then D is said to be complement, if $\mathbf{r}^C = (\mathbf{r}_0^C, \dots, \mathbf{r}_a^C) \in D$, for any $\mathbf{r} = (\mathbf{r}_0, \dots, \mathbf{r}_a) \in D$, where $\mathbf{r}_i = (r_0^i, r_1^i, \dots, r_{\alpha_i-1}^i) \in R_i^{\alpha_i}$ for $i = 0, 1, \dots, a$.

Definition 5.26 Let D be an $R_0R_1R_2 \cdots R_a$ linear code of block length $(\alpha_0, \dots, \alpha_a)$. Then, D is said to be reversible complement, if $\mathbf{r}^{RC} = (\mathbf{r}_0^{RC}, \dots, \mathbf{r}_a^{RC}) \in D$, for any $\mathbf{r} = (\mathbf{r}_0, \dots, \mathbf{r}_a) \in D$, where $\mathbf{r}_i = (r_0^i, r_1^i, \dots, r_{\alpha_i-1}^i) \in R_i^{\alpha_i}$ for $i = 0, 1, \dots, a$.

Theorem 5.27 Let $C = C_{\alpha_0} \times \cdots \times C_{\alpha_i}$ be separable $R_0R_1R_2 \cdots R_i$ -cyclic code of block length $(\alpha_0, \dots, \alpha_i)$, where C_{α_i} are cyclic codes of length α_i over R_i , for $i = 0, 1, 2, \dots, a$. Then C is reversible if and only if $C_{\alpha_0}, C_{\alpha_1}, \dots, C_{\alpha_i}$ are reversible codes over R_i , for $i = 0, 1, 2, \dots, a$, respectively.

Proof Let C be a reversible code and let $\mathbf{r} = (\mathbf{r}_0, \mathbf{r}_1, \dots, \mathbf{r}_a) \in C$, $\mathbf{r}_i = (r_0^i, r_1^i, \dots, r_{\alpha_i-1}^i) \in C_{\alpha_i}$ for $i = 0, 1, \dots, a$. By using the fact that C is a reversible, we have $\mathbf{r}^R = (\mathbf{r}_0^R, \mathbf{r}_1^R, \dots, \mathbf{r}_a^R) \in C$. So this shows that $\mathbf{r}_i^R \in C_{\alpha_i}$ where $i = 0, 1, 2, \dots, a$. Therefore, C_{α_i} are reversible codes of length α_i over R_i , for $i = 0, 1, \dots, a$, respectively. Conversely, let C_{α_i} be reversible codes of length α_i over R_i , for $i = 0, 1, \dots, a$, respectively and take $\mathbf{r} = (\mathbf{r}_0, \mathbf{r}_1, \dots, \mathbf{r}_a) \in C$ where $\mathbf{r}_i \in C_{\alpha_i}$ with $i = 0, 1, \dots, a$. By using the fact that C_{α_i} are reversible, then $\mathbf{r}_i^R \in C_{\alpha_i}$ for $i = 0, 1, \dots, a$. So $\mathbf{r}^R = (\mathbf{r}_0^R, \mathbf{r}_1^R, \dots, \mathbf{r}_a^R) \in C$. Hence C is reversible. \square

Theorem 5.28 Let $C = C_{\alpha_0} \times \cdots \times C_{\alpha_i}$ be separable $R_0R_1R_2 \cdots R_i$ -cyclic code of block length $(\alpha_0, \dots, \alpha_i)$, where C_{α_i} are cyclic codes of length α_i over R_i , for $i = 0, 1, 2, \dots, a$. Then, C is a reversible complement code if and only if $C_{\alpha_0}, C_{\alpha_1}, \dots, C_{\alpha_i}$ are reversible complement codes over R_i , for $i = 0, 1, 2, \dots, a$, respectively.

Proof Let C be a reversible complement code. Take $\mathbf{r} = (\mathbf{r}_0, \mathbf{r}_1, \dots, \mathbf{r}_a) \in C$, where $\mathbf{r}_i = (r_0^i, r_1^i, \dots, r_{\alpha_i-1}^i) \in C_{\alpha_i}$ for $i = 0, 1, \dots, a$. By using the fact that C is a reversible complement, we have $\mathbf{r}^{RC} = (\mathbf{r}_0^{RC}, \mathbf{r}_1^{RC}, \dots, \mathbf{r}_a^{RC}) \in C$. So this shows that $\mathbf{r}_i^{RC} \in C_{\alpha_i}$ where $i = 0, 1, 2, \dots, a$. Therefore C_{α_i} are reversible complement codes of length α_i over R_i , for $i = 0, 1, \dots, a$, respectively. Conversely, let C_{α_i} be reversible complement codes of length α_i over R_i , for $i = 0, 1, \dots, a$, respectively and take $\mathbf{r} = (\mathbf{r}_0, \mathbf{r}_1, \dots, \mathbf{r}_a) \in C$ where $\mathbf{r}_i \in C_{\alpha_i}$ where $i = 0, 1, \dots, a$. By using the fact that C_{α_i} are reversible complement, then $\mathbf{r}_i^{RC} \in C_{\alpha_i}$ for

$i = 0, 1, \dots, a$. So $\mathbf{r}^{RC} = (\mathbf{r}_0^{RC}, \mathbf{r}_1^{RC}, \dots, \mathbf{r}_a^{RC}) \in C$. Hence, C is a reversible complement. \square

Definition 5.29 Let C be an $R_0R_1R_2 \cdots R_a$ -linear code of block length $(\alpha_0, \dots, \alpha_a)$ and $\mathbf{r} = (\mathbf{r}_0, \dots, \mathbf{r}_a) = (r_0^0, \dots, r_{\alpha_0-1}^0, r_0^1, \dots, r_{\alpha_1-1}^1, \dots, r_0^a, \dots, r_{\alpha_a-1}^a) \in R_{\alpha_0, \dots, \alpha_a}$. By using the table, the map Δ is defined as follows

$$\begin{aligned} \Delta & : R_{\alpha_0, \dots, \alpha_a} \longrightarrow S_{D_4}^{\alpha_0 + 2\alpha_1 + \dots + 2^a \alpha_a} \\ \mathbf{r} = (\mathbf{r}_0, \dots, \mathbf{r}_a) & \mapsto \Delta(\mathbf{r}) = (\Lambda_0(\mathbf{r}_0), \dots, \Lambda_a(\mathbf{r}_a)). \end{aligned}$$

Theorem 5.30 Let C be a separable $R_0R_1R_2 \cdots R_a$ cyclic DNA code of block length $(\alpha_0, \dots, \alpha_a)$ with $|C| = M$ and minimum Hamming distance d . Then, $\Delta(C)$ is a DNA code of length

$$\alpha_0 + 2\alpha_1 + \dots + 2^a \alpha_a$$

over the alphabet $\{A, T, G, C\}$ with the minimum Hamming distance at least d .

Example 5.31 Let $\Upsilon_{\alpha_0\alpha_1\alpha_2\alpha_3}(C) = \langle f_{0,0}(x) \rangle \times \langle f_{1,0}(x) \rangle \times \langle f_{2,0}(x) \rangle \times \langle f_{3,0}(x) \rangle$ is a separable $R_0R_1R_2R_3$ -cyclic code of block length $(9, 3, 5, 35)$. Let $f_{0,0}(x) = x^6 + x^3 + 1$. Then,

$$\zeta_0(C_{\alpha_0}) = \langle f_{0,0}(x) \rangle$$

is a cyclic codes over R_0 with length 9. As $f_{0,0}(x)$ is self-reciprocal polynomial and $(\bar{0}, \bar{0}, \dots, \bar{0}) \in C_{\alpha_0}$, C_{α_0} is reversible complement over R_0 . Similarly, if we take $\zeta_1(C_{\alpha_1}) = \langle f_{1,0}(x) \rangle = \langle x+1 \rangle$, $\zeta_2(C_{\alpha_2}) = \langle f_{2,0}(x) \rangle = \langle x^2 + wx + 1 \rangle$, $\zeta_3(C_{\alpha_3}) = \langle f_{3,0}(x) \rangle = \langle x^2 + (w+1)x + 1 \rangle$, C_{α_i} 's will be reversible complement codes over R_i , for $i = 1, 2, 3$. Hence, by Theorem 5.28, we get C as a reversible complement code. Then $\Delta(C)$ is a DNA code of length 315, size 4^{35} .

§6. Conclusion

In this paper, the structures of $R_0R_1R_2 \cdots R_a$ -cyclic codes are obtained with their generator polynomials, and a new inner product is defined. It was shown that if C is an $R_0R_1R_2 \cdots R_a$ -cyclic code, then C^\perp is an $R_0R_1R_2 \cdots R_a$ -cyclic code, and a separable $R_0R_1R_2 \cdots R_a$ -cyclic codes are introduced with necessary and sufficient conditions for them being reversible and reversible complement, and also the DNA codes can be constructed from them with examples.

References

- [1] Abualrub, Taher, Ali Ghrayeb and Xiang Nian Zeng, Construction of cyclic codes over $GF(4)$ for DNA computing, *Journal of the Franklin Institute*, 343.4-5 (2006), 448-457.
- [2] Adleman L., Molecular computation of the solutions to combinatorial problems, *Science*, 266(1994), 1021-1024.
- [3] Bayram, Aysegul, Elif Segah Oztas and Irfan Siap, Codes over $F_4 + vF_4$ and some DNA

- applications, *Designs, Codes and Cryptography*, 80.2 (2016), 379-393.
- [4] Benbelkacem N., Frederic M., Abualrub T. and Batoul A., Skew cyclic codes over F_4R , *arXiv* :1812.10692, 2018.
 - [5] Dertli Abdullah and Yasemin Cengellenmis, Reversible DNA codes over a family of the finite rings, *Mathematical Combinatorics*, Vol.2 (2020), 74-79.
 - [6] Dertli A., Skew Constacyclic codes over a family of finite rings and their applications to LCD and quantum codes, *Chinese Annals of Mathematics*, Series B, 46(6)(2025), 937-950.
 - [7] Dinh Hai Q., et al., New DNA codes from cyclic codes over mixed alphabets, *Mathematics*, November 2020, <https://www.mdpi.com/2227-7390/8/11/1977>.
 - [8] Hill Raymond, *A First Course in Coding Theory*, Oxford University Press, 1986.
 - [9] Massey James L., Reversible codes, *Information and Control*, Vol. 7, No.3 (1964), 369-380.

Obstructions for Connected Tree-width and Connected Path-width

Takaaki Fujita

(Independent Researcher, Shinjuku, Shinjuku-ku, Tokyo, Japan)

E-mail: takaaki.fujita060@gmail.com

Abstract: Graph theory investigates networks of vertices and edges and provides powerful tools for analyzing their structural properties. A central approach to quantifying graph complexity is through *graph parameters*. A graph is *connected* if every pair of vertices is joined by a path, ensuring mutual reachability. Among these measures, *graph width parameters* capture structural complexity, typically defined via decompositions, separators, or connectivity restrictions. Understanding how such parameters behave under connectivity constraints is a well-established line of research. In this paper, we introduce and investigate connected obstructions, structural certificates that determine the values of connected tree-width and connected path-width.

Key Words: Connected tree-width, connected path-width, tree-width, bramble.

AMS(2010): 05C62, 05C83.

§1. Introduction

1.1 Graphs and Applications

Graph theory studies networks of vertices and edges and analyzes their paths, structures, and properties [1]. Because graphs provide both visual and conceptual representations of relationships among real-world entities, they have become indispensable across many disciplines, including the natural and life sciences as well as the social sciences and engineering [2].

1.2 Graph Width Parameters

A *graph parameter* is a numerical invariant that assigns to each finite graph a value preserved under graph isomorphisms. A *graph width parameter* measures the structural complexity of graphs, typically through decompositions, separators, or connectivity restrictions.

A large body of research has investigated structural complexity via *graph parameters*. Among the most influential are the width-type parameters: tree-width [3], band-width [4, 5], hypertree-width [6], superhypertree-width [7], rank-width [8], branch-width [9], twin-width [10], mim-width [11], proper path-width [12], path-distance-width [13], and path-width [14, 15].

Two of the most widely studied width parameters are *treewidth* and *path-width*. Tree-width

¹Received August 29, 2025. Accepted November 16, 2025

measures how close a graph is to a tree structure, controlling decomposition bag size, guiding efficient algorithms, and influencing parameterized complexity [16, 17]. Path-width measures how close a graph is to a path structure, restricting decomposition sequence width, enabling simplified dynamic programming, and informing structural graph analysis.

These parameters are central to algorithm design: many problems that are otherwise intractable become fixed-parameter tractable or solvable in polynomial time on classes of graphs of bounded width [18, 19]. Moreover, they play a key role in practical applications ranging from machine learning to network optimization [20, 21].

1.3 Connected Width Parameters

A graph is *connected* if every pair of vertices is joined by a path, ensuring mutual reachability [22]. Understanding how width parameters behave under explicit connectivity constraints is an established theme [23, 24]. In particular, tree-width and path-width have connected variants—*connected tree-width* [25] and *connected path-width* [26, 27] that have attracted considerable recent attention. Connected width parameters ensure decompositions remain cohesive across components, preserving structural integrity, improving interpretability, and enhancing algorithmic efficiency for graph analysis.

1.4 Obstructions for Width Parameters

For many width notions, *obstructions* serve as min-max certificates that characterize large width and guide algorithms [28, 3]. Classical examples include tangles [3, 29], blockages [30], brambles [29, 31], and ultrafilters [32]. Obstructions provide concise min-max characterizations, certify large width, guide algorithmic design, unify structural insights, and extend naturally to broader combinatorial and connectivity frameworks. These ideas extend beyond undirected graphs to directed graphs [33], matroids [9, 34], and general connectivity systems constrained by symmetric submodularity [32, 35], with implications for both algorithms [36] and game-theoretic viewpoints [37].

1.5 Our Contribution

From the above, research on graph-width parameters and their related topics is highly significant. However, studies on Connected Obstructions for width parameters have not yet been fully developed. This paper develops *connected obstructions* tailored to the connected variants of width. We introduce and investigate *connected brambles* for connected tree-width and *connected blockages* for connected path-width, providing tools to certify large values of these parameters and to clarify their structural behavior.

§2. Basic Notation

This section fixes the terminology used throughout the paper. Unless otherwise stated, all graphs considered in this paper are finite, undirected, and simple. Furthermore, the empty set is regarded as a subset of every set.

Definition 2.1(Undirected graph) *An undirected graph is a pair $G = (V, E)$ where V is a finite set whose elements are vertices and*

$$E \subseteq \{ \{u, v\} \subseteq V \mid u \neq v \}$$

is a finite set of unordered pairs of distinct vertices, called edges. If $\{u, v\} \in E$, then u and v are adjacent, written $u \sim v$.

Definition 2.2(Tree, leaf, node) *A tree is a connected, acyclic graph. If a tree has $n := |V|$ vertices, then it has exactly $n - 1$ edges. A leaf is a vertex of degree 1. In this paper, the terms vertex and node are synonymous, a node may be a leaf or an internal (nonleaf) vertex depending on its degree.*

Definition 2.3(Connectedness and components) *Let $G = (V, E)$ be a graph. A path from u to v is a finite sequence of vertices $u = v_0, v_1, \dots, v_k = v$ such that $\{v_i, v_{i+1}\} \in E$ for all i . The graph G is connected if for every $u, v \in V$ there exists a path in G from u to v . If G is not connected, it is disconnected and decomposes into connected components, i.e., maximal connected subgraphs of G .*

We use the standard notion of a (vertex) *separation*.

Definition 2.4(Separation and order) *A separation of a graph $G = (V, E)$ is a pair (A, B) of vertex sets with*

$$A \cup B = V \quad \text{and} \quad E(G[A \setminus B], G[B \setminus A]) = \emptyset.$$

Its order is $|A \cap B|$. We write (B, A) for the opposite orientation.

Example 2.1(Separation and its order on a cycle) *Let $G = C_4$ be the cycle $v_1 - v_2 - v_3 - v_4 - v_1$. Define*

$$A = \{v_1, v_2, v_3\}, \quad B = \{v_1, v_3, v_4\}.$$

Then $A \cup B = \{v_1, v_2, v_3, v_4\} = V(G)$. Moreover, there are no edges between $A \setminus B = \{v_2\}$ and $B \setminus A = \{v_4\}$. Thus (A, B) is a separation of G . Its order is

$$|A \cap B| = |\{v_1, v_3\}| = 2.$$

The opposite orientation is (B, A) .

Definition 2.5(Induced subgraph, vertex deletion, and edge deletion) *Let $G = (V(G), E(G))$ be a finite undirected graph.*

(1) *For $X \subseteq V(G)$, the induced subgraph on X is*

$$G[X] := (X, \{ \{u, v\} \in E(G) \mid u, v \in X \}).$$

(2) For $X \subseteq V(G)$, the graph obtained by deleting X is

$$G - X := G[V(G) \setminus X].$$

(3) For $F \subseteq E(G)$, the graph obtained by deleting the edges in F is

$$G - F := (V(G), E(G) \setminus F).$$

§3. Obstructions for Connected Tree-Width

In this section we recall tree-decompositions and connected tree-decompositions, and fix notation for subgraphs. Standard references include [3, 17, 38], for broader surveys see [16, 39].

Definition 3.1(Tree-decomposition and tree-width, [3]) *A tree-decomposition of G is a pair $(T, (B_t)_{t \in V(T)})$ where T is a tree and each $B_t \subseteq V(G)$ is a bag, such that*

- (1) Vertex coverage: $V(G) = \bigcup_{t \in V(T)} B_t$;
- (2) Edge coverage: For every $\{u, v\} \in E(G)$ there exists $t \in V(T)$ with $\{u, v\} \subseteq B_t$;
- (3) Running intersection: For every $v \in V(G)$, the index set $T_v := \{t \in V(T) \mid v \in B_t\}$ induces a connected subtree of T .

The width of the decomposition is $\max_{t \in V(T)} (|B_t| - 1)$. The tree-width of G is

$$\text{tw}(G) := \min \left\{ \max_{t \in V(T)} (|B_t| - 1) : (T, (B_t)) \text{ is a tree-decomposition of } G \right\}.$$

Example 3.1(Tree-decomposition and tree-width of a cycle) Let $G = C_4$ with vertices v_1, v_2, v_3, v_4 and edges $v_1v_2, v_2v_3, v_3v_4, v_4v_1$. Take the tree T to be a single edge with nodes t_1-t_2 , and define the bags

$$B_{t_1} = \{v_1, v_2, v_3\}, \quad B_{t_2} = \{v_1, v_3, v_4\}.$$

The vertex coverage holds since $B_{t_1} \cup B_{t_2} = \{v_1, v_2, v_3, v_4\}$. Edge coverage holds: $v_1v_2, v_2v_3 \subseteq B_{t_1}$ and $v_3v_4, v_4v_1 \subseteq B_{t_2}$. For the running intersection, each vertex appears in a connected set of bags: v_1, v_3 appear in both B_{t_1}, B_{t_2} , while v_2 (resp. v_4) appears only in B_{t_1} (resp. B_{t_2}). Thus this is a tree-decomposition of width $\max(|B_{t_i}| - 1) = 3 - 1 = 2$. Since graphs of tree-width 1 are forests and C_4 contains a cycle, $\text{tw}(C_4) \geq 2$. Therefore $\text{tw}(C_4) = 2$.

Definition 3.2(Connected tree-decomposition and connected tree-width, [40]) *A connected tree-decomposition of G is a tree-decomposition $(T, (B_t)_{t \in V(T)})$ with the additional requirement*

$$\forall t \in V(T) \text{ the induced subgraph } G[B_t] \text{ is connected.}$$

Its width is again $\max_{t \in V(T)} (|B_t| - 1)$ and the connected tree-width of G is

$$\text{ctw}(G) := \min \left\{ \max_{t \in V(T)} (|B_t| - 1) : (T, (B_t)) \text{ is a connected tree-decomposition of } G \right\}.$$

Example 3.1(Connected tree-decomposition and connected tree-width of a path) Let $G = P_4$ be the path $v_1 - v_2 - v_3 - v_4$. Take a tree T that is a path on nodes $t_1 - t_2 - t_3$ and define bags

$$B_{t_1} = \{v_1, v_2\}, \quad B_{t_2} = \{v_2, v_3\}, \quad B_{t_3} = \{v_3, v_4\}.$$

Vertex and edge coverage hold, and for each vertex the index set of bags containing it is contiguous (e.g., v_2 appears exactly in B_{t_1}, B_{t_2}). Each bag induces a connected subgraph (an edge), so this is a *connected* tree-decomposition. The width is $\max_t(|B_t| - 1) = 2 - 1 = 1$. Hence, $ctw(P_4) = 1$.

Definition 3.3(Connected bramble) *A connected bramble in G is a family \mathcal{B} of vertex sets $X \subseteq V(G)$ such that*

- (1) Connectivity of elements: $G[X]$ is connected for every $X \in \mathcal{B}$;
- (2) Touching: For all $X, Y \in \mathcal{B}$, either $X \cap Y \neq \emptyset$ or there exists an edge $\{u, v\} \in E(G)$ with $u \in X$ and $v \in Y$.

A set $S \subseteq V(G)$ hits \mathcal{B} if $S \cap X \neq \emptyset$ for all $X \in \mathcal{B}$, and the order of \mathcal{B} is

$$\text{ord}(\mathcal{B}) := \min\{|S| \mid S \subseteq V(G) \text{ hits } \mathcal{B}\}.$$

Remark 3.1 *The condition (1) simply means each element $X \in \mathcal{B}$ induces a connected subgraph $G[X]$ and the condition (2) is the usual “touching” requirement; thus a connected bramble is the standard notion of a bramble with the connectivity of its elements emphasized explicitly.*

Example 3.2(A connected bramble of order 2 on a path) Again let $G = P_4$ with vertices $v_1 - v_2 - v_3 - v_4$. Consider

$$X_1 = \{v_1, v_2\}, \quad X_2 = \{v_2, v_3\}, \quad X_3 = \{v_3, v_4\}.$$

Each $G[X_i]$ is connected. Moreover, $X_1 \cap X_2 = \{v_2\} \neq \emptyset$ and $X_2 \cap X_3 = \{v_3\} \neq \emptyset$, while X_1 and X_3 touch via the edge v_2v_3 . Thus $\mathcal{B} := \{X_1, X_2, X_3\}$ is a connected bramble. Any single vertex fails to meet all three sets (e.g., v_2 misses X_3), but $\{v_2, v_3\}$ hits all. Hence $\text{ord}(\mathcal{B}) = 2$.

We establish a duality theorem for *connected* tree-width via the notions of connected partial ($< k$)-decompositions and k -flaps (cf. [14]). Let $G = (V, E)$ be a graph and $k \in \mathbb{N}$

Definition 3.4(Connected partial ($< k$)-decomposition, cf. [41]) *A connected partial ($< k$)-decomposition of G is a pair (T, ℓ) consisting of a tree T and a labelling $\ell : V(T) \rightarrow 2^V$, satisfying with $U := \bigcup_{t \in V(T)} \ell(t)$,*

- (1) Coverage inside U : For every edge $\{u, v\} \in E(G[U])$ there exists $t \in V(T)$ with $\{u, v\} \subseteq \ell(t)$;
- (2) Running intersection: For each $v \in U$, the set $\{t \in V(T) \mid v \in \ell(t)\}$ induces a connected subtree of T ;
- (3) Bag-connectivity: $G[\ell(t)]$ is connected for all $t \in V(T)$;

(4) Size bound on internal bags: *If t is not a leaf of T , then $|\ell(t)| \leq k$;*

(5) Nontriviality: *At least one bag has size $\leq k$.*

We call U the covered vertex set of (T, ℓ) . Note that U may be a proper subset of V .

Definition 3.5(k -flap, cf. [41]) *Let (T, ℓ) be a connected partial $(< k)$ -decomposition of G . If x is a leaf of T with unique neighbor x' , the set*

$$X := \ell(x) \setminus \ell(x')$$

is a k -flap provided $|\ell(x')| \leq k$. It is a connected k -flap if, in addition, $G[X]$ is connected.

Example 3.3(Connected partial $(< k)$ -decomposition) Let $G = P_5$ be the path $v_1-v_2-v_3-v_4-v_5$ and fix $k = 2$. Take the tree T to be the path $t_1-t_2-t_3$ and label

$$\ell(t_1) = \{v_1, v_2\}, \quad \ell(t_2) = \{v_2\}, \quad \ell(t_3) = \{v_2, v_3\}.$$

The covered set is $U = \{v_1, v_2, v_3\} \subsetneq V(G)$. Inside U , each edge is covered ($v_1v_2 \in \ell(t_1)$, $v_2v_3 \in \ell(t_3)$); for every $w \in U$, the bags containing w form a connected subtree of T ; each $G[\ell(t_i)]$ is connected; the unique internal node is t_2 with $|\ell(t_2)| = 1 \leq k$, and at least one bag has size $\leq k$. Hence (T, ℓ) is a connected partial $(< k)$ -decomposition of G .

Example 3.4(k -flap) In the decomposition above, t_1 is a leaf with neighbor t_2 . Then

$$X = \ell(t_1) \setminus \ell(t_2) = \{v_1, v_2\} \setminus \{v_2\} = \{v_1\}.$$

Since $|\ell(t_2)| = 1 \leq k$ and $G[X]$ is connected (a single vertex), X is a connected k -flap. (Analogously, using the other leaf t_3 yields the flap $\{v_3\}$.)

We use the standard notion of *touching* for vertex sets: for $A, B \subseteq V$ we say that A and B *touch* if either $A \cap B \neq \emptyset$ or there exists an edge $\{u, v\} \in E$ with $u \in A$ and $v \in B$.

Lemma 3.1(Gluing along a nested neighborhood, cf. [41]) *Let (T_X, ℓ^X) and (T_Y, ℓ^Y) be connected partial $(< k)$ -decompositions of a connected graph G . Let X (resp. Y) be a connected k -flap of (T_X, ℓ^X) (resp. (T_Y, ℓ^Y)). If $S := N_G(X) \subseteq N_G(Y)$, then identifying the leaves that carry X and Y , and relabelling the identified leaf by S , yields a connected partial $(< k)$ -decomposition of G .*

A Sketch of Proof Relabelling the two leaf bags by S preserves bag-connectivity and the running-intersection property (attach S along the unique paths from the old leaves to bags containing its vertices). Internal bags remain of size $\leq k$, and coverage inside the new U is unchanged. The operation merely replaces the two flaps by the small separator S . \square

Lemma 3.2(Separating non-touching flaps) *Let G be connected and let X and Y be connected k -flaps of connected partial $(< k)$ -decompositions (T_X, ℓ^X) and (T_Y, ℓ^Y) , respectively. If X and Y do not touch, then there exists a connected partial $(< k)$ -decomposition (T, ℓ) of G whose connected k -flaps are contained in those of (T_X, ℓ^X) and (T_Y, ℓ^Y) but exclude X and Y .*

Proof Since X and Y do not touch, there is a vertex separator $S \subseteq V(G)$ such that no component of $G - S$ meets both X and Y . Choose S of minimum size. By Menger's theorem, $|S| \leq |N_G(X)| \leq k$. Let A be the union of S and all components of $G - S$ that meet X , and set $B := (V(G) \setminus A) \cup S$. Then $X \subseteq A \setminus S$ and $Y \subseteq B \setminus S$, with $A \cap B = S$.

Trim (T_X, ℓ^X) to $G[B]$ by setting, for each $t \in V(T_X)$,

$$\ell^{X'}(t) : = (\ell^X(t) \cap B) \cup \{s \in S \mid t \text{ lies on the unique path from the } X\text{-leaf to some node containing } s\}.$$

The bag-connectivity and the running-intersection property are preserved; internal bags stay of size $\leq k$ (new vertices are added only along paths while at least one vertex of the corresponding $X \rightarrow S$ path is removed from the bag), and the trimmed family covers all edges of $G[B]$. Thus $(T_X, \ell^{X'})$ is a connected partial ($< k$)-decomposition of $G[B]$ whose connected k -flaps are among those of (T_X, ℓ^X) but X is replaced by the small leaf S . Symmetrically trim (T_Y, ℓ^Y) to $G[A]$. Finally, glue the two trimmed decompositions along the common small leaf S to obtain (T, ℓ) as required. \square

Using the above Lemma, we can prove the following theorem.

Theorem 3.1 *For $k \in \mathbb{N}$ and a graph G , the following are equivalent:*

$$ctw(G) \geq k \iff G \text{ contains a connected bramble of order } > k.$$

Proof \Rightarrow . Assume $ctw(G) \geq k$. Among all connected partial ($< k$)-decompositions of G , choose one whose set \mathcal{F} of connected k -flaps is inclusion-minimal. By Lemma 3.2, any two members of \mathcal{F} must touch (else we could strictly reduce the flap set). Hence, \mathcal{F} is a family of pairwise touching connected sets.

We claim that $ord(\mathcal{F}) > k$. Suppose towards a contradiction that some $S \subseteq V(G)$ with $|S| \leq k$ hits \mathcal{F} . Gluing repeatedly along S (Lemma 3.1) collapses all large leaves into the small set S , producing a connected partial ($< k$)-decomposition that covers more vertices (eventually all of $V(G)$). This yields a *connected* tree-decomposition of width $\leq k$, contradicting $ctw(G) \geq k$. Therefore, $ord(\mathcal{F}) > k$, and \mathcal{F} is the desired connected bramble.

\Leftarrow . Assume G contains a connected bramble \mathcal{B} of order $> k$. Let $(T, (B_t)_{t \in V(T)})$ be any connected tree-decomposition of G . For each edge $e = t_1 t_2 \in E(T)$, deleting e splits T into components T_1, T_2 with vertex unions $U_i := \bigcup_{t \in V(T_i)} B_t$ ($i = 1, 2$) and separator $X_e := B_{t_1} \cap B_{t_2}$. If X_e hits \mathcal{B} , then $|X_e| > k$ and the width is $> k$. Otherwise, some $B \in \mathcal{B}$ is disjoint from X_e ; since \mathcal{B} consists of connected sets and bags cover all edges, $B \subseteq U_1$ or $B \subseteq U_2$. In this case, orient e towards that side.

Orient every edge of T by this rule. A sink node t^* (which exists in any finite oriented tree) has the property that its bag B_{t^*} hits \mathcal{B} : if some $B \in \mathcal{B}$ were disjoint from B_{t^*} , then the unique edge of T on the path from t^* towards the side containing B would point away from t^* , contradicting sinkness. Hence $|B_{t^*}| \geq ord(\mathcal{B}) > k$, so the width of the decomposition is $> k$. As the decomposition was arbitrary, $ctw(G) \geq k$. \square

§4. Obstructions for Connected Path-Width

We study the relationship between (connected) path-width and a connected analogue of blockage. We first recall path decompositions and connected path decompositions, see, e.g., [26].

Definition 4.1(Path decomposition and (connected) path-width, cf. [26]) *Let $G = (V(G), E(G))$ be a finite simple graph. For $X \subseteq V(G)$ write*

$$G[X] := (X, \{\{u, v\} \in E(G) \mid u, v \in X\}).$$

A path decomposition of G is a finite sequence of bags

$$P = (X_1, \dots, X_m) \quad (X_i \subseteq V(G)),$$

such that

- (1) Vertex coverage: $\bigcup_{i=1}^m X_i = V(G)$;
- (2) Edge coverage: *For every $\{u, v\} \in E(G)$ there exists i with $\{u, v\} \subseteq X_i$;*
- (3) Running intersection: *For all $1 \leq i \leq j \leq k \leq m$, $X_i \cap X_k \subseteq X_j$ (equivalently: for each $v \in V(G)$, the set $\{i \mid v \in X_i\}$ is an interval of $\{1, \dots, m\}$).*

The width of P is $\max_i(|X_i| - 1)$. The path-width of G is

$$pw(G) := \min \{ \max_i (|X_i| - 1) : P \text{ a path decomposition of } G \}.$$

A path decomposition $P = (X_1, \dots, X_m)$ is connected if

$$G[X_1 \cup \dots \cup X_i] \text{ is connected for every } i \in \{1, \dots, m\}.$$

The connected path-width of G is

$$cpw(G) := \min \{ \max_i (|X_i| - 1) : P \text{ a connected path decomposition of } G \}.$$

Example 4.1(Connected partial ($< k$)-decomposition on a path) Let $G = P_5$ be the path $v_1 - v_2 - v_3 - v_4 - v_5$ and fix $k = 2$. Take the tree T with nodes $t_1 - t_2 - t_3$ (a path), and label

$$\ell(t_1) = \{v_1, v_2\}, \quad \ell(t_2) = \{v_2\}, \quad \ell(t_3) = \{v_2, v_3\}.$$

The covered set is $U = \{v_1, v_2, v_3\}$. Coverage inside U holds since the edges v_1v_2 and v_2v_3 lie in $\ell(t_1)$ and $\ell(t_3)$, respectively. For each vertex, the bags containing it form a connected subtree of T (v_2 appears in all three nodes; v_1 only in t_1 ; v_3 only in t_3). Thus, each $G[\ell(t_i)]$ is connected. The unique internal node is t_2 and $|\ell(t_2)| = 1 \leq k$; at least one bag has size $\leq k$. Thus (T, ℓ) is a connected partial ($< k$)-decomposition of G that covers $U \subsetneq V(G)$.

Example 4.2((Connected) path-width of a star) Let $G = K_{1,3}$ with center c and leaves a, b, d .

Define the path decomposition $P = (X_1, X_2, X_3)$ by

$$X_1 = \{c, a\}, \quad X_2 = \{c, b\}, \quad X_3 = \{c, d\}.$$

The vertex/edge coverage is immediate, and each vertex appears in a contiguous block of bags. Every prefix union is connected, $G[X_1] = G[\{c, a\}]$, $G[X_1 \cup X_2] = G[\{c, a, b\}]$, and $G[X_1 \cup X_2 \cup X_3] = G$. Hence, P is a *connected* path decomposition of width $\max_i(|X_i| - 1) = 2 - 1 = 1$, so $pw(G) = cpw(G) = 1$.

We next introduce a connected version of blockage tailored to connected path-width.

Definition 4.2(Attachment and connected blockage) *For $X \subseteq V(G)$ define the attachment of X in G by*

$$att_G(X) := \{x \in X \mid \exists y \in V(G) \setminus X \text{ with } \{x, y\} \in E(G)\},$$

and set $\alpha_G(X) := |att_G(X)|$. The connected complement of X is

$$X^{\mathbb{G}} := (V(G) \setminus X) \cup att_G(X).$$

A connected blockage of order k in G is a family $\mathcal{B} \subseteq 2^{V(G)}$ satisfying

- (1) Size bound: For every $X \in \mathcal{B}$, $\alpha_G(X) \leq k$;
- (2) Heredity (downward, under small attachment): If $X \in \mathcal{B}$ and $Y \subseteq X$ with $\alpha_G(Y) \leq k$, then $Y \in \mathcal{B}$;
- (3) Complementarity: If $X_1, X_2 \subseteq V(G)$ are complementary in the sense that $X_1^{\mathbb{G}} \subseteq X_2$ or $X_2^{\mathbb{G}} \subseteq X_1$, and $|X_1 \cap X_2| \leq k$, then exactly one of X_1, X_2 lies in \mathcal{B} ;
- (4) Connectivity: Each $X \in \mathcal{B}$ induces a connected subgraph $G[X]$.

Example 4.3(Connected blockage of order 1 on a path) Let $G = P_4$ be $v_1 - v_2 - v_3 - v_4$. For $X \subseteq V$ let $att_G(X) = \{x \in X : \exists y \notin X \text{ with } xy \in E(G)\}$. Set

$$\mathcal{B} = \{X_1, X_2, X_3\}, \quad X_1 = \{v_1\}, \quad X_2 = \{v_1, v_2\}, \quad X_3 = \{v_1, v_2, v_3\}.$$

Each $G[X_i]$ is connected. Moreover $att_G(X_1) = \{v_1\}$, $att_G(X_2) = \{v_2\}$, $att_G(X_3) = \{v_3\}$, so $|att_G(X_i)| = 1 \leq 1$ (size bound for order 1). Heredity holds within the chain $X_1 \subset X_2 \subset X_3$. For each i , the connected complement $X_i^{\mathbb{G}} = (V \setminus X_i) \cup att_G(X_i)$ satisfies $|X_i \cap X_i^{\mathbb{G}}| = |att_G(X_i)| = 1$, and exactly one of the complementary pair $\{X_i, X_i^{\mathbb{G}}\}$ is included in \mathcal{B} (namely X_i). Thus \mathcal{B} is a connected blockage of order 1 in P_4 .

Lemma 4.1(Prefix attachments are small) *Let $P = (X_1, \dots, X_m)$ be a connected path decomposition of width at most $k - 1$. For $i \in \{1, \dots, m - 1\}$ put $W_i := X_1 \cup \dots \cup X_i$ and $S_i := X_i \cap X_{i+1}$. Then,*

$$att_G(W_i) \subseteq S_i \quad \text{and} \quad |att_G(W_i)| \leq |S_i| \leq k.$$

Proof Take $x \in \text{att}_G(W_i)$. Then $x \in W_i$ and there is $y \notin W_i$ with $\{x, y\} \in E(G)$. Let j be the minimal index with $y \in X_j$. Then $j \geq i + 1$. Since $\{x, y\}$ is covered by some bag and the running-intersection property holds, we must have $x \in X_j$ as well. As $x \in W_i$, the interval property for appearances of x forces $x \in X_i \cap X_{i+1} = S_i$. Hence $\text{att}_G(W_i) \subseteq S_i$, and $|S_i| \leq \min(|X_i|, |X_{i+1}|) \leq k$. \square

Lemma 4.2(Prefix pairs are complementary) *With W_i as in Lemma 4.1, the pair $(W_i, W_i^{\mathbb{G}})$ is complementary and $|W_i \cap W_i^C| = \alpha_G(W_i) \leq k$.*

Proof By definition, $W_i^C = (V(G) \setminus W_i) \cup \text{att}_G(W_i)$, so $W_i^C \subseteq W_i^{\mathbb{G}}$ and thus $W_i^C \subseteq W_i^{\mathbb{G}}$ witnesses complementarity of $(W_i, W_i^{\mathbb{G}})$. Moreover, $W_i \cap W_i^C = \text{att}_G(W_i)$, which has size at most k by Lemma 4.1. \square

We can now state the obstruction theorem.

Theorem 4.1 *If $\text{cpw}(G) \leq k - 1$, then G admits no connected blockage of order k .*

Proof Suppose to the contrary that $\text{cpw}(G) \leq k - 1$ and \mathcal{B} is a connected blockage of order k . Fix a connected path decomposition $P = (X_1, \dots, X_m)$ of width at most $k - 1$ and write $W_i := X_1 \cup \dots \cup X_i$ for $i = 1, \dots, m$. By connectedness of P , each $G[W_i]$ is connected.

For each $i \in \{1, \dots, m - 1\}$, Lemma 4.2 shows that (W_i, W_i^C) is a complementary pair with $|W_i \cap W_i^C| \leq k$. The complementarity axiom of \mathcal{B} thus forces, for each such i , *exactly one* of W_i and W_i^C to lie in \mathcal{B} .

Define $I := \{i \in \{1, \dots, m - 1\} \mid W_i \in \mathcal{B}\}$. The heredity axiom implies that I is *downward closed*: if $i \in I$ and $1 \leq j \leq i$, then $W_j \subseteq W_i$, $G[W_j]$ is connected and $\alpha_G(W_j) \leq k$ by Lemma 4.1, hence $j \in I$.

Observe that $m \notin I$: if $W_m = V(G) \in \mathcal{B}$, then heredity (applied to $Y = \emptyset$ with $\alpha_G(\emptyset) = 0$) would force $\emptyset \in \mathcal{B}$, contradicting the connectivity requirement on members of \mathcal{B} . Thus, I is a proper (possibly empty) initial segment of $\{1, \dots, m - 1\}$. Let $i^* := \max I$ if $I \neq \emptyset$; if $I = \emptyset$ set $i^* := 0$.

We now reach a contradiction in either case.

Case 1. $I = \emptyset$.

Then, for every $i \in \{1, \dots, m - 1\}$ the complementarity axiom forces $W_i^C \in \mathcal{B}$. Pick $i = 1$. Since G is connected (as P is a connected path decomposition), $W_1 = X_1 \neq \emptyset$, and $W_1^C = (V \setminus X_1) \cup \text{att}_G(X_1)$ induces a subgraph that has at least two components (the part outside X_1 and the vertices of $\text{att}_G(X_1)$ that lie in X_1), contradicting the connectivity axiom of \mathcal{B} . Hence $I \neq \emptyset$.

Case 2. $I \neq \emptyset$.

Let $i^* = \max I$. Then, $W_{i^*} \in \mathcal{B}$ but $W_{i^*+1} \notin \mathcal{B}$. By Lemma 4.2, $(W_{i^*+1}, W_{i^*+1}^C)$ is a complementary pair with $|W_{i^*+1} \cap W_{i^*+1}^C| \leq k$, hence $W_{i^*+1}^C \in \mathcal{B}$. Now consider the pair

$$A := W_{i^*} \quad \text{and} \quad B := W_{i^*+1}^C.$$

We have $A \subsetneq W_{i^*+1}$ and $B \subseteq V \setminus W_{i^*} \cup (X_{i^*} \cap X_{i^*+1})$. A direct verification using Lemma 4.1 shows that

$$A^C \subseteq B \quad \text{and} \quad |A \cap B| = |\text{att}_G(A)| \leq k,$$

so A, B form a complementary pair of order at most k . By the complementarity axiom, exactly one of A, B may lie in \mathcal{B} , but we already have $A = W_{i^*} \in \mathcal{B}$ and $B = W_{i^*+1}^C \in \mathcal{B}$, a contradiction.

Thus no connected blockage of order k can exist when $\text{cpw}(G) \leq k - 1$. \square

§5. Connected Tangles and Their Relation to Connected Brambles

This section develops a *connected* version of tangles and proves a duality with connected brambles. We shall work with the (equivalent) *haven* formulation of tangles, adapted to enforce connectedness of the “large side” chosen by the tangle.

Definition 5.1(Connected haven and connected tangle (order $k+1$)) *Let $k \in \mathbb{N}$. A connected haven of order $k+1$ on G is a map*

$$\beta : \{S \subseteq V(G) \mid |S| \leq k\} \longrightarrow \{\text{vertex sets of components of } G - S\}$$

such that

- (1) Connectivity: *For every S with $|S| \leq k$, the subgraph $G[\beta(S)]$ is a (nonempty) connected component of $G - S$;*
- (2) Monotonicity: *If $S \subseteq T$ and $|T| \leq k$, then $\beta(T) \subseteq \beta(S)$.*

Such a haven induces an orientation T of all separations of order at most k by the rule

$$(A, B) \in T \iff \beta(A \cap B) \subseteq B.$$

We call any orientation T obtained this way a connected tangle of order $k+1$.

Example 5.1(A connected haven and its induced connected tangle on a path) Let $G = P_4$ with vertices $v_1 - v_2 - v_3 - v_4$ and fix $k = 1$ (haven of order $k + 1 = 2$). Define β on all $S \subseteq V(G)$ with $|S| \leq 1$ by

$$\begin{aligned} \beta(\emptyset) &= \{v_1, v_2, v_3, v_4\}, & \beta(\{v_1\}) &= \{v_2, v_3, v_4\}, & \beta(\{v_2\}) &= \{v_3, v_4\}, \\ \beta(\{v_3\}) &= \{v_4\}, & \beta(\{v_4\}) &= \{v_1, v_2, v_3\}. \end{aligned}$$

Each $\beta(S)$ is the vertex set of a (nonempty) component of $G - S$ and hence induces a connected subgraph. Monotonicity holds since the only proper inclusion with $|T| \leq 1$ is $\emptyset \subset \{v_i\}$, and $\beta(\{v_i\}) \subseteq \beta(\emptyset)$.

This haven induces an orientation T of all separations of order at most 1 by $(A, B) \in T \iff \beta(A \cap B) \subseteq B$. For example, for the separation (A, B) with $A = \{v_1, v_2, v_3\}$, $B = \{v_3, v_4\}$ (order 1, separator $\{v_3\}$), we have $\beta(A \cap B) = \beta(\{v_3\}) = \{v_4\} \subseteq B$; hence (A, B) is oriented toward B . Thus β is a connected haven of order 2 on P_4 , and T is the corresponding connected tangle.

We now prove the connected tangle-connected bramble duality (parameter shift $k+1 \leftrightarrow >k$), which parallels the classical tangle-bramble correspondence.

Theorem 5.1(Connected tangle-connected bramble duality) *Let $k \in \mathbb{N}$ and G be a graph. The following are equivalent.*

- (1) G admits a connected tangle of order $k+1$ (equivalently, a connected haven β of order $k+1$);
- (2) G contains a connected bramble of order $> k$.

Proof (1) \Rightarrow (2). Let β be a connected haven of order $k+1$. Define

$$\mathcal{B}_\beta := \{ \beta(S) \mid S \subseteq V(G), |S| \leq k \}.$$

Each $\beta(S)$ is connected by definition, so \mathcal{B}_β consists of connected sets.

Pairwise touching. Let $S_1, S_2 \subseteq V(G)$ with $|S_i| \leq k$. By monotonicity,

$$\beta(S_1 \cup S_2) \subseteq \beta(S_1) \cap \beta(S_2).$$

Since $\beta(S_1 \cup S_2)$ is a (nonempty) component of $G - (S_1 \cup S_2)$, the intersection $\beta(S_1) \cap \beta(S_2)$ is nonempty. Hence any two members of \mathcal{B}_β meet (and thus touch).

Order $> k$. Let $S \subseteq V(G)$ with $|S| \leq k$. Because $\beta(S) \subseteq V(G) \setminus S$ is a component of $G - S$, we have

$$S \cap \beta(S) = \emptyset.$$

Therefore S does *not* hit \mathcal{B}_β . Since this holds for every S of size at most k , any hitting set must have size at least $k+1$, i.e., $\text{ord}(\mathcal{B}_\beta) > k$. Thus \mathcal{B}_β is a connected bramble of order $> k$.

(2) \Rightarrow (1). Let \mathcal{B} be a connected bramble with $\text{ord}(\mathcal{B}) > k$. For any $S \subseteq V(G)$ with $|S| \leq k$, every set $X \in \mathcal{B}$ lies in some component of $G - S$; since $|S| < \text{ord}(\mathcal{B})$, no single vertex set S hits \mathcal{B} , hence at least one component of $G - S$ meets *all* members of \mathcal{B} . Because sets in \mathcal{B} are pairwise touching, such a component is unique: if two distinct components of $G - S$ both met all of \mathcal{B} , then taking $X \in \mathcal{B}$ meeting the first and $Y \in \mathcal{B}$ meeting the second would violate touching. Define $\beta(S)$ to be the vertex set of this unique component of $G - S$ that meets every member of \mathcal{B} .

By construction, $G[\beta(S)]$ is a (nonempty) connected component of $G - S$. If $S \subseteq T$ with $|T| \leq k$, then $G - T$ is obtained from $G - S$ by deleting additional vertices, so the component $\beta(T)$ of $G - T$ must lie inside the component $\beta(S)$ of $G - S$; hence $\beta(T) \subseteq \beta(S)$. Thus β is a connected haven of order $k+1$.

Finally, orient every separation (A, B) of order at most k toward the side containing $\beta(A \cap B)$, i.e., $(A, B) \in T \iff \beta(A \cap B) \subseteq B$. This T is a connected tangle of order $k+1$ witnessed by β . \square

Remark 5.1(Parameter shift and connection to connected tree-width) *The equivalence in Theorem 5.1 uses the standard shift: order $k+1$ tangles correspond to brambles of order $> k$.*

Combined with the connected bramble-connected tree-width duality proved earlier,

$$\begin{aligned} \text{ctw}(G) \geq k &\iff G \text{ has a connected bramble of order } >k-1 \\ &\iff G \text{ has a connected tangle of order } k. \end{aligned}$$

§6. Conclusion

In this work, we have examined the possibility of defining *connected obstructions* that characterize the values of connected tree-width and connected path-width.

Future research will further explore tree-width, path-width, and related width parameters in the context of biconnected graphs [42, 43] and triconnected graphs [44, 45]. In particular, following [46], we will study the tree-width of biconnected graphs under the name *biconnected tree-width*, along with corresponding notions such as *biconnected path-width* and *biconnected bramble*. Analogously, we plan to investigate *triconnected tree-width* and *triconnected path-width*. We also aim to extend tree-width, path-width, and other width parameters to bidirected acyclic graphs (BAGs) [47, 48], which generalize directed acyclic graphs (DAGs). Specifically, we will investigate *bag-tree-width* and *bag-path-width*, in analogy with the existing notions of *dag-tree-width* [49, 50] and *dag-path-width* [51].

Finally, we intend to generalize the graph-parameter concepts developed in this paper to two broader settings:

(i) uncertainty-aware graph models, including fuzzy graphs [52], intuitionistic fuzzy graphs [53], neutrosophic graphs [54, 55], quadripartioned neutrosophic graphs [56], pentapartioned neutrosophic graphs [57], and plithogenic graphs [58].

(ii) hierarchical graph models such as hypergraphs [59] and superhypergraphs [60, 61]. The study of width parameters within these extended frameworks promises new insights into structural graph theory under uncertainty and hierarchical modeling.

Acknowledgments

We wish to thank everyone whose guidance, ideas, and assistance contributed to this research. Our appreciation goes to the readers for their interest and to the scholars whose publications provided the groundwork for this study. We are also indebted to the individuals and institutions that supplied the resources and infrastructure necessary for completing and disseminating this paper. Lastly, we extend our gratitude to all who offered their support in various capacities.

References

- [1] Reinhard Diestel, *Graph Theory*, Springer (print edition); Reinhard Diestel (eBooks), 2024.
- [2] Jonathan L Gross, Jay Yellen and Mark Anderson, *Graph Theory and its Applications*, Chapman and Hall/CRC, 2018.
- [3] Neil Robertson and Paul D. Seymour, *Graph minors x, obstructions to tree-decomposition*,

- Journal of Combinatorial Theory*, Series B, 52(2): 153C190, 1991.
- [4] Phyllis Z Chinn, Jarmila Chvtalová, Alexander K Dewdney and Norman E Gibbs, The bandwidth problem for graphs and matrices - A survey, *Journal of Graph Theory*, 6(3): 223C254, 1982.
 - [5] Julia Böttcher, Klaas P Pruessmann, Anusch Taraz and Andreas Wrfl, Bandwidth, treewidth, separators, expansion, and universality, *Electronic Notes in Discrete Mathematics*, 31: 91C96, 2008.
 - [6] Isolde Adler, Georg Gottlob and Martin Grohe, Hypertree width and related hypergraph invariants, *European Journal of Combinatorics*, 28(8): 2167C2181, 2007.
 - [7] Takaaki Fujita and Talal Ali Al-Hawary, Short note of superhyperclique-width and local superhypertree-width, *Neutrosophic Sets and Systems*, 86: 811C837, 2025.
 - [8] Sang-il Oum, Rank-width is less than or equal to branch-width, *Journal of Graph Theory*, 57(3):239C244, 2008.
 - [9] James F Geelen, Albertus MH Gerards and Geoff Whittle, Branch-width and well-quasi-ordering in matroids and graphs, *Journal of Combinatorial Theory*, Series B, 84(2): 270C290, 2002.
 - [10] Édouard Bonnet, Colin Geniet, Eun Jung Kim, Stphan Thomassé and Rémi Watrigant, Twin-width ii: small classes, In *Proceedings of the 2021 ACM-SIAM Symposium on Discrete Algorithms (SODA)*, pages 1977C1996. SIAM, 2021.
 - [11] Lars Jaffke, O Joung Kwon and Jan Arne Telle, Mim-width i, induced path problems, *Discrete Applied Mathematics*, 278: 153C168, 2020.
 - [12] Atsushi Takahashi, Shuichi Ueno and Yoji Kajitani, Minimal acyclic forbidden minors for the family of graphs with bounded path-width, *Discrete Mathematics*, 127(1-3): 293C304, 1994.
 - [13] Takaaki Fujita, Bounding linear-width and distance-width using feedback vertex set and mm-width for graph, *Journal of Fundamental Mathematics and Applications (JFMA)*, 8(1): 33C50, 2025.
 - [14] Ephraim Korach and Nir Solel, Tree-width, path-width and cutwidth, *Discrete Applied Mathematics*, 43(1): 97 101, 1993.
 - [5] Haim Kaplan and Ron Shamir, Pathwidth, bandwidth and completion problems to proper interval graphs with small cliques, *SIAM Journal on Computing*, 25(3): 540C561, 1996.
 - [16] Daniel J Harvey and David R Wood., Parameters tied to treewidth, *Journal of Graph Theory*, 84(4): 364C385, 2017.
 - [17] Ton Kloks, *Treewidth: Computations and Approximations*, Springer, 1994.
 - [18] Hans L Bodlaender, John R Gilbert, Hjlmyr Hafsteinsson and Ton Kloks, Approximating treewidth, path width, frontsize, and shortest elimination tree, *Journal of Algorithms*, 18(2): 238C255, 1995.
 - [19] Hans L Bodlaender and Ton Kloks, Efficient and constructive algorithms for the pathwidth and treewidth of graphs, *Journal of Algorithms*, 21(2): 358C402, 1996.
 - [20] David R Karger and Nathan Srebro, Learning markov networks, maximum bounded tree-width graphs, In *SODA*, pages 392C401, 2001.
 - [21] Siqu Nie, Cassio P de Campos and Qiang Ji, Efficient learning of bayesian networks with

- bounded tree-width, *International Journal of Approximate Reasoning*, 80:412C427, 2017.
- [22] Maumita Chakraborty, Sumon Chowdhury, Joymallya Chakraborty, Ranjan Mehera and Rajat Kumar Pal, Algorithms for generating all possible spanning trees of a simple undirected connected graph: an extensive review, *Complex & Intelligent Systems*, 5:265C281, 2019.
- [23] Lali Barrire, Paola Flocchini, Fedor V Fomin, Pierre Fraigniaud, Nicolas Nisse, Nicola Santoro and Dimitrios M Thilikos, Connected graph searching, *Information and Computation*, 219:1C16, 2012.
- [24] Laura A Sanchis, Relating the size of a connected graph to its total and restricted domination numbers, *Discrete Mathematics*, 283(1-3): 205C216, 2004.
- [25] Pierre Fraigniaud and Nicolas Nisse, Connected treewidth and connected graph searching, In *Latin American Symposium on Theoretical Informatics*, pages 479C490. Springer, 2006.
- [26] Dariusz Dereniowski, From pathwidth to connected pathwidth, *SIAM Journal on Discrete Mathematics*, 26(4): 1709C1732, 2012.
- [27] Dariusz Dereniowski, Dorota Osula and Paweł Rzażewski, Finding small-width connected path decompositions in polynomial time, *Theoretical Computer Science*, 794: 85C100, 2019.
- [28] Shimon Even, *Graph Algorithms*, Cambridge University Press, 2011.
- [29] Martin Grohe and Dániel Marx, On tree width, bramble size, and expansion, *Journal of Combinatorial Theory, Series B*, 99(1): 218C228, 2009.
- [30] Daniel Bienstock, Neil Robertson, Paul D Seymour and Robin Thomas, Quickly excluding a forest, *J. Comb. Theory, Ser. B*, 52(2): 274C283, 1991.
- [31] Meike Hatzel, *Dualities in graphs and digraphs*, *Universitätsverlag der Technischen Universität Berlin*, 2023.
- [32] Takaaki Fujita, Analytical study on ultrafilter in digraph:, Directed tangle and directed ultrafilter, *Asian Research Journal of Mathematics*, 21(5): 132C146, 2025.
- [33] Joshua Erde, Directed path-decompositions, *SIAM Journal on Discrete Mathematics*, 34(1): 415C430, 2020.
- [34] Petr Hliněný and Geoff Whittle, Matroid tree-width, *European Journal of Combinatorics*, 27(7): 1117C1128, 2006.
- [35] Sang-il Oum and Paul Seymour, Testing branch-width, *Journal of Combinatorial Theory, Series B*, 97(3): 385–393, 2007.
- [36] Martin Grohe and Pascal Schweitzer, Computing with tangles, In *Proceedings of the Forty-Seventh Annual ACM Symposium on Theory of Computing*, pages 683C692, 2015.
- [37] Roman Rabinovich and Lehr- und Forschungsgebiet., Complexity measures of directed graphs, *Diss., Rheinisch Westfälische Technische Hochschule Aachen*, page 123, 2008.
- [38] Hans L Bodlaender and Arie MCA Koster, Treewidth computations ii. lower bounds, *Information and Computation*, 209(7): 1103C1119, 2011.
- [39] Hans L Bodlaender, A tourist guide through treewidth, *Acta Cybernetica*, 11(1-2): 1C21, 1993.
- [40] Reinhard Diestel and Malte Miller, Connected tree-width, *Combinatorica*, 38: 381C398, 2018.
- [41] Frdric Mazoit, A simple proof of the tree-width duality theorem, *arXiv*: 1309.2266, 2013.

- [42] Dmitri Karpov, The tree of decomposition of a biconnected graph, *arXiv*: 1405.7196, 2014.
- [43] DV Karpov, The decomposition tree of a biconnected graph, *Journal of Mathematical Sciences*, 204: 232C243, 2015.
- [44] Tsan-sheng Hsu, On four-connecting a triconnected graph, *Journal of Algorithms*, 35(2): 202C234, 2000.
- [45] Kiem-Phong Vo, Finding triconnected components of graphs, *Linear and Multilinear Algebra*, 13(2):143C165, 1983.
- [46] Remie Janssen, Mark Jones, Steven Kelk, Georgios Stamoulis and Taoyang Wu, Treewidth of display graphs, bounds, brambles and applications, *arXiv*: 1809.00907, 2018.
- [47] Vaithianathan Geetha and Niladhuri Sreenath, High concurrency for continuously evolving oodbms, In *Distributed Computing and Internet Technology: 8th International Conference, ICDCIT 2012*, Bhubaneswar, India, February 2-4, 2012. Proceedings 8, pages 94C105. Springer, 2012.
- [48] Yohei Rosen, Jordan Eizenga and Benedict Paten, Describing the local structure of sequence graphs, In *Algorithms for Computational Biology: 4th International Conference, AICoB 2017*, Aveiro, Portugal, June 5-6, 2017, Proceedings 4, pages 24C46. Springer, 2017.
- [49] Dietmar Berwanger, Anuj Dawar, Paul Hunter, Stephan Kreutzer and Jan Obdržálek, The dag-width of directed graphs, *Journal of Combinatorial Theory, Series B*, 102(4): 900C923, 2012.
- [50] Dietmar Berwanger, Anuj Dawar, Paul Hunter and Stephan Kreutzer, Dag-width and parity games, In *STACS 2006: 23rd Annual Symposium on Theoretical Aspects of Computer Science*, Marseille, France, February 23-25, 2006. Proceedings 23, pages 524C536. Springer, 2006.
- [51] Shoji Kasahara, Jun Kawahara, Shin-ichi Minato and Jumpei Mori, Dag-pathwidth: graph algorithmic analyses of dag-type blockchain networks, *IEICE TRANSACTIONS on Information and Systems*, 106(3): 272C283, 2023.
- [52] Azriel Rosenfeld, Fuzzy graphs, In *Fuzzy Sets and their Applications to Cognitive and Decision Processes*, pages 77C95. Elsevier, 1975.
- [53] R Parvathi, MG Karunambigai and Krassimir T Atanassov, Operations on intuitionistic fuzzy graphs, In *2009 IEEE International Conference on Fuzzy Systems*, pages 1396C1401. IEEE, 2009.
- [54] Said Broumi, Mohamed Talea, Assia Bakali and Florentin Smarandache, Single valued neutrosophic graphs, *Journal of New theory*, 10: 86C101, 2016.
- [55] Said Broumi, Mohamed Talea, Assia Bakali and Florentin Smarandache, Interval valued neutrosophic graphs, *Critical Review*, XII, 2016: 5C33, 2016.
- [56] Basavaraj V Hiremath, Durga Nagarajan, Satham Hussain S, Hossein Rashmanlou and Farshid Mofidnakhaei, m -polar quadripartitioned neutrosophic graphs with applications in decision-making for mobile network selection, *Neutrosophic Sets and Systems*, 82(1): 29, 2025.
- [57] Said Broumi, Assia Bakali, Mohamed Talea, Florentin Smarandache and V Venkateswara Rao, Interval complex neutrosophic graph of type., *Collected Papers, Volume XIV: Neu-*

- trosophics and Other Topics*, page 289, 2022.
- [58] Fazeelat Sultana, Muhammad Gulistan, Mumtaz Ali, Naveed Yaqoob, Muhammad Khan, Tabasam Rashid and Tauseef Ahmed, A study of plithogenic graphs: applications in spreading coronavirus disease (covid-19) globally, *Journal of Ambient Intelligence and Humanized Computing*, 14(10): 13139C13159, 2023.
 - [59] Yifan Feng, Haoxuan You, Zizhao Zhang, Rongrong Ji and Yue Gao, Hypergraph neural networks, In *Proceedings of the AAAI Conference on Artificial Intelligence*, volume 33, pages 3558C3565, 2019.
 - [60] Florentin Smarandache, Extension of hypergraph to n -superhypergraph and to plithogenic n -superhypergraph and extension of hyperalgebra to n -ary (classical-/neutro-/anti-) hyperalgebra, *Infinite Study*, 2020.
 - [61] Masoud Ghods, Zahra Rostami and Florentin Smarandache, Introduction to neutrosophic restricted superhypergraphs and neutrosophic restricted superhypertrees and several of their properties, *Neutrosophic Sets and Systems*, 50: 480C487, 2022

Enumeration the Number of Spanning Trees of Some Families of Graphs Based on Nonahedron Graphs

S. N. Daoud^{1,2,*} and Ahmed N. Elsayy^{1,3}

1. Department of Mathematics, Faculty of Science, Taibah University, Al-Madinah 30001, Saudi Arabia

2. Department of Mathematics, Faculty of Science, Menoufia University, Shebin El Kom 32511, Egypt

3. Department of Mathematics, Faculty of Science, Al-Azhar University, Cairo, Egypt

E-mail: salamadaoud@gmail.com, ahnoby@yahoo.com

Abstract: In physics, analogous transformations can be used to simplify complex circuits that require multiple mathematical operations for investigation. The number of spanning trees in particular graph families can also be determined using these adjustments. In this work, we utilize our knowledge of difference equations, electrically equivalent transformations, and weighted generating function rules to compute explicit formulae for the number of spanning trees in sequences of new families of graphs formed by certain Nonahedron graphs with the same average degree. We end by comparing the entropy of our graphs to that of comparable graphs with an average degree of four.

Key Words: Enumeration, spanning trees, Nonahedron graph, electrically equivalent transformations.

AMS(2010): 05C30, 05C50, 05C63.

§1. Introduction

There has been a lot of interest in the topic of finding closed-form formulations for the complexity (number of spanning trees) in various graph types. Enumerating chemical isomers [1]-[2], extending network analysis methods in psychological networks [3], counting Eulerian circuits [4]-[5] and resolving unsolvable issues like the traveling salesman and Steiner tree problems [6] are all important applications of this study area. Additionally, examining various graph types can help find the most complicated graphs, which has applications for network resilience [7]-[8]. The number of spanning trees $\tau(G)$ of a finite connected undirected graph G is an acyclic $(n-1)$ -edge spanning subgraph. This number can be found in a variety of ways. Kirchhoff [9] gave the famous matrix tree theorem: *if D is the diagonal matrix of the degrees of G and A denote the adjacency matrix of G , Kirchhoff matrix $L = D - A$ has all its cofactors equal to $\tau(G)$.* Another way to determine a graph's complexity is to use its Laplacian eigenvalues. Consider a graph with k vertices that is linked. The following formula was obtained by Kelmans and

¹Received July 4, 2025. Accepted November 18, 2025

Chelnokov [10]

$$\tau(G) = \frac{1}{k} \prod_{i=1}^{k-1} \mu_i, \quad (1.1)$$

where $k = \mu_1 \geq \mu_2 \geq \dots \geq \mu_k = 0$ are the eigenvalues of the Kirchhoff matrix L . Degenerating the graph through successive elimination of contraction of its edges represents the core of another way to compute the complexity of a graph [11]-[13]. If $G = (V, E)$ is a multigraph with $e \in E(G)$, then $G - e$ denotes the graph obtained by deleting an arbitrary edge e and $G.e$ is the graph obtained from G by contracting the degree until its endpoints are a single vertex. The formula for computing the number of spanning trees of a multigraph G is given by

$$\tau(G) = \tau(G - e) + \tau(G.e). \quad (1.2)$$

This formula is beautiful but not practically useful (grows exponentially with the size of the graph- may be as many as $2^{|E(G)|}$ terms. For a summary of further techniques and methods for calculating the number of spanning trees of graphs, see [14]-[17].

§2. Electrically Equivalent Transformations

An edge-weighted graph, whose weights represent the conductance of the corresponding edges, may be thought of as an electrical network, which is why Kirchhoff was motivated to research electrical networks. The quotient of the (weighted) number of spanning trees and the (weighted) number of so-called thicketsthat is, spanning forests with exactly two components, and the characteristic that each component contains precisely one of the vertices u, v can be used to express the effect conductance between two vertices u, v [18]-[21]. The impact of a few basic modifications on the quantity of spanning trees is listed below. The weighted number of spanning trees G is indicated by $\tau(G)$ and let G be an edge-weighted graph and G' be the associated electrically equivalent graph.

- *Parallel edges.* When two parallel edges in G , each with conductances u and v , are merged into a single edge in G' with a conductance of $u + v$, the count of spanning trees, $\tau(G')$, remains unchanged compared to $\tau(G)$.

- *Serial edges.* If two serial edges in G , with conductances u and v , are combined into a single edge in G' with a conductance of $uv/(u + v)$, then $\tau(G')$ can be calculated as $1/(u + v)$ multiplied by $\tau(G)$.

- *Δ -Y Transformation.* When a triangle in G , with conductances u, v and w is transformed into an electrically equivalent star graph in G' with conductances $x = (uv + vw + wu)/u, y = (uv + vw + wu)/v$, and $z = (uv + vw + wu)/w$, the count of spanning trees in $G', \tau(G')$, can be determined as $(uv + vw + wu)^2/uvw$ multiplied by $\tau(G)$.

- *Y- Δ Transformation.* If a star graph in G , with conductance u, v and w , is converted into an electrically equivalent triangle in G' with conductance $x = vw/(u+v+w), y = uw/(u+v+w)$, and $z = uv/(u+v+w)$, then $\tau(G')$ is given by $1/(u+v+w)$ multiplied by $\tau(G)$. In mathematics, it is common to derive new structures from existing ones. This principle extends to graphs,

where numerous new graphs can be generated from a given set. In this study, we determine the complexity for four novel types of graphs of the same average degree we named $G_1^{(n)}, G_2^{(n)}, G_3^{(n)}$ and $G_4^{(n)}$ respectively.

§3. Number of Spanning Trees in the Sequences of $G_1^{(n)}$ Graphs

The graph $G_1^{(n)}$ is defined recursively using the graphs $G_1^{(1)}$ (triangle or K_3) and $G_1^{(2)}$ as shown in Figure 1. The graph $G_1^{(n)}$, $n = 3$ is obtained by replacing the central triangle in the graph $G_1^{(2)}$ by a copy of $G_1^{(2)}$. In general, the graph $G_1^{(n)}$ is obtained by replacing the central triangle in $G_1^{(n-1)}$ with $G_1^{(2)}$. According to this construction, the number of total vertices $|V(G_1^{(n)})|$ and edges $|E(G_1^{(n)})|$ are $|V(G_1^{(n)})| = 9n - 6$ and $|E(G_1^{(n)})| = 15n - 12, n = 1, 2, \dots$. The average degree of the graph ($G_1^{(n)}$) in the large n limit is $10/3$.

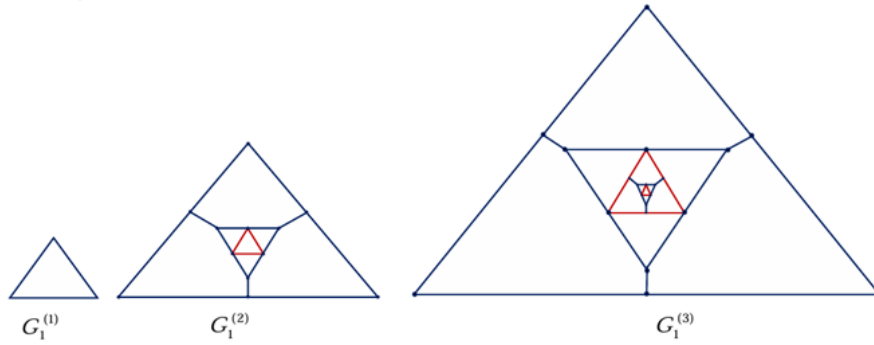


Figure 1. Some sequences of $G_1^{(n)}$ graphs.

Theorem 3.1 For $n \geq 1$, the number of spanning trees in the sequence of the graph $G_1^{(n)}$ is given by

$$\frac{4^{(n-4)}((-384 + 53\sqrt{42})(8749 + 1350\sqrt{42})^n + 17((13 - 2\sqrt{42})^n(48288 + 7451\sqrt{42}))^2)}{3(-17(337 + 52\sqrt{42}) + (31 + 4\sqrt{42})(337 + 52\sqrt{42})^n)^2}.$$

Proof We convert $G_1^{(i)}$ to $G_1^{(i-1)}$ via the electrically equivalent transformation. The conversion procedure from $G_1^{(2)}$ to $G_1^{(1)}$ is shown in Figures 2-7 following.

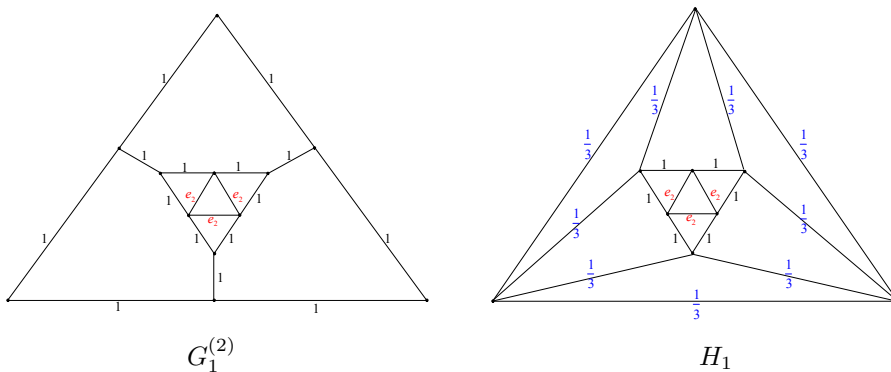


Figure 2

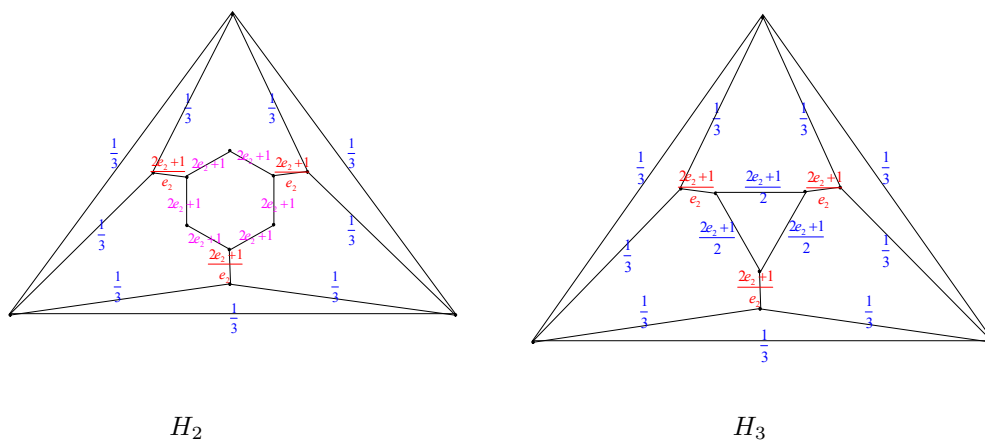


Figure 3

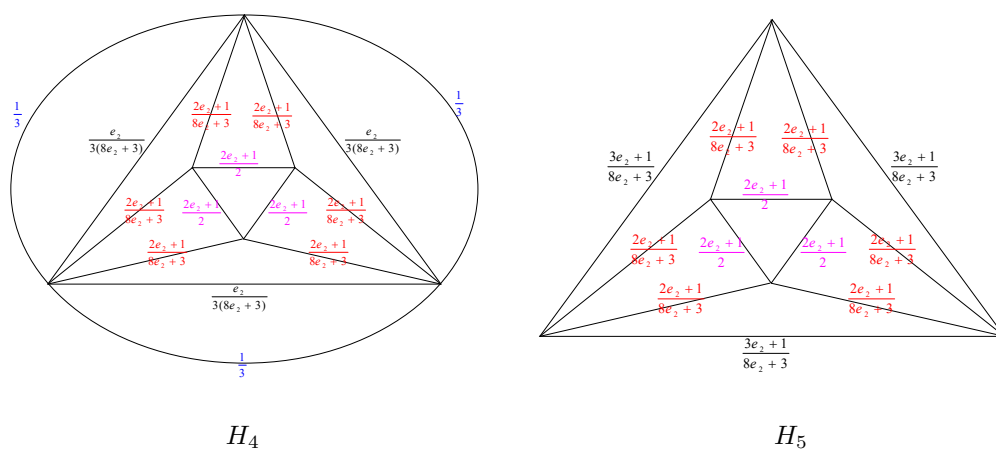


Figure 4

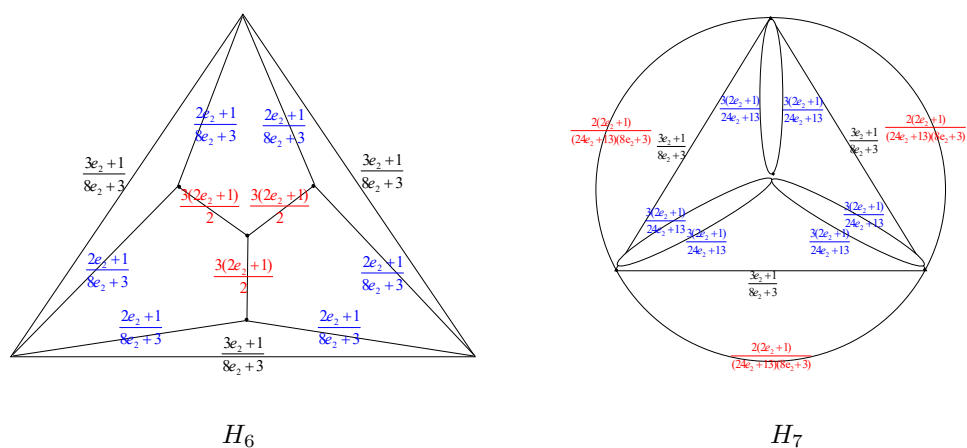


Figure 5

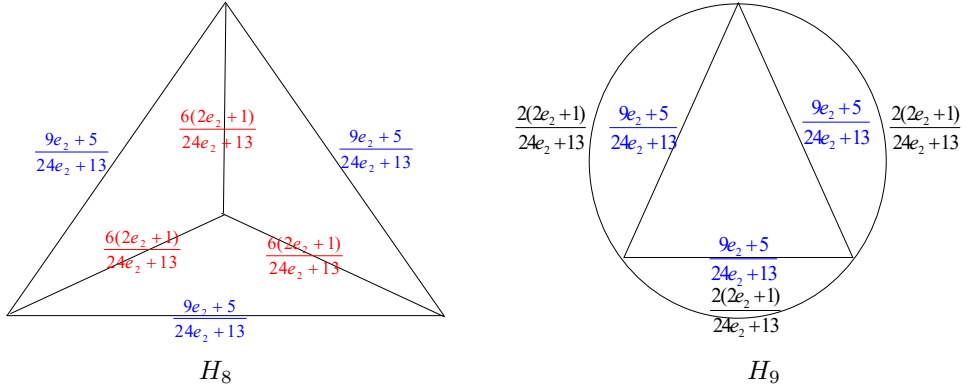


Figure 6

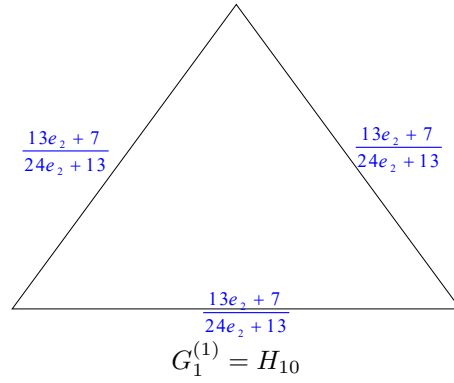


Figure 7

The following transformations result from using the attributes listed in Section 2

$$\begin{aligned} \tau(H_1) &= \left(\frac{1}{3}\right)^3 \tau(G_1^{(2)}), \quad \tau(H_2) = \left[\frac{(2e_2+1)^2}{e_2}\right]^3 \tau(H_1), \\ \tau(H_3) &= \left[\frac{1}{2(2e_2+1)}\right]^3 \tau(H_2), \quad \tau(H_4) = \left[\frac{3e_2}{8e_2+3}\right]^3 \tau(H_3), \\ \tau(H_5) &= \tau(H_4), \tau(H_6) = 9 \left[\frac{2e_2+1}{2}\right]^3 \tau(H_5), \quad \tau(H_7) = \left[\frac{2(8e_2+3)}{(24e_2+13)(2e_2+1)}\right]^3 \tau(H_6), \\ \tau(H_8) &= \tau(H_7), \tau(H_9) = \left[\frac{(24e_2+13)}{18(2e_2+1)}\right]^3 \tau(H_8), \quad \tau(G_1^{(1)}) = \tau(H_9). \end{aligned}$$

When these ten transformations are combined, we obtain

$$\tau(G_1^{(2)}) = 4(24e_2+13)^2 \tau(G_1^{(1)}). \tag{3.1}$$

Further, by

$$\tau(G_1^{(n)}) = \prod_{i=2}^n 4(24e_i+13)^2 \tau(G_1^{(1)})$$

where $h_0 = 0, k_0 = 1$ and $h_1 = 24, k_1 = 13$. By the expression $e_{n-1} = \frac{13e_n+7}{24e_n+13}$ and using Eqs. (3.6) and (3.7), we have

$$h_{i+1} = 26h_i - h_{i-1}; k_{i+1} = 26k_i - k_{i-1}. \quad (3.9)$$

Notice that Eq. (3.9) has the characteristic equation $u^2 - 26u + 1 = 0$. Its roots are $u_1 = 13+2\sqrt{42}$ and $u_2 = 13-2\sqrt{42}$. The general solutions of Eq.(3.9) are $h_i = a_1u_1^i + a_2u_2^i, k_i = b_1u_1^i + b_2u_2^i$. Given the initial conditions $h_0 = 0, k_0 = 1$ and $h_1 = 24, k_1 = 13$, we have

$$h_i = \frac{\sqrt{42}}{7}(13 + 2\sqrt{42})^i - \frac{\sqrt{42}}{7}(13 - 2\sqrt{42})^i; k_i = \frac{1}{2}(13 + 2\sqrt{42})^i + \frac{1}{2}(13 - 2\sqrt{42})^i. \quad (3.10)$$

There is no electrically similar transition for $G_1^{(n)}$ if $e_n = 1$. When Eq. (3.10) is inserted into Eq. (3.8), we obtain

$$\begin{aligned} \tau(G_1^{(n)}) = & 3 \times 4^{n-1} e_1^2 \left[\left(\frac{259 + 40\sqrt{42}}{14} \right) (13 + 2\sqrt{42})^{n-2} \right. \\ & \left. + \left(\frac{259 - 40\sqrt{42}}{14} \right) (13 - 2\sqrt{42})^{n-2} \right]^2 \end{aligned} \quad (3.11)$$

for integer $n \geq 2$. Notice that the equation (3.11) is satisfied for $n = 1$ and $\tau(G_1^{(1)}) = 3$. Thus, the number of spanning trees in the sequence of the graph $\tau(G_1^{(n)})$ is determined by

$$\begin{aligned} \tau(G_1^{(n)}) = & 3 \times 4^{n-1} e_1^2 \left[\left(\frac{259 + 40\sqrt{42}}{14} \right) (13 + 2\sqrt{42})^{n-2} \right. \\ & \left. + \left(\frac{259 - 40\sqrt{42}}{14} \right) (13 - 2\sqrt{42})^{n-2} \right]^2 \end{aligned} \quad (3.12)$$

for integer $n \geq 1$, where

$$e_1 = \frac{(337 + 52\sqrt{42})^{n-1}(168 + 31\sqrt{42}) + 17\sqrt{42}}{12(337 + 52\sqrt{42})^{n-1}(31 + 4\sqrt{42}) - 204}, n \geq 1. \quad (3.13)$$

The result is obtained by inserting Eq. (3.13) into Eq. (3.12).

§4. Number of Spanning Trees in Sequences of $G_2^{(n)}$ Graphs

The graph $G_2^{(n)}$ is defined recursively using the graphs $G_2^{(1)}$ (triangle or K_3) and $G_2^{(2)}$ as shown in Figure 8. The graph $G_2^{(n)}, n = 3$ is obtained by replacing the central triangle in the graph $G_2^{(2)}$ by a copy of $G_2^{(2)}$. In general, the graph $G_2^{(n)}$ is obtained by replacing the central triangle in $G_2^{(n-1)}$ with $G_2^{(2)}$. According to this construction, the number of total vertices $|V(G_2^{(n)})|$ and edges $|E(G_2^{(n)})|$ are $|V(G_2^{(n)})| = 9n - 6$ and $|E(G_2^{(n)})| = 15n - 12, n = 1, 2, \dots$. The average degree of the graph $G_2^{(n)}$ in the large n limit is $\frac{10}{3}$.

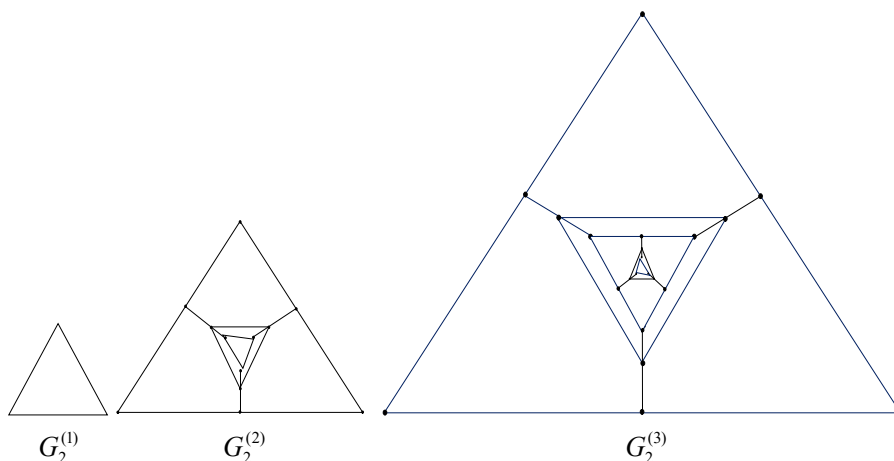


Figure 8. Some sequences of graphs $G_2^{(n)}$

Theorem 4.1 For $n \geq 1$, the number of spanning trees in the sequence of the graph $G_2^{(n)}$ is given by $\frac{A_1}{A_2}$, where

$$A_1 = 3 \times 2^{(n-5)}((38 - 27\sqrt{2})(17 + 12\sqrt{2})^n + (38 + 27\sqrt{2})(17 - 12\sqrt{2})^n)^2(1055 + 746\sqrt{2} + (5 + 4\sqrt{2})(577 + 408\sqrt{2})^n)^2,$$

$$B_1 = (-7(577 + 408\sqrt{2}) + (11 + 6\sqrt{2})(577 + 408\sqrt{2})^n)^2.$$

Proof We convert $G_2^{(i)}$ to $G_2^{(i-1)}$ via the electrically equivalent transformation. The conversion procedure from $G_2^{(2)}$ to $G_2^{(1)}$ is shown in Figures 9-14 following.

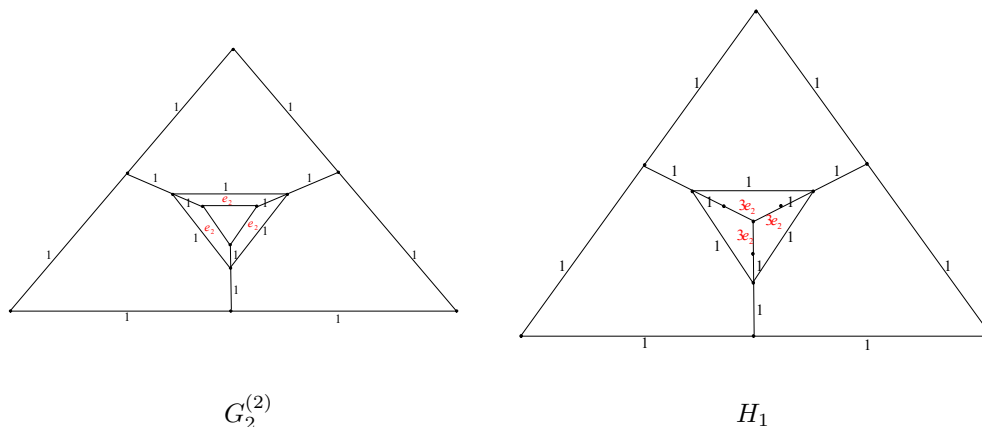


Figure 9

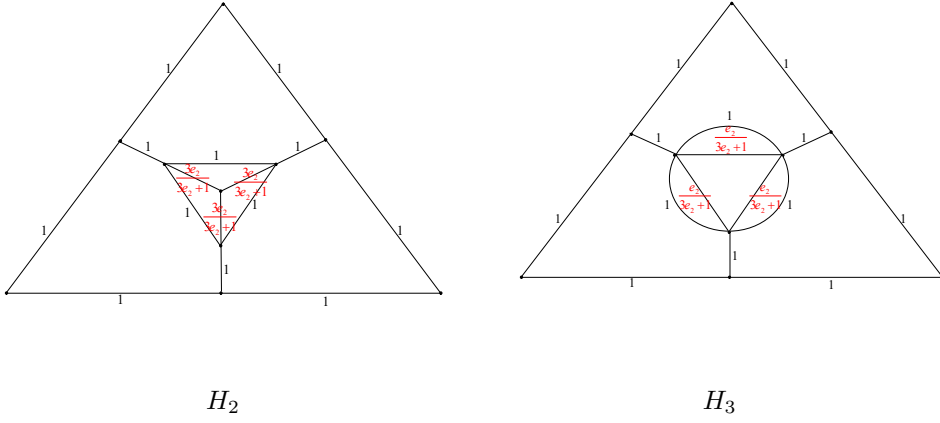


Figure 10

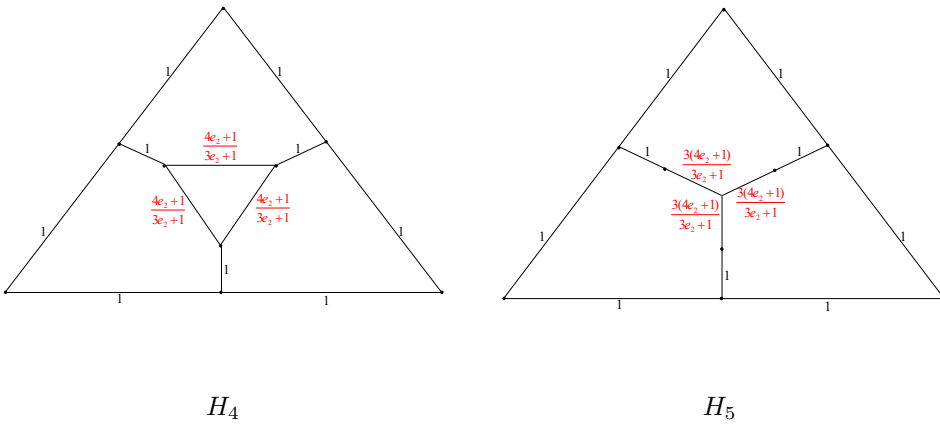


Figure 11

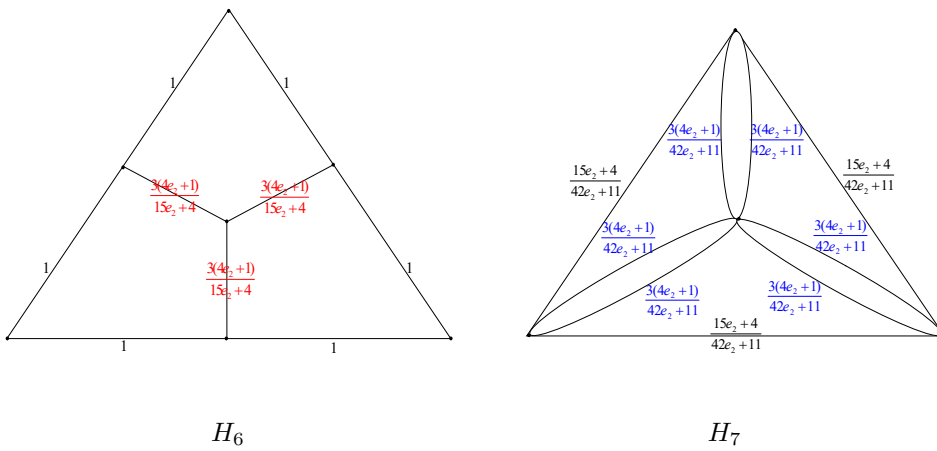


Figure 12

The following transformations result from using the attributes listed in Section 2.

$$\begin{aligned}
\tau(H_1) &= 9e_2\tau(G_2^{(2)}), \quad \tau(H_2) = \left[\frac{1}{3e_2+1}\right]^3 \tau(H_1), \\
\tau(H_3) &= \left[\frac{3e_2+1}{9e_2}\right] \tau(H_2), \quad \tau(H_4) = \tau(H_3), \\
\tau(H_5) &= 9\left[\frac{4e_2+1}{3e_2+1}\right] \tau(H_4), \quad \tau(H_6) = \left[\frac{3e_2+1}{15e_2+4}\right]^3 \tau(H_5), \\
\tau(H_7) &= \left[\frac{15e_2+4}{42e_2+11}\right]^3 \tau(H_6), \quad \tau(H_8) = \tau(H_7), \\
\tau(H_9) &= \left[\frac{(42e_2+11)}{18(4e_2+1)}\right] \tau(H_8), \quad \tau(G_2^{(1)}) = \tau(H_9).
\end{aligned}$$

When these ten transformations are combined, we obtain

$$\tau(G_2^{(2)}) = 2(42e_2+11)^2\tau(G_2^{(1)}). \quad (4.1)$$

Further,

$$\tau(G_2^{(n)}) = \prod_{i=2}^n 2(42e_i+11)^2\tau(G_2^{(1)}) = 3 \times 2^{n-1} e_1^2 \left[\prod_{i=2}^n (42e_i+11) \right]^2, \quad (4.2)$$

where,

$$e_{i-1} = \frac{23e_i+6}{42e_i+11}, \quad i = 2, 3, \dots, n.$$

Its characteristic equation is $21t^2 - 6t - 3 = 0$ with roots $t_1 = \frac{1-2\sqrt{2}}{7}$ and $t_2 = \frac{1+2\sqrt{2}}{7}$. Subtracting these two roots into both sides of $e_{i-1} = \frac{23e_i+6}{42e_i+11}$, we get

$$e_{i-1} - \frac{1-2\sqrt{2}}{7} = \frac{23e_i+6}{42e_i+11} - \frac{1-2\sqrt{2}}{7} = \frac{(17+12\sqrt{2})[e_i - \frac{1-\sqrt{2}}{7}]}{42e_i+11}, \quad (4.3)$$

$$e_{i-1} - \frac{1+2\sqrt{2}}{7} = \frac{23e_i+6}{42e_i+11} - \frac{1+2\sqrt{2}}{7} = \frac{(17-12\sqrt{2})[e_i - \frac{1+\sqrt{2}}{7}]}{42e_i+11}. \quad (4.4)$$

Let $x_i = \frac{e_i - \frac{1-2\sqrt{2}}{7}}{e_i - \frac{1+2\sqrt{2}}{7}}$, then by Eqs. (4.3) and (4.4) we get $x_{i-1} = (577 + 408\sqrt{2})x_i$ and $x_i = (577 + 408\sqrt{2})^{n-i}x_n$. Therefore,

$$e_i = \frac{(577 + 408\sqrt{2})^{n-i}(\frac{1+2\sqrt{2}}{7})x_n - \frac{1-2\sqrt{2}}{7}}{(577 + 408\sqrt{2})^{n-i}x_n - 1}.$$

Thus,

$$e_1 = \frac{(577 + 408\sqrt{2})^{n-1}(\frac{1+2\sqrt{2}}{7})x_n - \frac{1-2\sqrt{2}}{7}}{(577 + 408\sqrt{2})^{n-1}x_n - 1}. \quad (4.5)$$

Using the expression $e_{n-1} = \frac{23e_n+6}{42e_n+11}$ and denoting the coefficients of $23e_n+6$ and $42e_n+11$

for integer $n \geq 2$. Notice that Eq. (4.11) is satisfied for $n = 1$ and $\tau(G_2^{(1)}) = 3$. Thus, the number of spanning trees in the sequence of the graph \mathcal{N}_n is determined by

$$\begin{aligned} \tau(G_2^{(n)}) = & 3 \times 2^{n-1} e_1^2 \left[\left(\frac{106 + 75\sqrt{2}}{4} \right) (17 + 12\sqrt{2})^{n-2} \right. \\ & \left. + \left(\frac{106 - 75\sqrt{2}}{4} \right) (17 - 12\sqrt{2})^{n-2} \right]^2 \end{aligned} \quad (4.12)$$

for integer $n \geq 1$, where

$$e_1 = \frac{(577 + 408\sqrt{2})^{n-1} (5 + 4\sqrt{2}) - (1 - 2\sqrt{2})}{(577 + 408\sqrt{2})^{n-1} (11 + 6\sqrt{2}) - 7}, n \geq 1. \quad (4.13)$$

and the result is obtained by inserting Eq. (4.13) into Eq. (4.12). \square

§5. Number of Spanning Trees in Sequences of $G_3^{(n)}$ Graphs

The graph $G_3^{(n)}$ is defined recursively using the graphs $G_3^{(1)}$ (triangle or K_3) and $G_3^{(2)}$ as shown in Figure 15. The graph $G_3^{(n)}$, $n = 3$ is obtained by replacing the central triangle in the graph $G_3^{(2)}$ by a copy of $G_3^{(2)}$. In general, the graph $G_3^{(n)}$ is obtained by replacing the central triangle in $G_3^{(n-1)}$ with $G_3^{(2)}$. According to this construction, the number of total vertices $|V(G_3^{(n)})|$ and edges $|E(G_3^{(n)})|$ are $|V(G_3^{(n)})| = 9n - 6$ and $|E(G_3^{(n)})| = 15n - 12$, $n = 1, 2, \dots$. The average degree of the graph $G_3^{(n)}$ in the large n limit is $\frac{10}{3}$.

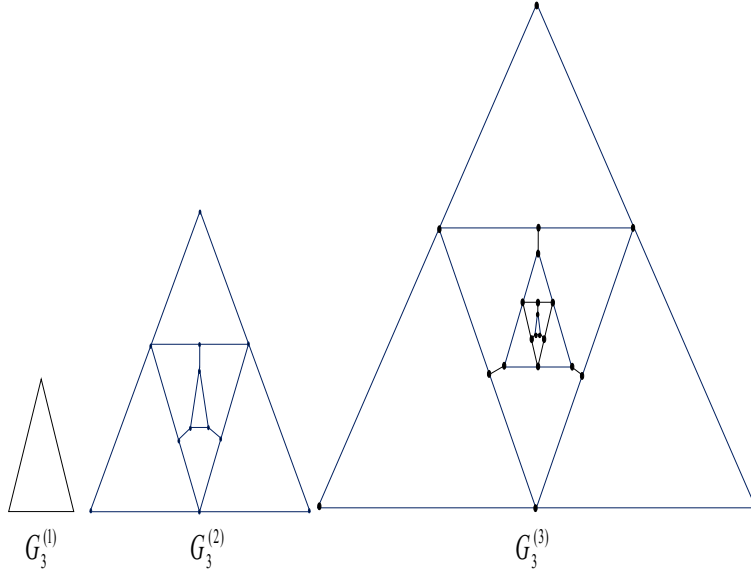


Figure 15. Some sequences of $G_3^{(n)}$ graphs.

Theorem 5.1 For $n \geq 1$ the number of spanning trees in the sequence of $G_3^{(n)}$ is given by $\frac{A_2}{B_2}$,

where

$$A_2 = (23782 + 3150\sqrt{57})^{2n} \left(-1 + \left(\frac{1}{8}(521 - 69\sqrt{57}) \right)^n \right)^2 (798 + 106\sqrt{57})$$

$$+ \left(\frac{1}{8}(521 - 69\sqrt{57}) \right)^n (3933 + 521\sqrt{57})^2,$$

$$B_2 = 38988(8^n(521 + 69\sqrt{57}) + 2(53 + 7\sqrt{57})(521 + 69\sqrt{57})^n)^2.$$

Proof We convert $G_3^{(i)}$ to $G_3^{(i-1)}$ via the electrically equivalent transformation. The conversion procedure from $G_3^{(2)}$ to $G_3^{(1)}$ is shown in Figures 16-20 following.

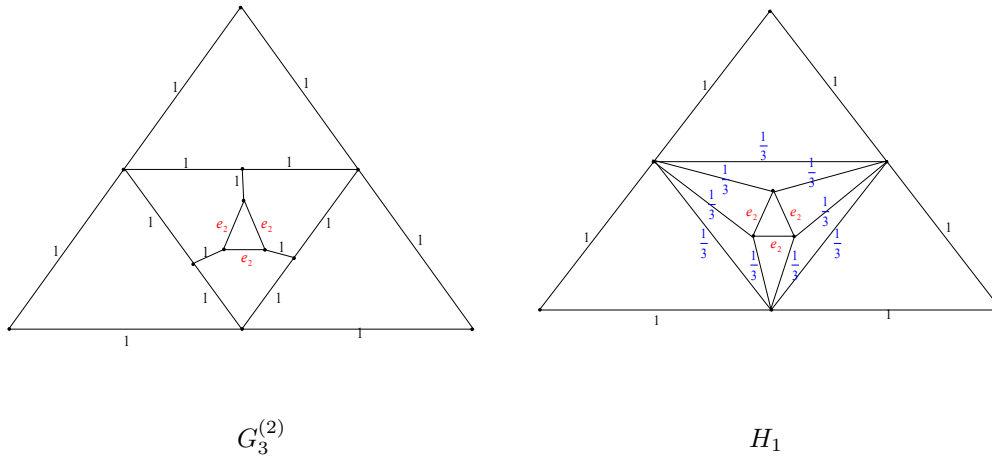


Figure 16

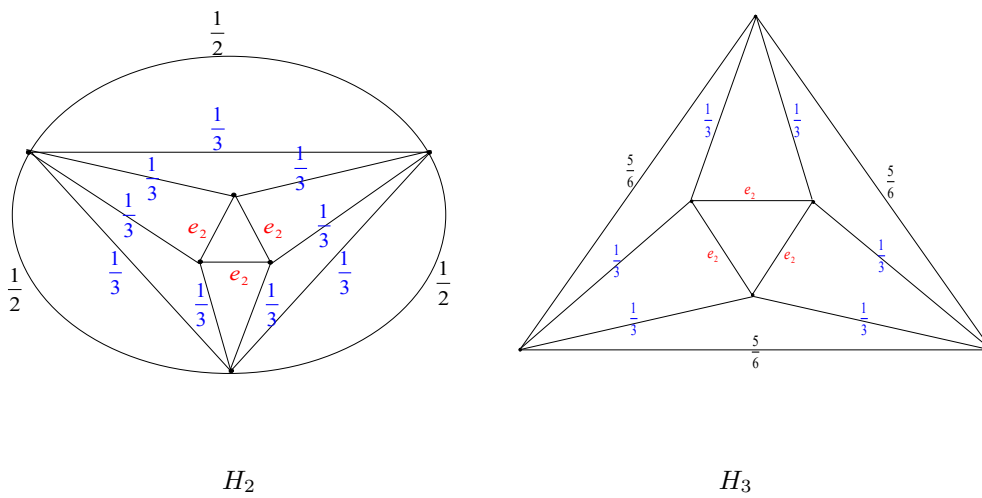


Figure 17

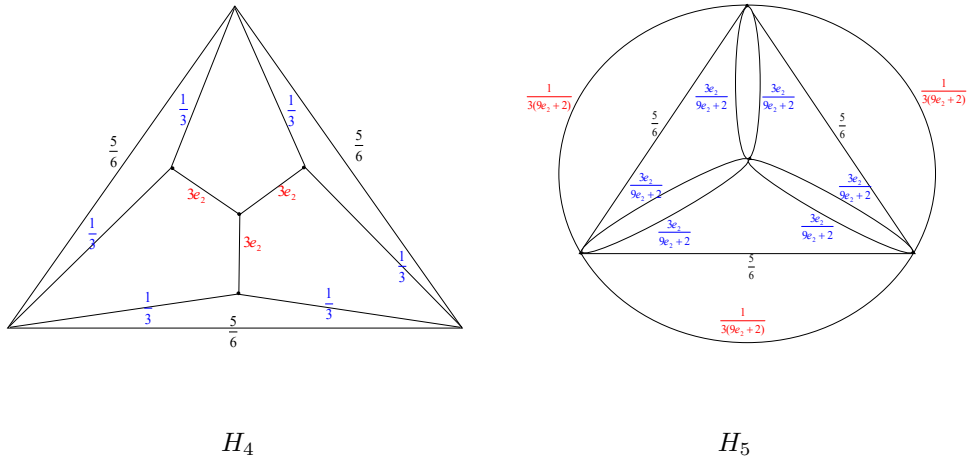


Figure 18

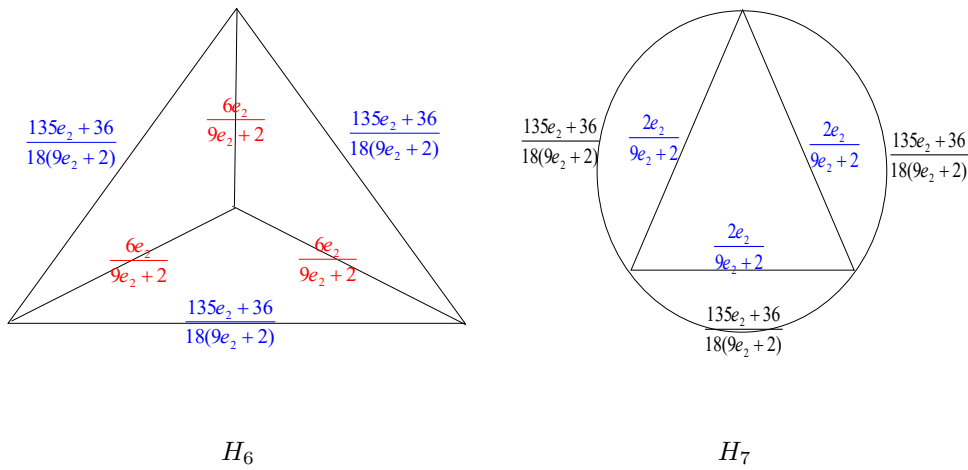


Figure 19

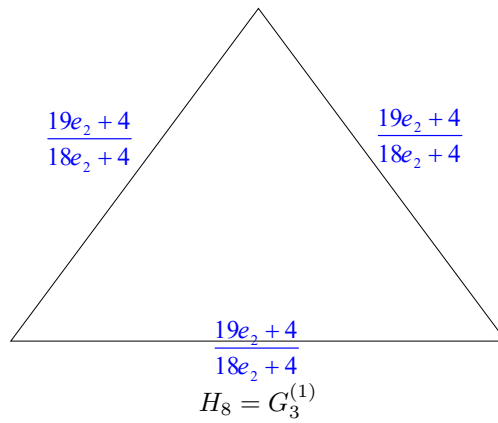


Figure 20

The following transformations result from using the attributes listed in Section 2.

$$\begin{aligned}\tau(H_1) &= \left[\frac{1}{3}\right]^3 \tau(G_3^{(2)}), \quad \tau(H_2) = \left[\frac{1}{2}\right]^3 \tau(H_1), \quad \tau(H_3) = \tau(H_2), \\ \tau(H_4) &= 9e_2\tau(H_3), \quad \tau(H_5) = \left[\frac{3}{9e_2+2}\right]^3 \tau(H_4), \quad \tau(H_6) = \tau(H_5), \\ \tau(H_7) &= \left[\frac{9e_2+2}{18e_2}\right] \tau(H_6) \quad \text{and} \quad \tau(G_3^{(1)}) = \tau(H_7).\end{aligned}$$

When these eight transformations are combined, we obtain

$$\tau(G_3^{(2)}) = 4(18e_2 + 4)^2 \tau(G_3^{(1)}). \quad (5.1)$$

Further,

$$\tau(G_3^{(n)}) = \prod_{i=2}^n 4(18e_i + 4)^2 \tau(G_3^{(1)}) = 3 \times 4^{n-1} e_1^2 \left[\prod_{i=2}^n (18e_i + 4) \right]^2, \quad (5.2)$$

where

$$e_{i-1} = \frac{19e_i + 4}{18e_i + 4}, \quad i = 2, 3, \dots, n.$$

Its characteristic equation is $18t^2 - 15t - 4 = 0$ with roots $t_1 = \frac{5-\sqrt{57}}{12}$ and $t_2 = \frac{5+\sqrt{57}}{12}$. Subtracting these two roots into both sides of $e_{i-1} = \frac{19e_i+4}{18e_i+4}$, we get

$$e_{i-1} - \frac{5 - \sqrt{57}}{12} = \frac{19e_i + 4}{18e_i + 4} - \frac{5 - \sqrt{57}}{12} = \frac{(23 + 3\sqrt{57})[e_i - \frac{5-\sqrt{57}}{12}]}{2(18e_i + 4)}, \quad (5.3)$$

$$e_{i-1} - \frac{5 + \sqrt{57}}{12} = \frac{19e_i + 4}{18e_i + 4} - \frac{5 + \sqrt{57}}{12} = \frac{(23 - 3\sqrt{57})[e_i - \frac{5+\sqrt{57}}{12}]}{2(18e_i + 4)}. \quad (5.4)$$

Let $x_i = \frac{e_{i-1} - \frac{5-\sqrt{57}}{12}}{e_{i-1} - \frac{5+\sqrt{57}}{12}}$ then by Eqs. (5.3) and (5.4), we get

$$x_{i-1} = \left(\frac{521 + 69\sqrt{57}}{8}\right)x_i \quad \text{and} \quad x_i = \left(\frac{521 + 69\sqrt{57}}{8}\right)^{n-i} x_n.$$

Therefore,

$$e_i = \frac{\left(\frac{521+69\sqrt{57}}{8}\right)^{n-i} \left(\frac{5+\sqrt{57}}{12}\right)x_n - \frac{5-\sqrt{57}}{12}}{\left(\frac{521+69\sqrt{57}}{8}\right)^{n-i} x_n - 1}.$$

Thus,

$$e_1 = \frac{\left(\frac{521+69\sqrt{57}}{8}\right)^{n-1} \left(\frac{5+\sqrt{57}}{12}\right)x_n - \frac{5-\sqrt{57}}{12}}{\left(\frac{521+69\sqrt{57}}{8}\right)^{n-1} x_n - 1}. \quad (5.5)$$

Using the expression $e_{n-1} = \frac{19e_n+4}{18e_n+4}$ and denoting the coefficients of $19e_n + 4$ and $18e_n + 4$

into Eq. (5.8), we obtain

$$\begin{aligned} \tau(G_3^{(n)}) = & 3 \times 4^{n-1} e_1^2 \left[\left(\frac{627 + 83\sqrt{57}}{57} \right) \left(\frac{23 + 3\sqrt{57}}{2} \right)^{n-2} \right. \\ & \left. + \left(\frac{627 - 83\sqrt{57}}{57} \right) \left(\frac{23 - 3\sqrt{57}}{2} \right)^{n-2} \right]^2 \end{aligned} \quad (5.11)$$

for integer $n \geq 2$. Notice that the Eq. (5.11) is satisfied for $n = 1$ and $\tau(G_3^{(1)}) = 3$. Thus, the number of spanning trees in the sequence of the graph $G_3^{(n)}$ is determined by

$$\begin{aligned} \tau(G_3^{(n)}) = & 3 \times 4^{n-1} e_1^2 \left[\left(\frac{627 + 83\sqrt{57}}{57} \right) \left(\frac{23 + 3\sqrt{57}}{2} \right)^{n-2} \right. \\ & \left. + \left(\frac{627 - 83\sqrt{57}}{57} \right) \left(\frac{23 - 3\sqrt{57}}{2} \right)^{n-2} \right]^2 \end{aligned} \quad (5.12)$$

for integer $n \geq 1$, where

$$e_1 = \frac{\left(\frac{521+69\sqrt{57}}{8}\right)^{n-1}(83 + 11\sqrt{57}) - \left(\frac{5-\sqrt{57}}{2}\right)}{\frac{3}{2}\left(\frac{521+69\sqrt{57}}{8}\right)^{n-1}(53 + 7\sqrt{57}) + 6}, \quad n \geq 1 \quad (5.13)$$

and the result is obtained by inserting Eq. (5.13) into Eq. (5.12). □

§6. Number of Spanning Trees in Sequences of $G_4^{(n)}$ Graphs

The graph $G_4^{(n)}$ is defined recursively using the graphs $G_4^{(1)}$ (triangle or K_3) and $G_4^{(2)}$ as shown in Figure 21. The graph $G_4^{(n)}$, $n = 3$ is obtained by replacing the central triangle in the graph $G_4^{(2)}$ by a copy of $G_4^{(2)}$. In general, the graph $G_4^{(n)}$ is obtained by replacing the central triangle in $G_4^{(n-1)}$ with $G_4^{(2)}$. According to this construction, the number of total vertices $|V(G_4^{(n)})|$ and edges $|E(G_4^{(n)})|$ are $|V(G_4^{(n)})| = 9n - 6$ and $|E(G_4^{(n)})| = 15n - 12, n = 1, 2, \dots$. The average degree of the graph $G_4^{(n)}$ in the large n limit $\frac{10}{3}$.

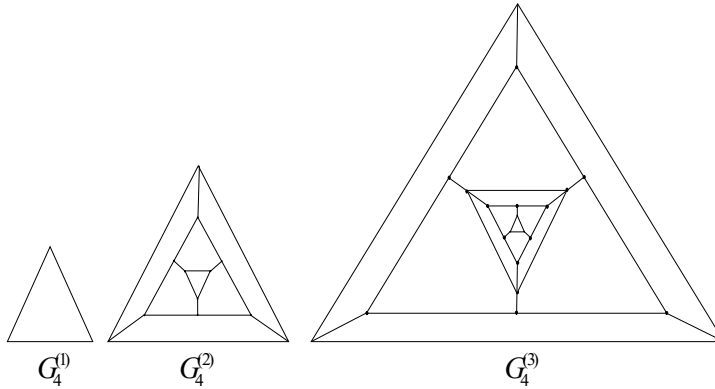


Figure 21. Some sequences of $G_4^{(n)}$ graph.

Theorem 6.1 For $n \geq 1$ the number of spanning trees in the sequence of $G_4^{(n)}$ is given by $\frac{A_3}{B_3}$, where

$$A_3 = 32^{-7+n} \left(2 \left(17 + 12\sqrt{2} \right)^n \left(58 + 41\sqrt{2} \right) - \left(17 - 12\sqrt{2} \right)^n \left(4756 + 3363\sqrt{2} \right) + \sqrt{2} \left(19601 + 13860\sqrt{2} \right)^n \right)^2,$$

$$B_3 = \left(577 + 408\sqrt{2} + \left(3 + 2\sqrt{2} \right) \left(577 + 408\sqrt{2} \right)^n \right)^2$$

Proof We convert $G_4^{(i)}$ to $G_4^{(i-1)}$ via the electrically equivalent transformation. The conversion procedure from $G_4^{(2)}$ to $G_4^{(1)}$ is shown in Figures 22-27.

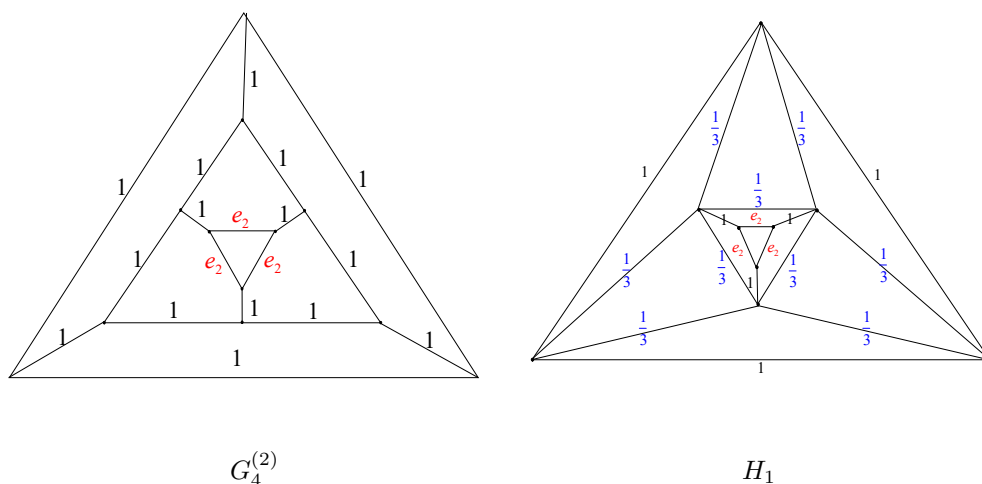


Figure 22

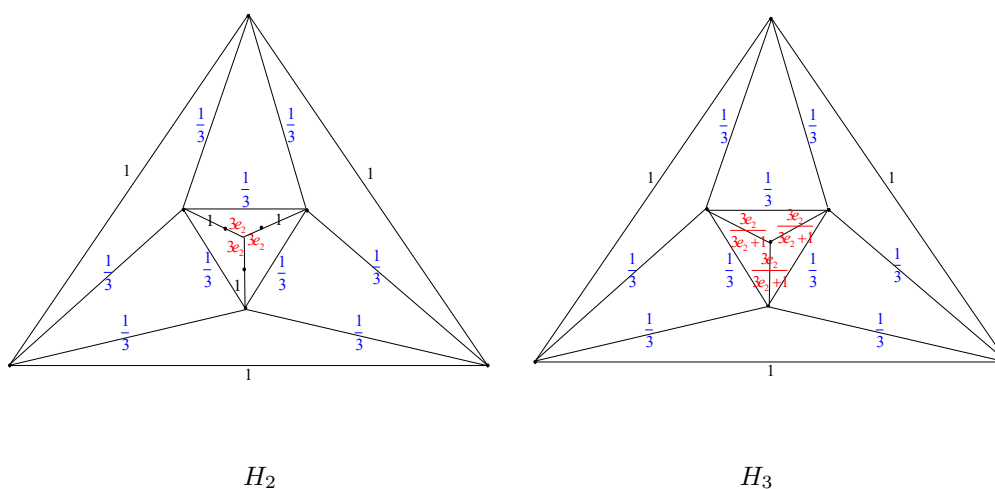


Figure 23

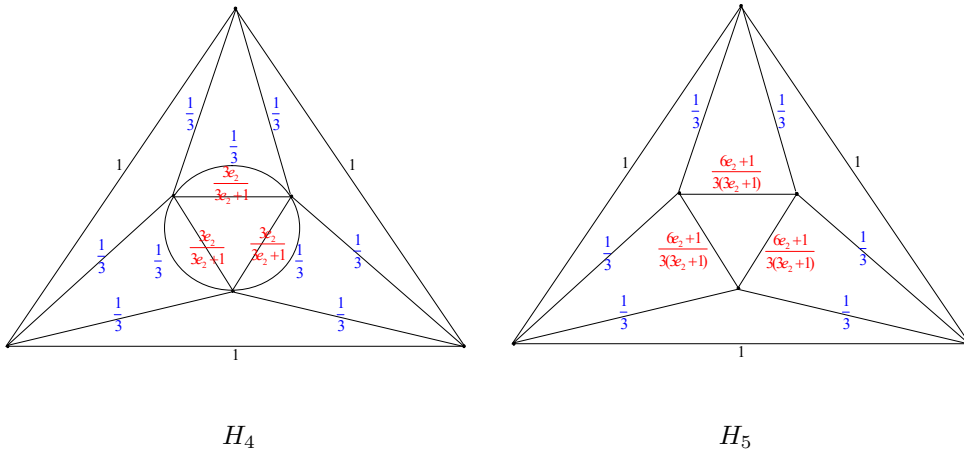


Figure 24

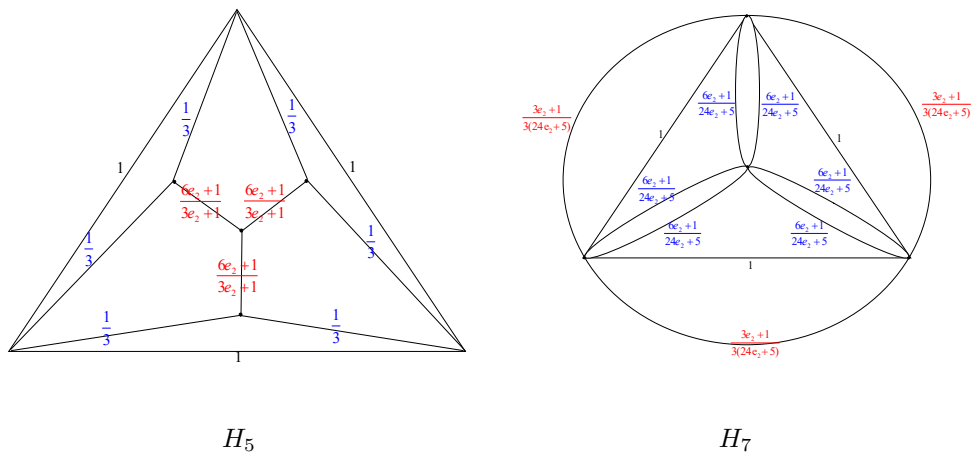


Figure 25

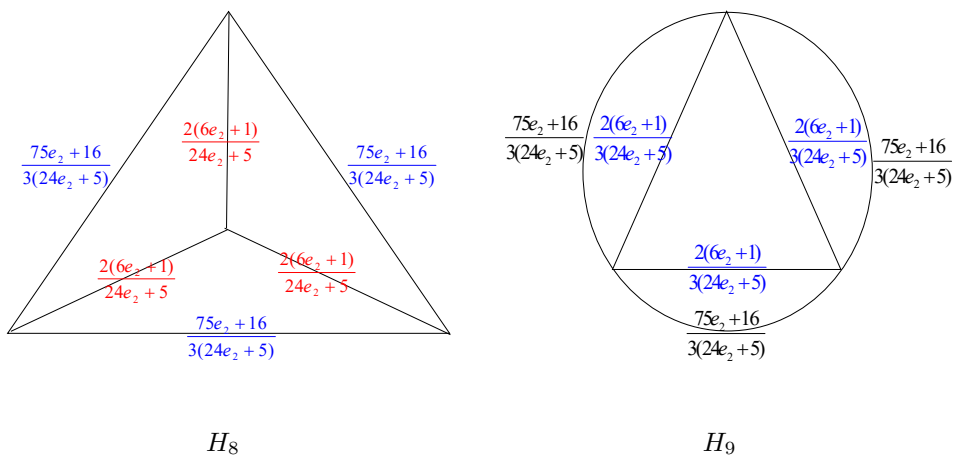


Figure 26

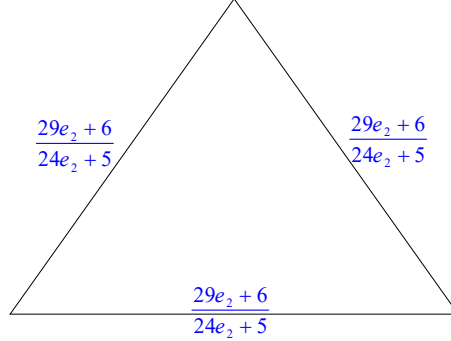


Figure 27. The transformations from $G_4^{(2)}$ to $G_4^{(1)}$

The following transformations result from using the attributes listed in Section 2.

$$\begin{aligned}\tau(H_1) &= \left[\frac{1}{3}\right]^3 \tau(G_4^{(2)}), \tau(H_2) = 9e_2\tau(H_1), \quad \tau(H_3) = \left[\frac{1}{3e_2 + 1}\right]^3 \tau(H_2), \\ \tau(H_4) &= \left[\frac{3e_2 + 1}{9e_2}\right] \tau(H_3), \quad \tau(H_5) = \tau(H_4), \\ \tau(H_6) &= \left[\frac{3(6e_2 + 1)}{3e_2 + 1}\right] \tau(H_5), \quad \tau(H_7) = \left[\frac{3(3e_2 + 1)}{24e_2 + 5}\right] \tau(H_6), \\ \tau(H_8) &= \tau(H_7), \quad \tau(H_9) = \left[\frac{24e_2 + 5}{6(6e_2 + 1)}\right] \tau(H_8) \quad \text{and} \quad \tau(G_4^{(1)}) = \tau(H_9).\end{aligned}$$

When these ten transformations are combined, we obtain

$$\tau(G_4^{(2)}) = 2(24e_2 + 5)^2 \tau(G_4^{(1)}). \quad (6.1)$$

and further

$$\tau(G_4^{(n)}) = \prod_{i=2}^n 2(24e_i + 5)^2 \tau(G_4^{(1)}) = 3 \times 2^{n-1} e_1^2 \left[\prod_{i=2}^n (24e_i + 5) \right]^2, \quad (6.2)$$

where $e_{i-1} = \frac{29e_i + 6}{24e_i + 5}$, $i = 2, 3, \dots, n$. Its characteristic equation is $4t^2 - 4t - 1 = 0$ with roots $t_1 = \frac{1-\sqrt{2}}{2}$ and $t_2 = \frac{1+\sqrt{2}}{2}$. Subtracting these two roots into both sides of $e_{i-1} = \frac{29e_i + 6}{24e_i + 5}$, we get

$$e_{i-1} - \frac{1 - \sqrt{2}}{2} = \frac{29e_i + 6}{24e_i + 5} - \frac{1 - \sqrt{2}}{2} = \frac{(17 + 12\sqrt{2})[e_i - \frac{1-\sqrt{2}}{2}]}{(24e_i + 5)}, \quad (6.3)$$

$$e_{i-1} - \frac{1 + \sqrt{2}}{2} = \frac{29e_i + 6}{24e_i + 5} - \frac{1 + \sqrt{2}}{2} = \frac{(17 - 12\sqrt{2})[e_i - \frac{1+\sqrt{2}}{2}]}{(24e_i + 5)}. \quad (6.4)$$

Let $x_i = \frac{e_{i-1} - \frac{1-\sqrt{2}}{2}}{e_{i-1} - \frac{1+\sqrt{2}}{2}}$. Then by Eq. (6.3) and (6.4) we get $x_{i-1} = (577 + 408\sqrt{2})x_i$ and $x_i = (577 + 408\sqrt{2})^{n-i} x_n$. Therefore,

$$e_i = \frac{(577 + 408\sqrt{2})^{n-i} \left(\frac{1+\sqrt{2}}{2}\right) x_n - \frac{1-\sqrt{2}}{2}}{(577 + 408\sqrt{2})^{n-i} x_n - 1}.$$

Thus

$$e_1 = \frac{(577 + 408\sqrt{2})^{n-1} \left(\frac{1+\sqrt{2}}{2}\right)x_n - \frac{1-\sqrt{2}}{2}}{(577 + 408\sqrt{2})^{n-1}x_n - 1}. \tag{6.5}$$

Using the expression $e_{n-1} = \frac{29e_n+6}{24e_n+5}$ and denoting the coefficients of $29e_n + 6$ and $24e_n + 5$ as h_n and k_n , we have

$$\begin{aligned} 24e_n + 5 &= h_0(29e_n + 6) + k_0(24e_n + 5), \\ 24e_{n-1} + 5 &= \frac{h_1(29e_n + 6) + k_1(24e_n + 5)}{h_0(29e_n + 6) + k_0(24e_n + 5)}, \\ 24e_{n-2} + 5 &= \frac{h_2(29e_n + 6) + k_2(24e_n + 5)}{h_1(29e_n + 6) + k_1(24e_n + 5)}, \\ &\dots \dots \dots, \\ 24e_{n-i} + 5 &= \frac{h_i(29e_n + 6) + k_i(24e_n + 5)}{h_{i-1}(29e_n + 6) + k_{i-1}(24e_n + 5)}, \end{aligned} \tag{6.6}$$

$$\begin{aligned} 24e_{n-(i+1)} + 5 &= \frac{h_{i+1}(29e_n + 6) + k_{i+1}(24e_n + 5)}{h_i(29e_n + 6) + k_i(24e_n + 5)}, \\ &\dots \dots \dots, \end{aligned} \tag{6.7}$$

$$24e_2 + 5 = \frac{h_{n-2}(29e_n + 6) + k_{n-2}(24e_n + 5)}{h_{n-3}(29e_n + 6) + k_{n-3}(24e_n + 5)}.$$

Thus, we obtain,

$$\tau(G_4^{(n)}) = 3 \times 2^{n-1} e_1^2 [h_{n-2}(29e_n + 6) + k_{n-2}(24e_n + 5)]^2, \tag{6.8}$$

where $h_0 = 0, k_0 = 1$ and $h_1 = 24, k_1 = 5$. By the expression

$$e_{n-1} = \frac{29e_n + 6}{24e_n + 5}$$

and using Eqs. (6.6) and (6.7), we have

$$h_{i+1} = 34h_i - h_{i-1}; k_{i+1} = 34k_i - k_{i-1}. \tag{6.9}$$

Notice that Eq. (6.9) has the characteristic equation $\beta^2 - 34\beta + 1 = 0$. Its roots are $u_1 = 17+12\sqrt{2}$ and $u_2 = 17-12\sqrt{2}$ with the general solutions $h_i = a_1u_1^i + a_2u_2^i$, $k_i = b_1u_1^i + b_2u_2^i$ of Eq. (6.9). Using the initial conditions $h_0 = 0, k_0 = 1$ and $h_1 = 24, k_1 = 5$, yields

$$\begin{aligned} h_i &= \frac{\sqrt{2}}{2}(17 + 12\sqrt{2})^i - \frac{\sqrt{2}}{2}(17 - 12\sqrt{2})^i, \\ k_i &= \left(\frac{2 - \sqrt{2}}{4}\right) (17 + 12\sqrt{2})^i + \left(\frac{2 + \sqrt{2}}{4}\right) (17 - 12\sqrt{2})^i. \end{aligned} \tag{6.10}$$

There is no electrically similar transition for $G_4^{(n)}$ if $e_n = 1$. When Eq. (6.10) is entered

into Eq. (6.8), we obtain

$$\begin{aligned} \tau(G_4^{(n)}) = & 3 \times 2^{n-1} e_1^2 \left[\left(\frac{58 + 41\sqrt{2}}{4} \right) (17 + 12\sqrt{2})^{n-2} \right. \\ & \left. + \left(\frac{58 - 41\sqrt{2}}{4} \right) (17 - 12\sqrt{2})^{n-2} \right]^2 \end{aligned} \quad (6.11)$$

for integer $n \geq 2$. Notice that Eq. (6.11) is satisfied for $n = 1$ and $\tau(G_4^{(1)}) = 3$. Thus, the number of spanning trees in the sequence of the graph $G_4^{(n)}$ is determined by

$$\begin{aligned} \tau(G_4^{(n)}) = & 3 \times 2^{n-1} e_1^2 \left[\left(\frac{58 + 41\sqrt{2}}{4} \right) (17 + 12\sqrt{2})^{n-2} \right. \\ & \left. + \left(\frac{58 - 41\sqrt{2}}{4} \right) (17 - 12\sqrt{2})^{n-2} \right]^2, \end{aligned} \quad (6.12)$$

for integer $n \geq 1$, where

$$e_1 = \frac{(577 + 408\sqrt{57})^{n-1} (7 + 5\sqrt{2}) + (1 - \sqrt{2})}{2(577 + 408\sqrt{57})^{n-1} (3 + 2\sqrt{2}) + 2}, \quad n \geq 1. \quad (6.13)$$

The result is obtained by inserting Eq. (6.13) into Eq. (6.12).

§7. Numerical Results

The values of number of spanning trees in graphs $G_1^{(n)}, G_2^{(n)}, G_3^{(n)}, G_4^{(n)}$ are shown in Table 1.

Table 1. Illustrates some values of the number of spanning trees in graphs $G_1^{(n)}, G_2^{(n)}, G_3^{(n)}, G_4^{(n)}$.

n	$G_1^{(n)}$	$G_2^{(n)}$	$G_3^{(n)}$	$G_4^{(n)}$
1	3	3	3	3
2	4800	5046	6348	7350
3	12929328	11642700	13230000	16964652
4	34857345792	26871324504	27569719488	39154389144
5	93975197203200	62018970370608	57451908926208	90368262289200
6	253356573941563392	143139676130037600	119722720360320000	208569792745923936

§8. Spanning Tree Entropy

After having explicit Formulas for the number of spanning trees of the sequence of the three families of graphs $G_1^{(n)}, G_2^{(n)}, G_3^{(n)}$ and $G_4^{(n)}$ we can calculate its spanning tree entropy \mathcal{Z} which is a finite number and a very interesting quantity characterizing the network structure, defined

as in [22]-[23] as for a graph G ,

$$Z(G) = \lim_{n \rightarrow \infty} \frac{\ln \tau(G)}{|V(G)|}. \quad (7.1)$$

Then,

$$\begin{aligned} Z(G_1^{(n)}) &= \frac{1}{9}(\ln[4] - 2\ln[337 + 52\sqrt{42}] + 2\ln[8749 + 1350\sqrt{42}]) = 0.8777246967, \\ Z(G_2^{(n)}) &= \frac{1}{9}(\ln[2] + 2\ln[17 + 12\sqrt{2}]) = 0.8604595419, \\ Z(G_3^{(n)}) &= \frac{2}{9}(\ln[23782 + 3150\sqrt{57}] - \ln[521 + 69\sqrt{57}]) = 0.8491094948, \\ Z(G_4^{(n)}) &= \frac{1}{9}(\ln[2] - 2\ln[577 + 408\sqrt{2}] + 2\ln[19601 + 13860\sqrt{2}]) = 0.8604595419. \end{aligned}$$

Now, we compare the value of entropy in our graphs with other graphs. It is clear that the entropy of the $G_1^{(n)}$ graph is greater than the other three graphs and the entropy of the $G_3^{(n)}$ graph is smaller than the other three graphs and $G_2^{(n)}$ and $G_4^{(n)}$ have the same entropy. In addition the entropy of our studied graphs $G_1^{(n)}$, $G_2^{(n)}$, $G_3^{(n)}$ and $G_4^{(n)}$ is smaller than the fractal scale free lattice [24] which has the entropy and two dimensional Sierpinski gasket [25] which has the entropy of the same average degree 4.

§9. Conclusions

In this work, we enumerate the number of spanning trees in the sequences of four sequences of graphs of average degree four based on some nono-hedral graphs using electrically equivalent transformations. An advantage of this method lies in the avoidance of laborious computation of Laplacian spectra that is needed for a generic method for determining spanning trees.

References

- [1] Stavros D. Nikolopoulos, Leonidas Palios and Charis Papadopoulos, Counting spanning trees using modular decomposition, *Theoretical Computer Science*, 2014, Volume 526, Pages 41-57.
- [2] Durbar Maji, Ganesh Ghorai and YaeUlrich Gaba, On the reformulated second Zagreb index of graph operations, *Journal of Chemistry*, Volume 2021, Article ID 9289534, 17 pages <https://doi.org/10.1155/2021/9289534>.
- [3] Srebrenka Letina, Tessa F. Blanken, Marie K. Deserno and Denny Borsboom, Expanding network analysis tools in psychological networks: Minimal spanning trees, participation coefficients, and motif analysis applied to a network of 26 psychological attributes, *Complexity*, Volume 2019 — Article ID 9424605 — <https://doi.org/10.1155/2019/9424605>.
- [4] F. Zhang and X. Yong, Asymptotic enumeration theorems for the number of spanning trees and Eulerian trail in circular digraphs and graphs, *Sci. China*, Ser. A43(2)264-271(1999).
- [5] H.S. Zhang et al, On the number of spanning trees and Eulerian torus in iterated line digraph, *Discrete App. Math.*, 73 (1997), 59-67.

- [6] D. L. Applegate, R. E. V. Bixby, Chvátal, and W. J. Cook, *The Traveling Salesman Problem: A Computational Study*, Princeton University Press, (2006).
- [7] T. Atajan and H. Inaba, Network reliability analysis by counting the number of spanning trees, ISGIT 2004, *IEEE International Symposium on Communication and Information Technology*, 1 (2004) 601-604.
- [8] Petru Caşcaval, Approximate method to evaluate reliability of complex networks, *Complexity*, Volume 2018 — Article ID 5967604 — <https://doi.org/10.1155/2018/5967604>.
- [9] G. G. Kirchhoff, Über die Auflösung der Gleichungen auf welche man bei der Untersucher der linearen Verteilung galvanischer Ströme geföhrt wird, *Ann. Phg. Chem.*, 72 (1847), 497-508.
- [10] A. K. Kelmans and V. M. Chelnokov, A certain polynomial of a graph and graphs with an extremal number of trees, *Journal of Combinatorial Theory B*, Vol. 16(1974), 197C214.
- [11] N.L. Biggs, *Algebraic Graph Theory* (2nd Edn.), Cambridge Univ. Press, Cambridge, (1993) pp: 205.
- [12] S. N. Daoud, The deletion-contraction method for counting the number of spanning trees of graphs, *European Journal of Physical Plus*, Vol.130, No. 10, Oct. (2015), 1-14.
- [13] S. N. Daoud, Complexity of graphs generated by wheel graph and their asymptotic limits, *Journal of the Egyptian Math. Soc.*, Vol.25, Issue 4, October (2017), 424-433.
- [14] S. N. Daoud, Generating formulas of the number of spanning trees of some special graphs, *Eur. Phys. J. Plus*, Vol. 129 (2014), 1-14.
- [15] S. N. Daoud, Number of spanning trees in different product of complete and complete tripartite graphs, *Ars Combinatoria*, Vol. 139 (2018), 85-103.
- [16] Jia-Bao Liu and S. N. Daoud, Complexity of some of pyramid graphs created from a gear graph., *Symmetry*, 2018, 10, 689; doi:10.3390/sym10120689.
- [17] S. N. Daoud, Number of spanning trees of cartesian and composition products of graphs and Chebyshev polynomials, *IEEE Access.*, Vol.7 (2019), 71142 C 71157.
- [18] Teuff E., Wagner S., Determinant identities for Laplace matrices, *Linear Algebra Appl.*, 432,(2010), 441-457.
- [19] S. N. Daoud, Number of spanning Trees in the sequence of some Nonahedral graphs, *Utilitas Mathematica*, Vol. 115 (2020), 1-18.
- [20] S. N. Daoud and Wedad Saleha, Complexity trees of the sequence of some nonahedral graphs generated by triangle, *Heliyon*, 6(9) Sep (2020).
- [21] Jia-Bao Liu and S. N. Daoud, Number of spanning trees in the sequence of some graphs, *Complexity*, Volume 2019 — Article ID 4271783 — <https://doi.org/10.1155/2019/4271783>.
- [22] F.Y. Wu, Number of spanning trees on a lattice, *J. Phys. A: Math. Gen.*, 10 (1977), 113C115.
- [23] R. Lyons, Asymptotic enumeration of spanning trees, *Combin. Probab. Comput.*, 14 (2005) 491C522.
- [24] Z. Zhang, H. Liu., Wu B., Zou T., Spanning trees in a fractal scale Cfree lattice, *Phys. Rev. E*, 83(2011), 016116.
- [25] S. Chang, L. Chen, W. Yang, Spanning trees on the Sierpinski gasket, *J. Stat. Phys.*, 126 (2007), 649-667.

Common Fixed Point Results for Interpolative Reich–Rus–Ćirić–Meir–Keeler Contractions

Jaynendra Shrivastava*

Department of Mathematics, Govt. V.Y.T. PG Autonomous College, Durg (C.G.), 491001, India

Rohit Kumar Verma

Department of Mathematics, Govt Chandulal Chandrakar Arts and Science College
Patan, Dist.- Durg (C.G.), 491111, India

E-mail: jayshrivas95@gmail.com, rohitverma1967@rediffmail.com

Abstract: In this paper, we introduce a new class of interpolative Reich–Rus–Ćirić–Meir–Keeler pair contractions and establish common fixed point results in complete metric spaces. These results generalize and unify several known fixed point theorems in the literature. An application to a nonlinear integral equation is also provided to demonstrate the usability of the obtained results.

Key Words: Metric space, interpolative Reich–Rus–Ćirić contraction, Meir–Keeler condition, common fixed point, nonlinear integral equation.

AMS(2010): 47H10, 54H25.

§1. Introduction

The study of fixed point theorems has long been a central theme in nonlinear analysis due to its wide-ranging applications in integral and differential equations, optimization, and dynamic systems. A foundational result in this area is the Banach Contraction Principle [1], which ensures the existence and uniqueness of fixed points for contractive self-mappings in complete metric spaces. Over the decades, this classical theorem has been generalized in various directions to accommodate more complex nonlinear structures.

One such direction was initiated by Reich [8, 9], who relaxed the strict contraction requirement, followed by Rus [11, 12], who introduced generalized contractive conditions involving control functions and modified distance expressions. Simultaneously, the contribution of Meir and Keeler [7] introduced a dynamic contractive condition through a control function, enabling a more nuanced view of convergence behavior. Further developments by Ćirić enriched this landscape by incorporating multi-term conditions that compare multiple distances among points and their images.

In recent years, there has been growing interest in synthesizing these diverse contraction

¹Received August 28, 2025. Accepted November 20, 2025

^{2*} Corresponding author

principles into unified frameworks using interpolative techniques. These approaches have proven especially powerful in extending classical results while maintaining generality and applicability.

Motivated by this synthesis-based perspective, the present work introduces a new class of contractive pairs, namely the *interpolative Reich–Rus–Ćirić–Meir–Keeler-type contractions*. These contractions merge the essential features of several well-established contraction schemes and offer a unified structure that encompasses a wide range of fixed point results.

Our main contributions are as follows:

- We introduce a new contractive framework involving two self-maps that interpolate between Reich-type, Rus-type, Ćirić-type, and Meir–Keeler-type conditions.
- We establish fixed point theorems for such pairs in complete metric spaces and prove the existence and uniqueness of common fixed points under suitable conditions.
- We demonstrate, through examples, that our results properly generalize and extend several classical theorems.
- As an application, we explore a class of nonlinear integral equations and show how the developed fixed point results guarantee the existence of solutions.

The proposed results not only advance the theory of fixed points in metric spaces but also provide new tools for tackling nonlinear equations with complex contractive structures.

§2. Preliminaries

We begin by outlining key definitions and foundational results relevant to our study.

Definition 2.1([7]) *Let (X, d) be a complete metric space. A mapping $\mathfrak{T}: X \rightarrow X$ is said to be a Meir–Keeler contraction on X , if for every $\epsilon > 0$, there exists $\delta > 0$ such that*

$$\epsilon \leq d(a, b) < \epsilon + \delta \implies d(\mathfrak{T}a, \mathfrak{T}b) < \epsilon, \quad \forall a, b \in X. \quad (2.1)$$

We call (2.1) the Meir–Keeler contraction.

Theorem 2.2([7]) *On a complete metric space (X, d) , any Meir–Keeler contraction $\mathfrak{T}: X \rightarrow X$ has a unique fixed point.*

Definition 2.3([4]) *Let (X, d) be a complete metric space. A mapping $\mathfrak{T}: X \rightarrow X$ is said to be an interpolative Kannan type contraction on X , if there exist $\mu \in [0, 1)$ and $\alpha \in (0, 1)$ such that*

$$d(\mathfrak{T}a, \mathfrak{T}b) \leq \mu [d(a, \mathfrak{T}a)]^\alpha [d(b, \mathfrak{T}b)]^{1-\alpha}, \quad (2.2)$$

for every $a, b \in X \setminus \text{Fix}(\mathfrak{T})$, where $\text{Fix}(\mathfrak{T}) = \{a \in X \mid \mathfrak{T}a = a\}$.

Theorem 2.4([4]) *On a complete metric space (X, d) , any interpolative Kannan-contraction $\mathfrak{T}: X \rightarrow X$ has a fixed point.*

Definition 2.5([5]) *Let (X, d) be a complete metric space. A mapping $\mathfrak{T}: X \rightarrow X$ is said to be an interpolative Kannan–Meir–Keeler type contraction on X , if there exist $\mu \in [0, 1)$ such that*

for every $a, b \in X \setminus \text{Fix}(\mathfrak{T})$ we have

(1) Given $\epsilon > 0$, there exists $\delta > 0$ so that

$$\epsilon < [d(a, \mathfrak{T}a)]^\alpha [d(b, \mathfrak{T}b)]^{1-\alpha} < \epsilon + \delta \implies d(\mathfrak{T}a, \mathfrak{T}b) \leq \epsilon, \quad (2.3)$$

(2) There is

$$d(\mathfrak{T}a, \mathfrak{T}b) \leq \mu [d(a, \mathfrak{T}a)]^\alpha [d(b, \mathfrak{T}b)]^{1-\alpha}. \quad (2.4)$$

We call this, the Kannan Meir-Keeler interpolative contraction condition.

Theorem 2.6([5]) *On a complete metric space (X, d) , any generalized interpolative Kannan-Meir-Keeler type contraction $\mathfrak{T}: X \rightarrow X$ has a fixed point.*

The following theorem, independently established by Reich, Rus, and Ćirić [8, 9, 10, 11, 12], serves to unify and extend the classical fixed point results of Banach and Kannan [1, 2].

Theorem 2.7 *Let (X, d) be a complete metric space. Let $\mathfrak{T}: X \rightarrow X$ be a given mapping such that*

$$d(\mathfrak{T}a, \mathfrak{T}b) \leq \mu [d(a, b) + d(a, \mathfrak{T}a) + d(b, \mathfrak{T}b)],$$

for all $a, b \in X$, where $\mu \in [0, \frac{1}{3})$. Then, \mathfrak{T} has a unique fixed point in X .

Notice that several variations of the Reich contraction condition (2.7) can be formulated. One may state the following general forms or modifications

$$d(\mathfrak{T}a, \mathfrak{T}b) \leq \alpha d(a, b) + \beta d(a, \mathfrak{T}a) + \gamma d(b, \mathfrak{T}b),$$

for all $a, b \in X$, where α, β, γ are non-negative reals such that $\alpha + \beta + \gamma < 1$.

Inspired by the above theorem, Karapınar, Ravi Agarwal and Hassen Aydi [6] introduced the concept of interpolative Reich-Rus-Ćirić-type contractions.

Definition 2.8([6]) *Let (X, d) be a metric space. We say that the self-mapping $\mathfrak{T}: X \rightarrow X$ is an interpolative Reich-Rus-Ćirić type contraction if there exists $\mu \in [0, 1)$ and $\alpha, \beta, \gamma \in (0, 1)$ with $\alpha + \beta < 1$, such that*

$$d(\mathfrak{T}a, \mathfrak{T}b) \leq \mu [d(a, b)]^\beta [d(a, \mathfrak{T}a)]^\alpha [d(b, \mathfrak{T}b)]^{1-\alpha-\beta},$$

for all $a, b \in X \setminus \text{Fix}(\mathfrak{T})$.

Theorem 2.9([6]) *Let (X, d) be a complete metric space and $\mathfrak{T}: X \rightarrow X$ be an interpolative Reich-Rus-Ćirić type contraction. Then, \mathfrak{T} has a fixed point in X .*

This paper introduces a new class of interpolative Reich-Rus-Ćirić-Meir-Keeler-type contractions involving a pair of self-mappings and provides illustrative examples to support the theoretical findings.

§3. Main Results

Definition 3.1 Let (X, d) be a metric space. Two self-mappings $\mathfrak{T}, \mathfrak{S}: X \rightarrow X$ are said to form an interpolative Reich-Rus-Ćirić type contraction pair if there exist constants $\mu \in [0, 1)$ and $\alpha, \beta \in (0, 1)$ with $\alpha + \beta < 1$, such that for all $a, b \in X \setminus (\text{Fix}(\mathfrak{T}) \cap \text{Fix}(\mathfrak{S}))$, the following inequality holds

$$d(\mathfrak{T}a, \mathfrak{S}b) \leq \mu [d(a, b)]^\beta [d(a, \mathfrak{T}a)]^\alpha [d(b, \mathfrak{S}b)]^{1-\alpha-\beta}. \quad (3.1)$$

Theorem 3.2 Let (X, d) be a complete metric space and let $\mathfrak{T}, \mathfrak{S}: X \rightarrow X$ be two self-mappings that form an interpolative Reich-Rus-Ćirić type contraction pair. Then, \mathfrak{T} and \mathfrak{S} have a common fixed point in X .

Proof Let $a_0 \in X$ be arbitrary. Define a sequence $\{a_n\}_{n=0}^\infty$ in X by the rule:

$$a_{n+1} = \mathfrak{T}a_n \quad \text{for all } n \in \mathbb{N}.$$

Suppose there exists $n_0 \in \mathbb{N}$ such that $a_{n_0} = a_{n_0+1} = \mathfrak{T}a_{n_0}$. Then, $a_{n_0} \in \text{Fix}(\mathfrak{T})$. If further $a_{n_0} = \mathfrak{S}a_{n_0}$, then $a_{n_0} \in \text{Fix}(\mathfrak{T}) \cap \text{Fix}(\mathfrak{S})$ and the proof is complete.

Now suppose that $a_n \neq a_{n+1}$ for all $n \in \mathbb{N}$. We apply the contractive condition (3.1) to the pair $a = a_n$ and $b = a_{n-1}$:

$$d(\mathfrak{T}a_n, \mathfrak{S}a_{n-1}) \leq \mu [d(a_n, a_{n-1})]^\beta [d(a_n, \mathfrak{T}a_n)]^\alpha [d(a_{n-1}, \mathfrak{S}a_{n-1})]^{1-\alpha-\beta}.$$

But by construction, we have

$$a_{n+1} = \mathfrak{T}a_n, \quad a_n = \mathfrak{S}a_{n-1}, \quad \text{so that } d(\mathfrak{T}a_n, \mathfrak{S}a_{n-1}) = d(a_{n+1}, a_n).$$

Substituting back, we obtain

$$d(a_{n+1}, a_n) \leq \mu [d(a_n, a_{n-1})]^\beta [d(a_n, a_{n+1})]^\alpha [d(a_{n-1}, a_n)]^{1-\alpha-\beta}.$$

Combining the powers on the right-hand side:

$$[d(a_{n+1}, a_n)]^{1-\alpha} \leq \mu [d(a_{n-1}, a_n)]^{1-\alpha}.$$

Since $0 < \alpha < 1$, we can take $(1 - \alpha)$ -th root on both sides

$$d(a_{n+1}, a_n) \leq \mu^{\frac{1}{1-\alpha}} d(a_{n-1}, a_n).$$

Using recursive application of this inequality, we obtain

$$\begin{aligned} d(a_{n+1}, a_n) &\leq \mu^{\frac{1}{1-\alpha}} d(a_n, a_{n-1}) \\ &\leq \mu^{\frac{1+1}{1-\alpha}} d(a_{n-1}, a_{n-2}) \leq \cdots \leq \mu^{\frac{n}{1-\alpha}} d(a_1, a_0). \end{aligned}$$

Since $0 < \mu < 1$, this implies

$$\lim_{n \rightarrow \infty} d(a_{n+1}, a_n) = 0.$$

To show $\{a_n\}$ is Cauchy, for any $r \in \mathbb{N}$, we estimate

$$\begin{aligned} d(a_n, a_{n+r}) &\leq \sum_{k=0}^{r-1} d(a_{n+k}, a_{n+k+1}) \\ &\leq d(a_1, a_0) \sum_{k=0}^{r-1} \mu^{\frac{n+k}{1-\alpha}} = \mu^{\frac{n}{1-\alpha}} d(a_1, a_0) \sum_{k=0}^{r-1} \mu^{\frac{k}{1-\alpha}}. \end{aligned}$$

The geometric sum $\sum_{k=0}^{\infty} \mu^{\frac{k}{1-\alpha}}$ is convergent, so,

$$d(a_n, a_{n+r}) \leq C \cdot \mu^{\frac{n}{1-\alpha}}, \quad \text{for some } C > 0.$$

Hence, $\lim_{n \rightarrow \infty} d(a_n, a_{n+r}) = 0$ for each fixed r , and so $\{a_n\}$ is a Cauchy sequence.

Since (X, d) is complete, there exists $a^* \in X$ such that

$$\lim_{n \rightarrow \infty} a_n = a^*.$$

Now, we prove that a^* is a common fixed point of \mathfrak{T} and \mathfrak{S} .

Assume, for contradiction, that $a^* \neq \mathfrak{T}a^*$. Then $d(a^*, \mathfrak{T}a^*) > 0$. Applying (3.1) to the pair $a = a_n$ and $b = a^*$, we get

$$d(\mathfrak{T}a_n, \mathfrak{S}a^*) \leq \mu [d(a_n, a^*)]^\beta [d(a_n, \mathfrak{T}a_n)]^\alpha [d(a^*, \mathfrak{S}a^*)]^{1-\alpha-\beta}.$$

Denoting $A_n = d(a_{n+1}, \mathfrak{S}a^*)$, $B_n = d(a_n, a_{n+1})$, we rewrite

$$A_n \leq \mu A_n^\beta B_n^\alpha [d(a^*, \mathfrak{S}a^*)]^{1-\alpha-\beta}.$$

Dividing both sides by A_n^β (for large n where $A_n > 0$), we obtain

$$A_n^{1-\beta} \leq \mu B_n^\alpha [d(a^*, \mathfrak{S}a^*)]^{1-\alpha-\beta}.$$

Letting $n \rightarrow \infty$, we find $B_n \rightarrow 0$, so $A_n \rightarrow 0$. Hence,

$$\lim_{n \rightarrow \infty} d(a_{n+1}, \mathfrak{S}a^*) = 0 \quad \Rightarrow \quad \mathfrak{S}a^* = a^*.$$

Since $a_{n+1} = \mathfrak{T}a_n$ and $a_n \rightarrow a^*$, we also get:

$$\lim_{n \rightarrow \infty} a_{n+1} = \mathfrak{T}a^* = a^*.$$

Therefore, $a^* \in \text{Fix}(\mathfrak{T}) \cap \text{Fix}(\mathfrak{S})$. This completes the proof. \square

Definition 3.3 Let (X, d) be a metric space. We say that two self-mappings $\mathfrak{T}, \mathfrak{S}: X \rightarrow X$ form

an interpolative Reich-Rus-Ćirić-Meir-Keeler type contraction pair if there exists $\mu \in [0, 1)$ and $\alpha, \beta \in (0, 1)$ with $\alpha + \beta < 1$ such that for all $a, b \in X \setminus \text{Fix}(\mathfrak{T}) \cap \text{Fix}(\mathfrak{S})$,

(1) Given $\epsilon > 0$, there exists $\delta > 0$ such that

$$\epsilon < \mu[d(a, b)]^\beta [d(a, \mathfrak{T}a)]^\alpha [d(b, \mathfrak{S}b)]^{1-\alpha-\beta} < \epsilon + \delta \implies d(\mathfrak{T}a, \mathfrak{S}b) \leq \epsilon, \quad (3.2)$$

(2) There is

$$d(\mathfrak{T}a, \mathfrak{S}b) \leq \mu[d(a, b)]^\beta [d(a, \mathfrak{T}a)]^\alpha [d(b, \mathfrak{S}b)]^{1-\alpha-\beta}. \quad (3.3)$$

Theorem 3.4 Let (X, d) be a complete metric space. Suppose that $\mathfrak{T}, \mathfrak{S}: X \rightarrow X$ satisfy the interpolative Reich-Rus-Ćirić-Meir-Keeler type contraction conditions as defined above. Then, \mathfrak{T} and \mathfrak{S} have a unique common fixed point in X .

Proof Let $a_0 \in X$ be arbitrary. Define a sequence $\{a_n\}$ recursively by

$$a_{2n+1} = \mathfrak{T}(a_{2n}), \quad a_{2n+2} = \mathfrak{S}(a_{2n+1}) \quad \text{for all } n \geq 0.$$

Assume $a_n \neq a_{n+1}$ for all $n \in \mathbb{N}$. Otherwise, if $a_n = a_{n+1}$ for some n , then a_n is a common fixed point of both \mathfrak{T} and \mathfrak{S} , and the proof is complete.

We now show that the sequence $\{a_n\}$ is Cauchy. From the construction

$$a_{2n+1} = \mathfrak{T}(a_{2n}), \quad a_{2n+2} = \mathfrak{S}(a_{2n+1}),$$

apply the contractive condition (3.3) to the pair (a_{2n}, a_{2n+1}) by

$$\begin{aligned} d(a_{2n+2}, a_{2n+1}) &= d(\mathfrak{S}a_{2n+1}, \mathfrak{T}a_{2n}) \\ &\leq \mu[d(a_{2n}, a_{2n+1})]^\beta [d(a_{2n}, \mathfrak{T}a_{2n})]^\alpha [d(a_{2n+1}, \mathfrak{S}a_{2n+1})]^{1-\alpha-\beta} \\ &= \mu[d(a_{2n}, a_{2n+1})]^\beta [d(a_{2n}, a_{2n+1})]^\alpha [d(a_{2n+1}, a_{2n+2})]^{1-\alpha-\beta}. \end{aligned}$$

Rewriting, we get

$$d(a_{2n+2}, a_{2n+1}) \leq \mu[d(a_{2n}, a_{2n+1})]^{\alpha+\beta} [d(a_{2n+2}, a_{2n+1})]^{1-\alpha-\beta}.$$

Dividing both sides by $[d(a_{2n+2}, a_{2n+1})]^{1-\alpha-\beta}$ (note: positive as $a_n \neq a_{n+1}$), we get

$$d(a_{2n+2}, a_{2n+1})^{\alpha+\beta} \leq \mu[d(a_{2n}, a_{2n+1})]^{\alpha+\beta}. \quad (3.4)$$

Since $\mu \in [0, 1)$ and $\alpha + \beta > 0$, the sequence $\{d(a_{2n}, a_{2n+1})^{\alpha+\beta}\}$ is decreasing and converges to 0. Hence,

$$\lim_{n \rightarrow \infty} d(a_n, a_{n+1}) = 0.$$

We now prove that $\{a_n\}$ is a Cauchy sequence. For $m > n$, consider

$$d(a_n, a_m) \leq \sum_{k=n}^{m-1} d(a_k, a_{k+1}).$$

As $d(a_k, a_{k+1}) \rightarrow 0$, this implies that $\{a_n\}$ is Cauchy. Since (X, d) is complete, there exists $a^* \in X$ such that

$$\lim_{n \rightarrow \infty} a_n = a^*.$$

We now show that a^* is a common fixed point. From the construction

$$a_{2n+1} = \mathfrak{T}(a_{2n}), \quad a_{2n+1} \rightarrow a^*, \quad a_{2n} \rightarrow a^* \quad \Rightarrow \mathfrak{T}(a^*) = a^*.$$

,

$$a_{2n+2} = \mathfrak{S}(a_{2n+1}), \quad a_{2n+1} \rightarrow a^*, \quad a_{2n+2} \rightarrow a^* \quad \Rightarrow \mathfrak{S}(a^*) = a^*.$$

Thus, a^* is a common fixed point of both \mathfrak{T} and \mathfrak{S} .

To prove uniqueness, suppose $u, v \in X$ are two distinct common fixed points, i.e., $\mathfrak{T}u = u$ and $\mathfrak{S}v = v$. Then, from condition (3.3) we have

$$\begin{aligned} d(u, v) &= d(\mathfrak{T}u, \mathfrak{S}v) \\ &\leq \mu[d(u, v)]^\beta [d(u, \mathfrak{T}u)]^\alpha [d(v, \mathfrak{S}v)]^{1-\alpha-\beta} \\ &= \mu[d(u, v)]^\beta \cdot 0^\alpha \cdot 0^{1-\alpha-\beta} = 0, \end{aligned}$$

which implies $d(u, v) = 0$, i.e., $u = v$. Hence, the common fixed point is unique. \square

§4. Numerical Example

Example 4.1 Let (X, d) be the real line \mathbb{R} with the usual metric $d(x, y) = |x - y|$, which is a complete metric space. Define the self-mappings $\mathfrak{T}, \mathfrak{S}: \mathbb{R} \rightarrow \mathbb{R}$ by

$$\mathfrak{T}(x) = \frac{x}{4}, \quad \mathfrak{S}(x) = \frac{x}{6}.$$

- First, we observe that both mappings are contractions. Moreover, $\mathfrak{T}(x) = x$ and $\mathfrak{S}(x) = x$ imply $x = 0$ is the unique common fixed point, i.e.,

$$\text{Fix}(\mathfrak{T}) \cap \text{Fix}(\mathfrak{S}) = \{0\}.$$

- Let $\mu = \frac{3}{4}$, $\alpha = \beta = \frac{1}{4}$, so that $\alpha + \beta = \frac{1}{2} < 1$. We show that the pair $(\mathfrak{T}, \mathfrak{S})$ satisfies the interpolative Reich–Rus–Ćirić–Meir–Keeler type contraction condition.

For any $a, b \in \mathbb{R} \setminus \{0\}$, we compute

$$d(\mathfrak{T}a, \mathfrak{S}b) = \left| \frac{a}{4} - \frac{b}{6} \right| = \left| \frac{3a - 2b}{12} \right|,$$

$$d(a, \mathfrak{T}a) = \left| a - \frac{a}{4} \right| = \frac{3|a|}{4}, \quad d(b, \mathfrak{S}b) = \left| b - \frac{b}{6} \right| = \frac{5|b|}{6},$$

$$d(a, b) = |a - b|.$$

The right-hand side of the inequality from Definition 3.3 (inequality (3.3)) is

$$\mu \cdot [d(a, b)]^\beta \cdot [d(a, \mathfrak{T}a)]^\alpha \cdot [d(b, \mathfrak{S}b)]^{1-\alpha-\beta} = \frac{3}{4} \cdot |a - b|^{1/4} \cdot \left(\frac{3|a|}{4} \right)^{1/4} \cdot \left(\frac{5|b|}{6} \right)^{1/2}.$$

As $|a|, |b|$ vary, it is easy to verify numerically or analytically that

$$d(\mathfrak{T}a, \mathfrak{S}b) \leq \mu \cdot [d(a, b)]^\beta \cdot [d(a, \mathfrak{T}a)]^\alpha \cdot [d(b, \mathfrak{S}b)]^{1-\alpha-\beta},$$

and also the implication form of the inequality (condition (1)) is satisfied due to continuity of the involved expressions.

- Next, we verify that \mathfrak{T} and \mathfrak{S} each satisfy the Meir-Keeler condition.

For $\mathfrak{T}(x) = \frac{x}{4}$, we have

$$d(\mathfrak{T}x, \mathfrak{T}y) = \left| \frac{x}{4} - \frac{y}{4} \right| = \frac{1}{4}|x - y| = \frac{1}{4}d(x, y).$$

Given $\varepsilon > 0$, choose $\delta = 3\varepsilon$. Then, for all x, y with $\varepsilon < d(x, y) < \varepsilon + \delta$,

$$d(\mathfrak{T}x, \mathfrak{T}y) = \frac{1}{4}d(x, y) < \frac{1}{4}(\varepsilon + \delta) = \frac{1}{4}(4\varepsilon) = \varepsilon.$$

Thus, \mathfrak{T} satisfies the Meir-Keeler condition. Similarly, $\mathfrak{S}(x) = \frac{x}{6}$ satisfies

$$d(\mathfrak{S}x, \mathfrak{S}y) = \frac{1}{6}d(x, y),$$

and choosing $\delta = 5\varepsilon$ ensures

$$d(\mathfrak{S}x, \mathfrak{S}y) < \frac{1}{6}(\varepsilon + \delta) = \frac{1}{6}(6\varepsilon) = \varepsilon.$$

- Therefore, both \mathfrak{T} and \mathfrak{S} satisfy the Meir-Keeler condition, and the pair $(\mathfrak{T}, \mathfrak{S})$ satisfies the interpolative Reich-Rus-Ćirić -Meir-Keeler type contraction conditions.

By Theorem 3.4, \mathfrak{T} and \mathfrak{S} have a unique common fixed point in \mathbb{R} , namely,

$$\mathfrak{T}(0) = 0 = \mathfrak{S}(0).$$

§5. Application to Nonlinear Integral Equations

In this section, we demonstrate how the fixed point theorem for interpolative Reich-Rus-Ćirić -Meir-Keeler type contraction pairs can be applied to prove the existence and uniqueness of a

solution to a class of nonlinear integral equations.

Consider the nonlinear integral equation of the Volterra–Hammerstein type

$$u(t) = \int_0^t K(t, s)f(s, u(s)) ds, \quad t \in [0, 1], \quad (5.1)$$

where $K : [0, 1] \times [0, 1] \rightarrow \mathbb{R}$ is a continuous kernel and $f : [0, 1] \times \mathbb{R} \rightarrow \mathbb{R}$ is a continuous nonlinearity.

Let $X := C([0, 1], \mathbb{R})$ be the Banach space of real-valued continuous functions on $[0, 1]$ equipped with the supremum norm

$$d(u, v) := \|u - v\|_\infty = \sup_{t \in [0, 1]} |u(t) - v(t)|.$$

Define two self-mappings $\mathfrak{T}, \mathfrak{S} : X \rightarrow X$ by

$$(\mathfrak{T}u)(t) := \int_0^t K(t, s)f(s, u(s)) ds, \quad (\mathfrak{S}u)(t) := \int_0^t K(t, s)f(s, u(t)) ds.$$

Assume that the following conditions hold

(A1) The kernel $K(t, s)$ is continuous and satisfies $|K(t, s)| \leq M$ for all $t, s \in [0, 1]$, for some $M > 0$.

(A2) The function $f(t, x)$ satisfies a generalized Hölder condition: there exist constants $L > 0$ and $\gamma \in (0, 1)$ such that

$$|f(t, x) - f(t, y)| \leq L|x - y|^\gamma, \quad \forall t \in [0, 1], x, y \in \mathbb{R}.$$

(A3) The parameters $\mu \in [0, 1]$, $\alpha, \beta \in (0, 1)$ satisfy $\alpha + \beta < 1$ and

$$\mu := ML < 1.$$

Now, we verify the interpolative condition. Let $u, v \in X$. Then we have

$$\begin{aligned} d(\mathfrak{T}u, \mathfrak{S}v) &= \sup_{t \in [0, 1]} \left| \int_0^t K(t, s) [f(s, u(s)) - f(s, v(t))] ds \right| \\ &\leq \sup_{t \in [0, 1]} \int_0^t |K(t, s)| \cdot |f(s, u(s)) - f(s, v(t))| ds \\ &\leq M \int_0^1 L \cdot |u(s) - v(t)|^\gamma ds \leq ML \cdot \|u - v\|^\gamma = \mu \cdot [d(u, v)]^\gamma. \end{aligned}$$

To obtain the full interpolative structure, note

$$d(\mathfrak{T}u, \mathfrak{S}v) \leq \mu \cdot [d(u, v)]^\beta \cdot [d(u, \mathfrak{T}u)]^\alpha \cdot [d(v, \mathfrak{S}v)]^{1-\alpha-\beta}$$

for suitable values of μ, α, β satisfying $\mu = ML < 1$, $\alpha + \beta < 1$. Moreover, the continuity of f and K ensures that the Meir–Keeler condition is satisfied due to the smooth behavior of the

modulus of continuity.

Hence, by Theorem 3.4, the mappings \mathfrak{T} and \mathfrak{S} have a unique common fixed point in X , which is a unique solution of the integral equation (5.1).

Example 5.1 Let us consider

$$K(t, s) = ts, \quad f(s, x) = \frac{x}{1+x^2}, \quad \text{for } t, s \in [0, 1], \quad x \in \mathbb{R}.$$

Then,

$$|K(t, s)| \leq 1 \cdot 1 = 1, \quad \text{so } M = 1.$$

For $f(s, x) = \frac{x}{1+x^2}$, we compute

$$|f(s, x) - f(s, y)| \leq |x - y|^\gamma, \quad \text{with } \gamma = \frac{1}{2}, \quad \text{and } L = 1.$$

Thus, the Hölder condition is satisfied, and we can choose $\mu = ML = 1 \cdot 1 = 1$, but for contraction we need $\mu < 1$. So, slightly modify

$$f(s, x) = \frac{1}{2} \cdot \frac{x}{1+x^2}, \quad \Rightarrow L = \frac{1}{2}, \quad \mu = \frac{1}{2} < 1.$$

Then, all assumptions are satisfied with

$$\alpha = \frac{1}{4}, \quad \beta = \frac{1}{2}, \quad \alpha + \beta = \frac{3}{4} < 1.$$

Hence, the integral equation

$$u(t) = \int_0^t ts \cdot \frac{u(s)}{2(1+u(s)^2)} ds,$$

has a unique solution in $C([0, 1], \mathbb{R})$ by our theorem.

By Theorem 3.4, we conclude that the mappings \mathfrak{T} and \mathfrak{S} have a unique common fixed point in $C[0, 1]$. Therefore, the boundary value problem has a unique solution $u^* \in C[0, 1]$ which satisfies

$$u^*(t) = \lambda \int_0^1 G(t, s) \frac{1}{1+(u^*(s))^2} ds = \lambda \int_0^1 G(t, s) e^{-(u^*(s))^2} ds.$$

This illustrates the effectiveness of the fixed point approach for establishing the existence and uniqueness of solutions to nonlinear differential equations.

§6. Conclusion

This paper introduced common fixed point results for interpolative Reich–Rus–Ćirić–Meir–Keeler type contraction pairs in complete metric spaces. The results generalize several known theorems and were supported by illustrative examples. An application to nonlinear integral

equations demonstrated the usefulness of the theory. These findings open potential directions for further research in generalized metric settings and applications.

References

- [1] S. Banach, Sur les opérations dans les ensembles abstraits et leur application aux équations intégrales, *Fund. Math.*, 3 (1922), 133–181.
- [2] R. Kannan, Some results on fixed points, *Bull. Calcutta Math. Soc.*, 60 (1968), 71–76.
- [3] R. Kannan, Some results on fixed points II, *Amer. Math. Monthly*, 76 (1969), 405–408.
- [4] E. Karapınar, Revisiting the Kannan type contractions via interpolation, *Adv. Theor. Nonlinear Anal. Appl.*, 2 (2018), no. 2, 85–87.
- [5] E. Karapınar, Interpolative Kannan–Meir–Keeler type contraction, *Adv. Theor. Nonlinear Anal. Appl.*, 5 (2021), No.4, 611–614.
- [6] E. Karapınar, O. Alqahtani and H. Aydi, Interpolative Reich–Rus–Ćirić type contractions on partial metric spaces, *Mathematics*, 11 (2018), no. 6, 256.
- [7] A. Meir and E. Keeler, A theorem on contraction mappings, *J. Math. Anal. Appl.*, 28 (1969), 326–329.
- [8] S. Reich, Some remarks concerning contraction mappings, *Canad. Math. Bull.*, 14 (1971), 121–124.
- [9] S. Reich, Fixed point of contractive functions, *Boll. Unione Mat. Ital.*, 4 (1972), 26–42.
- [10] S. Reich, Kannan’s fixed point theorem, *Boll. Unione Mat. Ital.*, 4 (1971), 1–11.
- [11] I. A. Rus, *Principles and Applications of the Fixed Point Theory*, Editura Dacia, Cluj-Napoca, Romania, 1979.
- [12] I. A. Rus, *Generalized Contractions and Applications*, Cluj University Press, Cluj-Napoca, Romania, 2001.

Group Divisible Designs $(5, n, n + 1, 4; \lambda_1, \lambda_2)$

Didas Ngabirano*, Kasifa Namyalo and Olivia Nabawanda

(Department of Mathematics, Faculty of Science, Mbarara University of Science and Technology, Uganda)

E-mail: didasngabirano2014@gmail.com

Abstract: In this paper, we present new results on group divisible designs (GDDs) of block size four on three groups of different sizes $n_1 = 5$, $n_2 = n$ and $n_3 = n + 1$ where $n \geq 5$ with indices λ_1 and λ_2 . Here, we first establish necessary conditions for the existence of $\text{GDD}(5, n, n + 1, 4; \lambda_1, \lambda_2)$ using relationships between parameters of the GDD. Secondly, we prove that these conditions are sufficient for several families of the GDDs and later give a general construction where parameters satisfy all the necessary conditions.

Key Words: Blocks, balanced incomplete block designs, group divisible designs.

AMS(2010): 05B05.

§1. Introduction

The arrangements of numbers in different patterns have a long history which dates back to the eighteenth and nineteenth centuries such as in the works of Euler, Kirkman, Cayley, Hamilton, Sylvester, Moore and others [9]. Such arrangements generally are called designs. Design theory is categorized into three designs that is combinatorial, algebraic and algorithmic also called computational. Combinatorial design theory is a branch of mathematics which deals with the study of existence, construction and properties of finite sets whose arrangements satisfy concepts of balance and symmetry [9]. For example equality of the size of the subsets and equality of occurrence of a particular element or pair of distinct elements may be needed. In combinatorial design theory, balanced incomplete block designs (BIBDs), pairwise balanced designs (PBDs), latin squares, and group divisible designs (GDDs) has been regarded as the most studied areas in mathematics with many designs [3]. Group divisible designs have been studied for their usefulness in statistics [1] and there are important applications in construction of other types of combinatorial designs such as packings and frames [2] and moreover, are also applicable to designs of different sizes (that is non-uniform GDDs) that are used to fit in various situations [2]. Unfortunately, comparing with uniform GDDs, much less is known on the construction of non-uniform ones. One major reason is that no appropriate algebraic or geometric structures have been found for the construction. In this research, focus shall be put on group divisible designs with block size four solving the problem when the design has three groups of different sizes.

¹Received August 22, 2025. Accepted November 24, 2025

^{2*} Corresponding author

Definition 1.1 A group divisible design-GDD $(n, m, k, \lambda_1, \lambda_2)$ is a collection of k -element subsets, called blocks, of an nm set (V -set), where the elements of V are partitioned into m subsets (called groups) of size n each; each point of V appearing in $r = \frac{\lambda_1(n-1) + \lambda_2 n(m-1)}{(k-1)}$ blocks, and $b = \frac{nmr}{k}$ blocks.

A GDD with parameters $(n_1 + n_2 + n_3, k; \lambda_1, \lambda_2)$ has three groups of different sizes n_1, n_2 and n_3 . For example, the GDD $(1+2+n, 3; \lambda_1, \lambda_2)$ [6], GDD $(1+1+n, 3; 1, \lambda_2)$ [4], GDD $(1, n, n+1, 4; \lambda_1, \lambda_2)$, GDD $(2, n, n+1, 4; \lambda_1, \lambda_2)$, GDD $(3, n, n+1, 4; \lambda_1, \lambda_2)$ [7], and GDD $(4, n, n+1, 4; \lambda_1, \lambda_2)$ [7] have been studied. Though, there are many parameter sets where the answer to the existence of particular designs is not yet known [11]. For this reason therefore, this research paper intends to study and establish the necessary conditions for the existence of GDD $(5, n, n+1, 4; \lambda_1, \lambda_2)$ when $n_1 = 5, n_2 = n$ and $n_3 = n+1$ when $\lambda_1 \equiv 0 \pmod{3}$, and $\lambda_2 \equiv 0 \pmod{6}$ where $\lambda_1 = 3t$ for all $t \geq 1$ using relationships between parameters of the GDD. Secondly, we prove that these conditions are sufficient for several families of the GDDs and later give a general construction where parameters satisfy all the necessary conditions.

Example 1.1 A GDD $(3, 3, 4, 3, 1)$ has a pair of elements from the same group occurs together in three blocks and a pair of elements from different groups occurs together in one block, that is if $V = \{1, 2, 3, 4, 5, 6, 7, 8, 9\}$, $G_1 = \{1, 2, 3\}$, $G_2 = \{4, 5, 6\}$, and $G_3 = \{7, 8, 9\}$ and the blocks $\{1, 2, 3, 4\}, \{1, 2, 3, 5\}, \{1, 2, 3, 6\}, \{4, 5, 6, 7\}, \{4, 5, 6, 8\}, \{4, 5, 6, 9\}, \{7, 8, 9, 1\}, \{7, 8, 9, 2\}$ and $\{7, 8, 9, 3\}$.

Theorem 1.1([5]) If $n \equiv 0, 4 \pmod{6}$, then there exists a minimal odd GDD $(n, 3, 4; 2n, n-1)$. If $n \equiv 2 \pmod{6}$, then there exists a minimal odd GDD $(n, 3, 4; 6n, 3(n-1))$.

Proof For $n \equiv 0, 4 \pmod{6}$ there exists a BIBD $(n, 3, 2)$ with replication number $n-1$. Use the size three blocks from n copies of such a design based on the n points of group 1 to fill three of the spaces of a size four block. Fill in the fourth place with, say, point x_1 from group 2. Do this for every point from group 2 using the n copies of the BIBD. This puts each point of Group 1 in a block with every other group-mate $2n$ times, and $\lambda_1 = 2n$. Now, using n copies of a BIBD $(n, 3, 2)$ based on group 2, fill in with the points from Group 3. Using n copies of a BIBD $(n, 3, 2)$ on group 3, fill in with the points from group 1. This creates the desired GDD. When $n \equiv 2 \pmod{6}$, there exists a BIBD $(n, 3, 6)$ with replication number $3(n-1)$. Repeat the previous construction for this n . \square

Lemma 1.1([8]) Relationship between the parameters of a BIBD (v, b, r, k, λ) . In a BIBD (v, b, r, k, λ) , the parameters must satisfy the necessary conditions.

- (i) $\lambda(v-1) = r(k-1)$;
- (ii) A (v, k, λ) has exactly $vr = k \times b$, implies $b = \frac{vr}{k}$.

Theorem 2.2([8]) In a (v, k, λ) BIBD,

- (i) Every point occurs in exactly $r = \frac{\lambda(v-1)}{(k-1)}$ blocks;
- (ii) There are $b = \frac{vr}{k} = \frac{\lambda v(v-1)}{k(k-1)}$.

Corollary 1.1([8]) If a (v, k, λ) BIBD exists, then $\lambda(v-1) \equiv 0 \pmod{k-1}$ and $\lambda v(v-1) \equiv 0$

$(\text{mod } k(k-1))$.

§2. Results on the Existence of GDD $(5, n, n+1, 4; \lambda_1, \lambda_2)$

Here, we establish and prove that the necessary conditions for the existence of group divisible design-GDD $(5, n, n+1, 4; \lambda_1, \lambda_2)$ exist as well as giving its general construction.

2.1. Parameters of the GDD $(5, n, n+1, 4; \lambda_1, \lambda_2)$

For GDD $(5, n, n+1, 4; \lambda_1, \lambda_2)$ with block size four and three groups of different sizes $5, n$ and $n+1$, has replication numbers, r_i for $i = 1, 2, 3$ are from $r_1 = \frac{4\lambda_1 + (2n+1)\lambda_2}{3}$, $r_2 = \frac{(n-1)\lambda_1 + (n+6)\lambda_2}{3}$ and $r_3 = \frac{n\lambda_1 + (n+5)\lambda_2}{3}$. The GDD has $(n^2+10)\lambda_1$ first associate pairs and $(n^2+11n+5)\lambda_2$ second associate pairs.

2.2. Necessary Conditions for the GDD $(5, n, n+1, 4; \lambda_1, \lambda_2)$

- (i) $4\lambda_1 + (2n+1)\lambda_2 \equiv 0 \pmod{3}$ and $(2n+1)\lambda_2 \equiv 0 \pmod{3}$;
- (ii) $(n-1)\lambda_1 + (n+6)\lambda_2 \equiv 0 \pmod{3}$;
- (iii) $n\lambda_1 + (n+5)\lambda_2 \equiv 0 \pmod{3}$;
- (iv) $(n^2+10)\lambda_1 + (n^2+11n+5)\lambda_2 \equiv 0 \pmod{6}$.

§3. Main Results

Theorem 3.1 *A GDD $(5, n, n+1, 4; \lambda_1, \lambda_2)$ exists if the necessary condition $4\lambda_1 + (2n+1)\lambda_2 \equiv 0 \pmod{3}$ and $(2n+1)\lambda_2 \equiv 0 \pmod{3}$ holds.*

Proof By counting the replication numbers r_i for elements of the i^{th} group, the replication number for elements in G_1 is obtained from $r_1 = \frac{4\lambda_1 + (2n+1)\lambda_2}{3}$. Since r_1 is a positive integer, then $4\lambda_1 + (2n+1)\lambda_2 \equiv 0 \pmod{3}$. Again $3|4\lambda_1$ remains and for the case of $3|(2n+1)\lambda_2$, gives $(2n+1)\lambda_2 \equiv 0 \pmod{3}$. Now, consider the parameters of the GDD $(v, g, m, k; \lambda_1, \lambda_2)$ where block size $k = 4$, group size $g = n$ and number of groups $m = n+1$, let us proceed with the proof. Assuming that a GDD $(5, n, n+1, 4; \lambda_1, \lambda_2)$ exists, then the design has the following parameters: block size $k = 4$, group size $g = n$, number of groups $m = n+1$, total number of elements $V = gm = n(n+1)$ together with indices λ_1 , and λ_2 . Consider an arbitrary element x in the GDD. let r be the number of blocks containing x . Now, let us consider the possible values of $n \pmod{3}$.

Case 1. $n \equiv 0 \pmod{3}$.

The first congruence becomes $(0-1)\lambda_1 + 0^2\lambda_2 \equiv -\lambda_1 \equiv 0$ and this implies $\lambda_1 \equiv 0 \pmod{3}$. The second congruence becomes: $\lambda_1 + (2(0)+1)\lambda_2 \equiv 0 + \lambda_2 \equiv \lambda_2 \pmod{3}$. Since $\lambda_1 \equiv 0$, from $3r = (n-1)\lambda_1 + n^2\lambda_2$, we have $3r = (-1)(0) + (0)\lambda_2 = 0$, which gives no direction constraint on λ_2 . However, for the GDD to exist, the parameters must be consistent.

Case 2. $n \equiv 1 \pmod{3}$.

The first congruence becomes $(1 - 1)\lambda_1 + 1^2\lambda_2 \equiv 0\lambda_1 + \lambda_2 \equiv \lambda_2 \equiv 0 \pmod{3}$. The second congruence becomes: $\lambda_1 + (2(1) + 1)\lambda_2 \equiv \lambda_1 + 3\lambda_2 \equiv \lambda_1 + 0\lambda_2 \equiv \lambda_1 \pmod{3}$. From $3r = (n - 1)\lambda_1 + n^2\lambda_2$, we have $3r \equiv (0)\lambda_1 + 1\lambda_2$. Since $3r \equiv 0 \pmod{3}$, then $\lambda_2 \equiv 0 \pmod{3}$ which is consistent and thus $\lambda_1 \equiv 0 \pmod{3}$.

Case 3. $n \equiv 2 \pmod{3}$.

The first congruence becomes $(2 - 1)\lambda_1 + 2^2\lambda_2 \equiv \lambda_1 + 4\lambda_2 \equiv \lambda_1 + \lambda_2 \equiv 0$. This implies $\lambda_1 \equiv -\lambda_2 \equiv 2\lambda_2 \pmod{3}$. The second congruence becomes: $\lambda_1 + (2(2) + 1)\lambda_2 \equiv \lambda_1 + 5\lambda_2 \equiv \lambda_1 + 2\lambda_2 \pmod{3}$. Now, substituting $\lambda_1 \equiv 2\lambda_2$, we get $2\lambda_2 + 2\lambda_2 \equiv 4\lambda_2 \equiv \lambda_2 \pmod{3}$. From $3r = (n - 1)\lambda_1 + n^2\lambda_2$, we have $3r \equiv (1)\lambda_1 + (1)\lambda_2 \equiv \lambda_1 + \lambda_2$. Since $3r \equiv 0$, $\lambda_1 + \lambda_2 \equiv 0$, which is consistent with $\lambda_1 \equiv -\lambda_2 \pmod{3}$. Thus, $\lambda_2 \equiv 0 \pmod{3}$, which implies $\lambda_1 \equiv 0 \pmod{3}$ and this satisfies the necessary condition. \square

Remark 3.1 *In all cases, the condition $(n - 1)\lambda_1 + 2^2\lambda_2 \equiv 0 \pmod{3}$ and this leads to $\lambda_1 + (2n + 1)\lambda_2 \equiv 0 \pmod{3}$ which gives the necessary condition $4\lambda_1 + (2n + 1)\lambda_2 \equiv 0 \pmod{3}$ and $(2n + 1)\lambda_2 \equiv 0 \pmod{3}$.*

Theorem 3.2 *A GDD $(5, n, n + 1, 4; \lambda_1, \lambda_2)$ exists if the necessary condition $(n - 1)\lambda_1 + (n + 6)\lambda_2 \equiv 0 \pmod{3}$ holds.*

Proof The replication number for elements in G_2 is obtained from $r_2 = \frac{(n-1)\lambda_1 + (6+n)\lambda_2}{3}$. Since r_2 is a positive integer, then $(n - 1)\lambda_1 + (6 + n)\lambda_2 \equiv 0 \pmod{3}$. First, we prove that the necessary conditions for the GDD $(5, n, n + 1, 4; \lambda_2, \lambda_2)$ exists. Let $V = n(n + 1)$ be the total number of elements. Let b be the number of blocks. We derive the necessary conditions by considering the counting of pairs. Counting pairs involving a specific element: Consider an arbitrary element x which belongs to one group of size $n + 1$. Within its group, there are n other elements. Each pair involving x and another element in the same group appears in λ_1 blocks. There are $n - 1$ other groups, each of size $n + 1$. So, there are $(n - 1)(n + 1)$ elements in the other groups. Each pair involving x and an element from a different group appears in λ_2 blocks. Now, let us count how many times x appears in all the blocks. Let r be the number of blocks containing x . Each block has size 4, so counting the pairs involve x in two ways, i.e.,

$$\begin{aligned} (4 - 1)r &= (n)\lambda_1 + (n - 1)(n + 1)\lambda_2, \\ 3r &= (n)\lambda_1 + (n^2 - 1)\lambda_2. \end{aligned} \tag{1}$$

Since the total number of pairs is $\binom{n(n+1)}{2}$ and each block contains $\binom{4}{2} = 6$ pairs, we also relate the total number of pairs to λ_1 and λ_2 , i.e.,

$$\begin{aligned} b\binom{4}{2} &= n\binom{n+1}{2}\lambda_1 + \binom{n}{2}(n+1)^2\lambda_2, \\ 6b &= n\left(\frac{(n+1)n}{2}\lambda_1\right) + \frac{n(n-1)(n+1)^2}{2}\lambda_2, \\ 12b &= n^2(n+1)\lambda_1 + n(n-1)(n+1)^2\lambda_2 \end{aligned} \tag{2}$$

Also, by counting the total number of elements in all blocks, we have $4b = vr = n(n + 1)r$,

so $b = \frac{n(n+1)r}{4}$, substituting this into

$$12\frac{n(n+1)r}{4} = n^2(n+1)\lambda_1 + n(n-1)(n+1)^2\lambda_2, \quad (3)$$

i.e.,

$$3nr(n+1) = n^2(n+1)\lambda_1 + n(n-1)(n+1)^2\lambda_2.$$

Dividing it by $n(n+1)$ (assuming $n \geq 1$), we get

$$3r = n\lambda_1 + (n-1)(n+1)\lambda_2 = n\lambda_1 + (n^2-1)\lambda_2.$$

However, this is consistent with equation (1). Now, let us look at the modular conditions. The proof involves counting arguments modulo 3, considering the number of blocks and the nature of the design. The condition $(n-1)\lambda_1 + (n+6)\lambda_2 \equiv 0 \pmod{3}$ can be re-written as $(n-1)\lambda_1 + n\lambda_2 \equiv 0 \pmod{3}$ (since $6 \equiv 0 \pmod{3}$). Given $\lambda_1 \equiv 0 \pmod{3}$, this simplifies to $n\lambda_1 \equiv 0 \pmod{3}$. From the second derived condition $(2n+1)\lambda_2 \equiv (-n+1)\lambda_2 \equiv 0 \pmod{3}$. If the $\gcd(-n+1, n) = \gcd(-n+1+n, n) = \gcd(1, n) = 1$, then we must have $\lambda_2 \equiv 0 \pmod{3}$, which satisfies $n\lambda_2 \equiv 0 \pmod{3}$. If the $\gcd(-n+1, n) \neq 1$, then $n \equiv 1 \pmod{3}$. In this case, $(-n+1)\lambda_2 \equiv 0 \pmod{3}$, and the second condition is satisfied regardless of λ_2 . The first condition becomes: $(1)\lambda_2 \equiv \lambda_2 \equiv 0 \pmod{3}$, so $n\lambda_2 \equiv 1 \cdot 0 \equiv 0 \pmod{3}$. Thus, the necessary condition $(n-1)\lambda_1 + (n+6)\lambda_2 \equiv 0 \pmod{3}$ hold. \square

Theorem 3.3 *A GDD $(5, n, n+1, 4; \lambda_1, \lambda_2)$ exists if the necessary condition $n\lambda_1 + (5+n)\lambda_2 \equiv 0 \pmod{3}$ holds.*

Proof The replication number for elements in G_3 is obtained from $r_3 = \frac{n\lambda_1 + (5+n)\lambda_2}{3}$. Since r_3 is a positive integer, then $n\lambda_1 + (5+n)\lambda_2 \equiv 0 \pmod{3}$. For a GDD $(5, n, n+1, 4; \lambda_1, \lambda_1)$, we have the fundamental equations: $3r = (n)\lambda_1 + (n^2-1)\lambda_2$ and $12b = n^2(n+1)\lambda_1 + n(n-1)(n+1)^2\lambda_2$ and the derived necessary modular condition: $4\lambda_1 + (2n+1)\lambda_2 \equiv 0 \pmod{3}$ and this implies $\lambda_1 + (2n+1)\lambda_2 \equiv 0 \pmod{3}$ which gives $(2n+1)\lambda_2 \equiv 0 \pmod{3}$. From these, we deduce that $\lambda_1 \equiv 0 \pmod{3}$. Now, we want to show that $n\lambda_1 + (5+n)\lambda_2 \equiv 0 \pmod{3}$ must hold. This condition simplifies to

$$n\lambda_1 + (2+n)\lambda_2 \equiv 0 \pmod{3}. \quad (*)$$

Substituting $\lambda_1 \equiv 0 \pmod{3}$ into (*), gives $n(0) + (2+n)\lambda_2 \equiv 0 \pmod{3}$ and this yields

$$(2+n)\lambda_2 \equiv 0 \pmod{3}. \quad (**)$$

Now, let us consider the second derived modular in necessary condition one $(2n+1)\lambda_2 \equiv 0 \pmod{3}$, which is equivalent to $(-n+1)\lambda_2 \equiv 0 \pmod{3}$. We have two congruences involving λ_2 : $(n+2)\lambda_2 \equiv 0 \pmod{3}$ and $(-n+1)\lambda_2 \equiv 0 \pmod{3}$. Adding these two congruences gives $(n+2)\lambda_2 + (-n+1)\lambda_2 \equiv 0 + 0 \pmod{3}$ and this gives $3\lambda_2 \equiv 0 \pmod{3}$ and this implies $0 \equiv 0 \pmod{3}$. This does not directly give information about n or λ_2 . Now, let us consider

the possible values of $n \pmod{3}$.

Case 1. $n \equiv 0 \pmod{3}$.

From (**), $(2 + 0)\lambda_2 \equiv 2\lambda_2 \equiv 0 \pmod{3}$ and this implies $\lambda_2 \equiv 0 \pmod{3}$. The target condition (*) becomes: $0(0) + (2 + 0)(0) \equiv 0 \pmod{3}$, which holds.

Case 2. $n \equiv 1 \pmod{3}$.

From (**), $(2 + 1)\lambda_2 \equiv 3\lambda_2 \equiv 0 \pmod{3}$. This gives no information about λ_2 . Now, from second derived condition: $(-1 + 1)\lambda_2 \equiv 0\lambda_2 \equiv 0 \pmod{3}$. This also gives no information about λ_2 . The target condition (*) becomes: $(1(0) + (2 + 1))\lambda_2 \equiv 3\lambda_2 \equiv 0 \pmod{3}$, which holds.

Case 3. $n \equiv 2 \pmod{3}$.

From (**), $(2 + 2)\lambda_2 \equiv 4\lambda_2 \equiv 0 \pmod{3}$. The target condition (*) becomes: $(2)(0) + (2 + 2)(0) \equiv 0 \pmod{3}$, which holds. \square

Remark 3.2 *In all cases, the necessary condition $n\lambda_1 + (5 + n)\lambda_2 \equiv 0 \pmod{3}$ is satisfied and thus it is a necessary condition for the existence of the the GDD.*

Theorem 3.4 *A GDD $(5, n, n + 1, 4; \lambda_1, \lambda_2)$ exists if the necessary condition $(n^2 + 10)\lambda_1 + (n^2 + 11n + 5)\lambda_2 \equiv 0 \pmod{6}$ holds.*

Proof The number of blocks of the GDD is obtained from $b = \frac{(n^2+10)\lambda_1+(n^2+11n+5)\lambda_2}{6}$ and that $(n^2 + 10)\lambda_1 + (n^2 + 11n + 5)\lambda_2 \equiv 0 \pmod{6}$. For a GDD $(5, n, n + 1, 4 : \lambda_1, \lambda_1)$, we have the fundamental equations: $3r = (n)\lambda_1 + (n^2 - 1)\lambda_2$ and $12b = n^2(n + 1)\lambda_1 + n(n - 1)(n + 1)^2\lambda_2$ and the necessary modular conditions derived earlier: For the number of blocks b to be an integer, $12b \equiv 0 \pmod{12}$, which implies $n^2(n + 1)\lambda_1 + n(n - 1)(n + 1)^2\lambda_2 \equiv 0 \pmod{12}$. This congruence modulo 12 gives us information modulo its divisors, including 2. Let us consider the equation modulo 2: $n^2(n + 1)\lambda_1 + n(n - 1)(n + 1)^2\lambda_2 \equiv 0 \pmod{2}$.

Case 1. $n \equiv 0 \pmod{2}$.

We have, $0^2(0 + 1)\lambda_1 + (0)(0 - 1)(0 + 1)^2\lambda_2 \equiv 0 \pmod{2}$, which implies $0 \equiv 0 \pmod{2}$. This gives no constraint on λ_1 or λ_2 when n is even.

Case 2. $n \equiv 1 \pmod{2}$.

We have, $1^2(1 + 1)\lambda_1 + (1)(1 - 1)(1 + 1)^2\lambda_2 \equiv 1 \pmod{2}$, which implies $1(0)\lambda_1 + (1)(0)(1 + 1)^2\lambda_2 \equiv 0 \pmod{2}$ and this gives $0 \equiv 0 \pmod{2}$. This also gives no constraint on λ_1 or λ_2 when n is odd. Now, let us consider the target conditions modulo 2 and 3 separately.

Modulo 2. In this case, we have $(n^2 + 0)\lambda_1 + (n^2 + n + 1)^2\lambda_2 \equiv 0 \pmod{2}$, which implies $(n)^2\lambda_1 + (n^2 + n + 1)^2\lambda_2 \equiv 0 \pmod{2}$.

If n is even, $0\lambda_1 + (0^2 + 0 + 1)\lambda_2 \equiv 0 \pmod{2}$, which gives $\lambda_2 \equiv 0 \pmod{2}$; If n is odd, $1\lambda_1 + (1^2 + 1 + 1)\lambda_2 \equiv 0 \pmod{2}$ and this gives $\lambda_1 + (1^2 + 1 + 1)\lambda_2 \equiv 0 \pmod{2} \equiv \lambda_1 + 2\lambda_2 \equiv \lambda_1 + \lambda_2 \equiv 0 \pmod{2}$. So, $\lambda_1 \equiv \lambda_2 \pmod{2}$.

Modulo 3. In this case, we have $(n^2 + 1)\lambda_1 + (n^2 + 2n + 2)\lambda_2 \equiv 0 \pmod{3}$. Using $\lambda_1 \equiv 0$

(mod 3); , $(n^2 + 1)(0) + (n^2 + 2n + 2)\lambda_2 \equiv 0 \pmod{3}$ and this implies $(n^2 + 2n + 2)\lambda_2 \equiv 0 \pmod{3}$. Now, we know that $n\lambda_2 \equiv 0 \pmod{3}$, then,

If $n \equiv 0 \pmod{3}$, $(0 + 0 + 2)\lambda_2 \equiv 2\lambda_2 \equiv \lambda_2 \equiv 0 \pmod{3}$; If $n \equiv 1 \pmod{3}$: then, $(1 + 2 + 2)\lambda_2 \equiv 5\lambda_2 \equiv 2\lambda_2 \equiv \lambda_2 \equiv 0 \pmod{3}$. If $n \equiv 2 \pmod{3}$: then, $(4 + 4 + 2)\lambda_2 \equiv 10\lambda_2 \equiv 2\lambda_2 \equiv \lambda_2 \equiv 0 \pmod{3}$. So, we have $\lambda_1 \equiv 0 \pmod{3}$ and $\lambda_2 \equiv 0 \pmod{3}$. Now, let us check the target condition modulo 6 with these congruences: $(n^2 + 10)\lambda_1 + (n^2 + 11n + 5)\lambda_2 \equiv 0 \pmod{6}$. If $\lambda_1 \equiv 0 \pmod{3}$ and $\lambda_2 \equiv 0 \pmod{3}$, then the target condition becomes $(n^2 + 10)(3k_1) + (n^2 + 11n + 5)(3k_2) \equiv 3[(n^2 + 10)k_1 + (n^2 + 11n + 5)k_2] \equiv 0 \pmod{3}$. We need to show that it is also 0 (mod 2). If λ_1 and λ_2 are even, then the target condition is 0 (mod 2). If λ_1 and λ_2 are odd, then the modulo 2 becomes: $(n^2 + 0)(1) + (n^2 + n + 1)(1) \equiv (n^2 + n^2 + n + 1) \equiv n + 1 \equiv 0 \pmod{2}$, so n is odd and thus, the necessary condition $(n^2 + 10)\lambda_1 + (n^2 + 11n + 5)\lambda_2 \equiv 0 \pmod{6}$ hold. \square

Remark 3.3. *Combining these conditions modulo 2 and 3 gives the required necessary conditions $(n^2 + 10)\lambda_1 + (n^2 + 11n + 5)\lambda_2 \equiv 0 \pmod{6}$ for λ_1 and λ_2 either being even or odd.*

These necessary conditions on b and r_i determine possibilities for the parameter n and the indices λ_1 and λ_2 which are summarized in the Table 3.1 where Does not means that the design does not exist for any value of n .

Table 1. The restrictions on n for $GDD(5, n, n + 1, 4; \lambda_1, \lambda_2)$

$\lambda_1 \setminus \lambda_2$	3	6	9	12	15	18
3	Does not	Exist	Does not	Exist	Does not	Exist
6	Does not	Exist	Does not	Exist	Does not	Exist
9	Does not	Exist	Does not	Exist	Does not	Exist
12	Does not	Exist	Does not	Exist	Does not	Exist
15	Does not	Exist	Does not	Exist	Does not	Exist
18	Does not	Exist	Does not	Exist	Does not	Exist

Theorem 3.5 *Necessary conditions are sufficient for a $GDD(n, 3, 4; \lambda, 2\lambda)$ for $\lambda_1 = \lambda_2 \equiv 0 \pmod{6}$, then a $BIBD(5 + n, 4, \lambda)$, a $BIBD(6 + n, 4, \lambda)$ and a $BIBD(2n + 1, 4, \lambda)$ exists.*

Proof Let $\lambda_1 = t$, and $\lambda_2 = 2t$. The blocks of t copies of a $4-(n, 4, 6)$ on G_1 as well as on G_2 and G_3 give the required 4-GDDs where groups $G_1 = a_1, \dots, a_n$, $G_2 = b_1, \dots, b_n$ and $G_3 = c_1, \dots, c_n$. It is well known that a $BIBD(n, 4, 6)$ exists for $n \geq 5$ [10] and thus a $GDD(5, n, n + 1, 4; 3, 6)$ will always exist. Hence a $GDD(5, n, n + 1, 4; 3t, 6t)$ always exists for all positive integers, t . \square

Here, we typically denote these groups as $G_1, G_2, G_3, \dots, G_m$ where m is the number of groups, G_i is a subset of treatment set, the union of all the groups is the entire treatment set $\bigcup_{i=1}^m G_i = V$ written as $V = G_1 \cup G_2 \cup \dots \cup G_i$, and $G_i \cap G_j = \emptyset$ for $i \neq j$.

Example 3.1 Construction of $GDD(5, 6, 7, 4; 3, 6)$ exists with $r_1 = 30$, $r_2 = 29$, and $r_3 = 28$. We now show that if $n \equiv 0 \pmod{6}$. Using our necessary conditions from theorem 3.4 then

a GDD $(5,6,7,4;3,6)$ exists through the following construction. When $\lambda_1 = 3$, $\lambda_2 \equiv 0 \pmod{6}$ implies $\lambda_2 = 6t$ for $t \geq 1$. The GDD has groups, $G_1 = \{0,1,2,3,4\}$, $G_2 = \{5,6,7,8,9,10\}$ and $G_3 = \{11, 12,13,14,15,16,17\}$. Then using direct construction of blocks of a BIBD $(40,4,1)$, we get 130 blocks.

[0, 1, 2, 12]	[0, 3, 6, 9]	[0, 4, 8, 10]	[0, 5, 7, 11]	[0, 13, 26, 39]	[0, 14, 25, 28]
[0, 15, 27, 38]	[0, 16, 22, 32]	[0, 17, 23, 34]	[0, 18, 24, 33]	[0, 19, 29, 35]	[0, 20, 31, 37]
[0, 21, 30, 36]	[1, 3, 8, 11]	[1, 4, 7, 9]	[1, 5, 6, 10]	[1, 13, 28, 38]	[1, 14, 27, 39]
[1, 15, 25, 26]	[1, 16, 24, 34]	[1, 17, 22, 33]	[1, 18, 23, 32]	[1, 19, 31, 36]	[1, 20, 30, 35]
[1, 21, 29, 37]	[2, 3, 7, 10]	[2, 4, 6, 11]	[2, 5, 8, 9]	[2, 13, 25, 27]	[2, 14, 26, 38]
[2, 15, 28, 39]	[2, 16, 23, 33]	[2, 17, 24, 32]	[2, 18, 22, 34]	[2, 19, 30, 37]	[2, 20, 29, 36]
[2, 21, 31, 35]	[3, 4, 5, 12]	[3, 13, 32, 35]	[3, 14, 34, 37]	[3, 15, 33, 36]	[3, 16, 29, 39]
[3, 17, 25, 31]	[3, 18, 30, 38]	[3, 19, 22, 26]	[3, 20, 23, 28]	[3, 21, 24, 27]	[4, 13, 34, 36]
[4, 14, 33, 35]	[4, 15, 32, 37]	[4, 16, 31, 38]	[4, 17, 30, 39]	[4, 18, 25, 29]	[4, 19, 24, 28]
[4, 20, 22, 27]	[4, 21, 23, 26]	[5, 13, 33, 37]	[5, 14, 32, 36]	[5, 15, 34, 35]	[5, 16, 25, 30]
[5, 17, 29, 38]	[5, 18, 31, 39]	[5, 19, 23, 27]	[5, 20, 24, 26]	[5, 21, 22, 28]	[6, 7, 8, 12]
[6, 13, 22, 29]	[6, 14, 23, 31]	[6, 15, 24, 30]	[6, 16, 26, 35]	[6, 17, 28, 37]	[6, 18, 27, 36]
[6, 19, 32, 39]	[6, 20, 25, 34]	[6, 21, 33, 38]	[7, 13, 24, 31]	[7, 14, 22, 30]	[7, 15, 23, 29]
[7, 16, 28, 36]	[7, 17, 27, 35]	[7, 18, 26, 37]	[7, 19, 34, 38]	[7, 20, 33, 39]	[7, 21, 25, 32]
[8, 13, 23, 30]	[8, 14, 24, 29]	[8, 15, 22, 31]	[8, 16, 27, 37]	[8, 17, 26, 36]	[8, 18, 28, 35]
[8, 19, 25, 33]	[8, 20, 32, 38]	[8, 21, 34, 39]	[9, 10, 11, 12]	[9, 13, 16, 19]	[9, 14, 17, 20]
[9, 15, 18, 21]	[9, 22, 35, 39]	[9, 23, 25, 37]	[9, 24, 36, 38]	[9, 26, 29, 32]	[9, 27, 30, 33]
[9, 28, 31, 34]	[10, 13, 17, 21]	[10, 14, 18, 19]	[10, 15, 16, 20]	[10, 22, 37, 38]	[10, 23, 36, 39]
[10, 24, 25, 35]	[10, 26, 30, 34]	[10, 27, 31, 32]	[10, 28, 29, 33]	[11, 13, 18, 20]	[11, 14, 16, 21]
[11, 15, 17, 19]	[11, 22, 25, 36]	[11, 23, 35, 38]	[11, 24, 37, 39]	[11, 26, 31, 33]	[11, 27, 29, 34]
[11, 28, 30, 32]	[12, 13, 14, 15]	[12, 16, 17, 18]	[12, 19, 20, 21]	[12, 22, 23, 24]	[12, 25, 38, 39]
[12, 26, 27, 28]	[12, 29, 30, 31]	[12, 32, 33, 34]	[12, 35, 36, 37]	<i>130 Blocks.</i>	

(1) **Necessary conditions are sufficient for** a GDD $(n, 3, 4; \lambda_1, \lambda_2)$ when $\lambda_1 = \lambda_2$.

We can view that the existence of a GDD with unequal group sizes as a consequence of the existence of GDDs with equal group sizes. Applying Wilson's Existence Theorem for GDDs, a GDD $(k, n, m; \lambda_1, \lambda_1)$ exists for sufficiently large $v = nm$ if necessary conditions are satisfied. For small order v , known existence results cover specific cases. Now, our total $v = 5 + 6 + 7 = 18$ is the modest with $\lambda_1 = 6$ and $\lambda_2 = 6$. Since both pair frequencies are equal, this GDD behaves similarly to a balanced incomplete block design (BIBD) within and between groups, but with group structure restrictions. Thus, we construct 13 blocks of BIBD $(13,4,1)$, add 63 blocks of BIBD $(28,4,1)$. The remaining blocks are formed by constructing 77 blocks of BIBD $(22,4,2)$. This is because from known theorem 2.2 $b = \frac{vr}{k} = \frac{\lambda v(v-1)}{k(k-1)}$, which gives in total 130 blocks.

Remark 3.4 A $GDD(5, n, n+1, 4; 0, \lambda_2)$ does not exist. This is because there are only three groups and the block size is four. So, each block must contain at least a pair from the same group ($\lambda_1 \geq 6$) to complete the block size. A $GDD(5, n, n+1, 4; \lambda_1, 0)$ exists as a $(2n+6, 4, \lambda_1)$ BIBD for particular values of n and λ_1 . So, a $GDD(5, n, n+1, 4; 0, 0)$ does not exist.

Example 3.2 Construction of $GDD(5, 6, 7, 4; 6, 6)$ exists with $r_1 = 34$, $r_2 = 34$, $r_3 = 34$ and $b = 153$ blocks. The GDD has groups, $G_1 = \{0, 1, 2, 3, 4\}$, $G_2 = \{5, 6, 7, 8, 9, 10\}$ and $G_3 = \{11, 12, 13, 14, 15, 16, 17\}$. The total number of blocks can be obtained by adding 13 blocks of a $BIBD(13, 4, 1)$ together with 63 blocks of a $(28, 4, 1)$ BIBD and then plus 77 blocks of a $BIBD(22, 4, 2)$.

In general, a $GDD(5, 6t, 6t+1, 4; 6t, 6t)$ exists with $r_1 = 24t^2 + 10t$, $r_2 = 24t^2 + 10t$, $r_3 = 24t^2 + 10t$ and $b = 72t^3 + 66t^2 + 15t$ where t is a positive integer.

(2) **Necessary conditions are sufficient for a GDD** $(5, n, n+1, 4; 2\lambda_1, \lambda_2)$ when $\lambda_1 \geq \lambda_2$

Theorem 3.6 A $GDD(5, n, n+1, 4; \lambda_1, \lambda_2)$ exist for $\lambda_1 \geq \frac{(n^2+10)\lambda_1 + (n^2+11n+5)\lambda_2}{6}$.

Proof The design has three groups of size $n_1 \geq 5$ and block size 4, then each block must have at least one first associate pair. This means that the total number of first associate pairs is at least equal to the number of blocks. Since there are $(n^2+10)\lambda_1$ first associate pairs and $\frac{(n^2+10)\lambda_1 + (n^2+11n+5)\lambda_2}{6}$ blocks, and so

$$\begin{aligned} (n^2+10)\lambda_1 &\geq \frac{(n^2+10)\lambda_1 + (n^2+11n+5)\lambda_2}{6}, \\ 5(n^2+10)\lambda_1 &\geq (n^2+11n+5)\lambda_2, \\ \lambda_1 &\geq \frac{(n^2+11n+5)\lambda_2}{(5n^2+50)}. \end{aligned}$$

This completes the proof. □

Corollary 3.1 From $b = \frac{vr}{k}$, if $GDD(5, n, n+1, 4; \lambda_1, \lambda_2)$ exists, then it has $(n^2+10)\lambda_1$ first associate pairs and $(n^2+11n+5)\lambda_2$ second associate pairs with $b \leq (n^2+10)\lambda_2$.

Proof The design has b blocks and $(n^2+10)\lambda_2$ first associate pairs. The total number of blocks cannot exceed the total number of first associate pairs. Thus $b \leq (n^2+10)\lambda_2$. □

Remark 3.5 A $GDD(5, n, n+1, 4; 2\lambda, \lambda)$ exists if and only if $BIBD(5+n, 4, \lambda)$ and $BIBD(2n+1, 4, \lambda)$ exists. Here, a $BIBD(n, 4, 6)$ exists for $n \geq 5$ and thus a $GDD(5, n, n+1, 4; 12, 6)$ will always exist. Hence a $GDD(5, n, n+1, 4; 12t, 6t)$ always exists for all positive integers, t .

Example 3.3 Construction of $GDD(5, 6, 7, 4; 9, 12)$ exists with $r_1 = 64$, $r_2 = 63$, $r_3 = 62$ and $b = 283$ blocks. The groups of the GDD are $G_1 = \{0, 1, 2, 3, 4\}$, $G_2 = \{5, 6, 7, 8, 9, 10\}$ and $G_3 = \{11, 12, 13, 14, 15, 16, 17\}$. We construct the total number of blocks by taking the 18 blocks of a $BIBD(9, 4, 3)$ on $G_1 \cup G_2$ add 55 blocks of a $BIBD(11, 4, 6)$ on $G_1 \cup G_3$ together with two copies of the 105 blocks of a $BIBD(15, 4, 6)$ on $G_2 \cup G_3$.

Example 3.4 Construction of $GDD(5, 6, 7, 4; 18, 18)$ exists with $r_1 = 102$, $r_2 = 102$, $r_3 =$

102 and $b = 459$ blocks. The total number of blocks can be obtained by constructing 210 blocks as 203 blocks of BIBD(29,4,3) and then add 7 blocks of BIBD(7,4,2) by normalizing a regular hadamard matrix of order 8 plus 242 blocks which has groups, $G_1 = \{0,1,2,3,4\}$, $G_2 = \{5,6,7,8,9,10\}$ and $G_3 = \{11,12,13,14, 15,16,17\}$ that will form 153 blocks and these blocks can be obtained by adding 13 blocks of BIBD(13,4,1) plus 63 blocks of (28,4,1)BIBD together with 77 blocks of BIBD(22,4,2) and then plus 50 blocks of BIBD(25,4,1) together with 39 blocks of BIBD (13,4,3). We generalise that, a GDD(5, 6t, 6t + 1, 4; 18t, 18t) exists with $r_1 = 72t^2 + 30t$, $r_2 = 72t^2 + 30t$, $r_3 = 72t^2 + 30t$ and $b = 216t^3 + 198t^2 + 45t$ where t is a positive integer.

Acknowledgement

I wish to express sincere gratitude to my beloved wife Ainembabazi Scholastic and our boys Ainomugisha Johnbillz and Ariguma Don, Parents Mr. and Mrs. Tumwesigye Isaaya and Kahima Peace and without forgetting the Staff St Kagwa Bushenyi High School lead by the Head teacher Mr. PK who supported me whole heartedly. Staff Mbarara University of Science and Technology with special thanks to my Supervisor Dr. Kasifa Namyalo and Dr. Olivia Nabawanda.

References

- [1] C. J. Colbourn, *CRC Handbook of Combinatorial Designs*, CRC press, 2010.
- [2] C. Colbourne and J. Dinitz, *Handbook of Combinatorial Designs*, CRC press Boca Raton, FL, 2007.
- [3] H. H. Crapo and G.-C. Rota, *On the Foundations of Combinatorial Theory: Combinatorial Geometries*, MIT press Cambridge, Mass., 1970.
- [4] F. Gao and G. Ge, A complete generalization of clatworthy group divisible designs, *SIAM Journal on Discrete Mathematics*, 25(4): 1547C1561, 2011.
- [5] D. Henson, D. G. Sarvate, and S. P. Hurd, Group divisible designs with three groups and block size four, *Discrete Mathematics*, 307(14): 1693C1706, 2007.
- [6] N. Pabhapote and N. Punnim, Group divisible designs with two associate classes and $\lambda_2 = 1$, *Int. J. Math. Math. Sci.*, 2011: 148580C1, 2011.
- [7] D. Sarvate, N. Mishra and K. Namyalo, Group divisible designs with block size five from clatworthy's table, *Communications in Statistics-Theory and Methods*, 47(9): 2085C2097, 2018.
- [8] D. R. Stinson, Introduction to balanced incomplete block designs, *Combinatorial Designs: Constructions and Analysis*, pages 1C21, 2004.
- [9] D. R. Stinson, Combinatorial designs: constructions and analysis, *ACM SIGACT News*, 39(4): 17C21, 2008.
- [10] D. R. Stinson, Weak and strong nestings of bibds, *arXiv*: 2405.12820, 2024.
- [11] M. Zhu and G. Ge, Mixed group divisible designs with three groups and block size 4, *Discrete mathematics*, 310(17-18): 2323C2326, 2010.

Hyperfloorplans and Superhyperfloorplans – Definitions, Properties and Perspectives (Revisit)

Takaaki Fujita

(Independent Researcher, Shinjuku, Shinjuku-ku, Tokyo, Japan)

E-mail: takaaki.fujita060@gmail.com

Abstract: Floorplans are geometric arrangements of modules within defined boundaries, adhering to constraints such as area and aspect ratio [1-3]. They are well known for applications in VLSI design and have been the subject of extensive algorithmic research. Hyperstructures extend the concept of the powerset into advanced mathematical models, while superhyperstructures further generalize these models via n -th iterated powersets, enabling multi-layered hierarchical abstractions [4-5]. Floorplans have a wide range of applications, and because hyperstructures and superhyperstructures can represent hierarchical structures in the real world, they are recognized as highly important research areas. However, the fusion of these concepts has only just begun to be explored. Therefore, with the aim of contributing to the dissemination of knowledge, in this paper, we revisit floorplans and examine the notions of *hyperfloorplan* and *superhyperfloorplan* as defined in [6]. We hope that our analysis provides valuable insights and aids in the broader understanding of floorplan theory and its applications.

Key Words: Hyperfloorplan, superhyperfloorplan, hyperStructure, superHyperStructure, powerset.

AMS(2010): 05C65, 08C10.

§1. Preliminaries

This section introduces the fundamental concepts and definitions that underpin the discussions in this paper. Throughout, all sets are assumed to be finite. Furthermore, any integer n used in the context of superhyperstructures and related constructs is taken to be a non-negative integer. For detailed information on the operations associated with each concept, the reader is referred to the relevant literature as appropriate.

1.1. Hyperstructures and Superhyperstructures

This subsection presents the formal foundations of *hyperstructures* and their higher-order generalization, *superhyperstructures*, which serve as powerful mathematical tools for modeling multi-tiered relational systems. Mathematical concepts such as networks, graphs, topology, and alge-

¹Received August 12, 2025. Accepted November 26, 2025

bra, as well as various real-world models, are defined on a daily basis; however, in some cases, these frameworks cannot adequately represent hierarchical structures. To address this limitation, the notions of hyperstructure and superhyperstructure have been introduced in recent years.

A *hyperstructure* is defined over the powerset of a base set, allowing operations not on individual elements but on subsets of the underlying domain. This generalization offers a flexible and expressive framework for capturing interactions and dependencies within complex systems [7-12].

Building on this concept, a *superhyperstructure* extends the idea further by employing the n -th iterated powerset of a set. This construction facilitates the representation of deeply nested or hierarchical relationships, where elements can themselves be subsets of subsets, and so forth. Such structures are particularly useful in applications involving recursive abstraction or multilayer decision architectures [4,13C16]. Closely related frameworks include the theory of *superhypergraphs* [17C20].

We now proceed to provide precise mathematical definitions of these two foundational concepts.

Definition 1.1(Set,[21]) *A set is a collection of distinct, well-defined objects, referred to as elements. For any object x , it can be determined whether x is an element of a given set. If x belongs to a set A , this is denoted as $x \in A$. Sets are often represented using curly braces.*

Definition 1.2(Base set,[22]) *A base set is a primary set S from which more complex structures, such as powersets and hyperstructures, are derived. It is formally expressed as:*

$$S = \{x \mid x \text{ is an element in the defined domain}\}.$$

The elements of advanced structures, such as $\mathcal{P}(S)$ or $\mathcal{P}_n(S)$, are drawn from this base set S .

Definition 1.3(Power set,[23, 24]) *The powerset of a set S , denoted as $\mathcal{P}(S)$, is the set containing all subsets of S , including both the empty set and S itself. Formally, it is defined as:*

$$\mathcal{P}(S) = \{A \mid A \subseteq S\}.$$

Definition 1.4(n -th Powerset, cf. [14,25,26]) *The n -th powerset of a set H , denoted by $\mathcal{P}_n(H)$, is constructed iteratively. Starting from the basic powerset, it is defined as:*

$$\mathcal{P}_1(H) = \mathcal{P}(H), \quad \mathcal{P}_{n+1}(H) = \mathcal{P}(\mathcal{P}_n(H)), \quad \text{for } n \geq 1.$$

Similarly, the n -th non-empty powerset, denoted by $\mathcal{P}_n^(H)$, is defined iteratively as:*

$$\mathcal{P}_1^*(H) = \mathcal{P}^*(H), \quad \mathcal{P}_{n+1}^*(H) = \mathcal{P}^*(\mathcal{P}_n^*(H)).$$

Here, $\mathcal{P}^(H)$ represents the powerset of H excluding the empty set.*

Example 1.5(Real-world example of an n -th powerset) Consider a company H with three employees:

$$H = \{\text{Satoshi, Yuko, Kenji}\}.$$

The first powerset $\mathcal{P}_1(H)$ lists all possible groups of employees, such as $\{\text{Satoshi, Yuko}\}$ or $\{\text{Kenji}\}$.

The second powerset $\mathcal{P}_2(H)$ then treats each element of $\mathcal{P}_1(H)$ (i.e., each possible group of employees) as a single unit and forms all possible collections of such groups. For example, one element of $\mathcal{P}_2(H)$ could be:

$$\{ \{\text{Satoshi}\}, \{\text{Yuko, Kenji}\} \},$$

which represents a scenario where the company organizes two independent task forces: one consisting solely of Satoshi, and another consisting of Yuko and Kenji.

In practical terms, the n -th powerset models higher-order organizational structures, such as teams of teams, or committees formed from existing working groups, thereby capturing multiple hierarchical levels of arrangement.

To establish a formal foundation for the concepts of Hyperstructures and Superhyperstructures, we present the following definitions and propositions.

Definition 1.6(Classical structure, cf. [14,26]) *A classical structure is a mathematical framework defined on a non-empty set H , equipped with one or more Classical Operations that satisfy specified classical axioms. Specifically, a classical operation is a function of the form*

$$\#_0 : H^m \rightarrow H,$$

where $m \geq 1$ is a positive integer, and H^m denotes the m -fold Cartesian product of H . Common examples include addition and multiplication in algebraic structures such as groups, rings, and fields.

Definition 1.7(Hyperstructure, cf. [14,26]) *A Hyperstructure extends the notion of a Classical Structure by operating on the powerset of a base set. Formally, it is defined as:*

$$\mathcal{H} = (\mathcal{P}(S), \circ),$$

where S is the base set, $\mathcal{P}(S)$ is the powerset of S , and \circ is an operation defined on subsets of $\mathcal{P}(S)$. Hyperstructures allow for generalized operations that can apply to collections of elements rather than single elements.

Example 1.8(Real-world example of a hyperstructure) Let $S = \{\text{Satoshi, Yuko, Kenji}\}$ represent the set of individual project members in a company. The powerset $\mathcal{P}(S)$ consists of all possible project teams, such as $\{\text{Satoshi, Yuko}\}$ or $\{\text{Kenji}\}$.

Define an operation \circ on $\mathcal{P}(S)$ where, given two subsets of S (teams), the result of \circ is the set of all possible joint committees that can be formed by taking at least one member from

each team. For example:

$$\{\text{Satoshi, Yuko}\} \circ \{\text{Kenji}\} = \{\{\text{Satoshi, Kenji}\}, \{\text{Yuko, Kenji}\}\}.$$

This construction forms a hyperstructure $\mathcal{H} = (\mathcal{P}(S), \circ)$, where the operation acts on *subsets* (teams) instead of on individual people. In practical terms, this models scenarios such as cross-team collaboration in organizations, where operations combine groups rather than single members.

Definition 1.9(n -Superhyperstructure, cf.[14,26]) *An n -Superhyperstructure further generalizes a Hyperstructure by incorporating the n -th powerset of a base set. It is formally described as:*

$$\mathcal{SH}_n = (\mathcal{P}_n(S), \circ),$$

where S is the base set, $\mathcal{P}_n(S)$ is the n -th powerset of S , and \circ represents an operation defined on elements of $\mathcal{P}_n(S)$. This iterative framework allows for increasingly hierarchical and complex representations of relationships within the base set.

Example 1.10(2-Superhyperstructure over $S = \{a, b\}$) Let

$$S = \{a, b\}.$$

Then the first powerset is

$$\mathcal{P}_1(S) = \{\emptyset, \{a\}, \{b\}, \{a, b\}\},$$

and the second powerset is

$$\mathcal{P}_2(S) = \mathcal{P}(\mathcal{P}_1(S)) = \{X \mid X \subseteq \mathcal{P}_1(S)\},$$

which has $2^4 = 16$ elements. Define a hyperoperation

$$\circ_2 : \mathcal{P}_2(S) \times \mathcal{P}_2(S) \longrightarrow \mathcal{P}(\mathcal{P}_2(S))$$

by

$$X \circ_2 Y = \{Z \in \mathcal{P}_2(S) \mid X \cup Y \subseteq Z\}.$$

Then, $(\mathcal{P}_2(S), \circ_2)$ is a concrete 2-superhyperstructure.

Concrete computation. Choose

$$X = \{\{a\}, \{a, b\}\}, \quad Y = \{\{b\}\}.$$

Then

$$X \cup Y = \{\{a\}, \{b\}, \{a, b\}\},$$

and

$$X \circ_2 Y = \{Z \subseteq \mathcal{P}_1(S) \mid \{a\}, \{b\}, \{a, b\} \in Z\}.$$

The two minimal members of $X \circ_2 Y$ are

$$Z_1 = \{\{a\}, \{b\}, \{a, b\}\}, \quad Z_2 = Z_1 \cup \{\emptyset\}.$$

All other elements of $X \circ_2 Y$ are obtained by adding any of the remaining subsets of $\mathcal{P}_1(S)$ to Z_1 .

1.2. Floorplan

Floorplans are geometric arrangements of modules within defined boundaries, adhering to constraints such as area and aspect ratio [3,27,28]. The definition of a general floorplan is provided below.

Definition 1.11(Floorplan, [3,27,28]) *A floorplan is a geometric arrangement of a given set of rectangular modules within a bounding rectangle, satisfying specific constraints related to module dimensions, aspect ratios, and interconnections. It is formally defined as follows:*

1. *Modules.* The floorplan consists of m rectangular modules $\{M_1, M_2, \dots, M_m\}$, where each module M_i is characterized by

- *Area.* $A_i > 0$, the total area of the module;
- *Aspect ratio bounds.* l_i and u_i , the lower and upper bounds for the height-to-width ratio $\frac{h_i}{w_i}$, such that

$$w_i \cdot h_i = A_i, \quad l_i \leq \frac{h_i}{w_i} \leq u_i;$$

- *A module is rigid if $l_i = u_i$, and flexible otherwise;*
- *A module may have a fixed orientation (dimensions w_i, h_i are fixed) or a free orientation (dimensions can be interchanged).*

2. *Bounding Rectangle.* The modules are arranged within a bounding rectangle R with dimensions W (width) and H (height), such that

$$p \leq \frac{H}{W} \leq q, \quad \text{where } p, q > 0$$

3. *Partitioning* The rectangle R is partitioned into m non-overlapping rectangular regions $\{r_1, r_2, \dots, r_m\}$, each corresponding to a module M_i . Each region r_i satisfies:

$$x_i \cdot y_i \geq A_i, \quad l_i \leq \frac{y_i}{x_i} \leq u_i$$

where x_i and y_i are the width and height of r_i , respectively.

4. *Objective Function.* The quality of a floorplan is measured using the following objective function:

$$\text{Score} = \lambda \cdot (W \cdot H) + \sum_{i=1}^m \sum_{j=1}^m c_{ij} \cdot d_{ij}$$

where

- $W \cdot H$: Total area of the bounding rectangle R ;

- c_{ij} : Connection cost between modules M_i and M_j ($c_{ij} \geq 0$);
- d_{ij} : Manhattan distance between the centers of r_i and r_j ;
- $\lambda > 0$: User-defined weight balancing the importance of area and wirelength.

5. *Slicing Floorplans.* A slicing floorplan is a recursive partitioning of R using horizontal and vertical cuts, represented as

- *Slicing Tree.* A binary tree where internal nodes represent cuts and leaves represent modules;
- *Polish Expression.* A postfix expression encoding the slicing structure.

For slicing floorplans, the bounding rectangle R is recursively divided into smaller regions $\{r_1, r_2, \dots, r_m\}$ using slicing operators $+$ (horizontal cut) and \times (vertical cut).

6. *Feasibility.* A floorplan is feasible if all regions r_i satisfy:

$$x_i \cdot y_i = A_i, \quad l_i \leq \frac{y_i}{x_i} \leq u_i$$

and no two regions overlap.

Example 1.12(3-module slicing floorplan) Let $m = 3$ and consider modules M_1, M_2, M_3 with parameters:

$$\begin{aligned} A_1 &= 10, & l_1 &= 0.8, & u_1 &= 1.2, & \text{free orientation,} \\ A_2 &= 20, & l_2 &= u_2 = 1.0, & \text{rigid, fixed orientation,} \\ A_3 &= 15, & l_3 &= 0.5, & u_3 &= 2.0, & \text{free orientation.} \end{aligned}$$

Choose module region dimensions (x_i, y_i) satisfying $x_i y_i = A_i$ and $l_i \leq y_i/x_i \leq u_i$:

$$(x_1, y_1) = (\sqrt{10}, \sqrt{10}), \quad (x_2, y_2) = (\sqrt{20}, \sqrt{20}), \quad (x_3, y_3) = (3, 5).$$

a slicing tree with a vertical root cut (\times) separating

$$\underbrace{(M_1 + M_3)}_{\text{horizontal cut}} \text{ and } M_2,$$

whose Polish expression is

$$M_1 M_3 + M_2 \times .$$

Then,

$$W = \underbrace{\max\{x_1, x_3\}}_{= \sqrt{10}} + x_2 = \sqrt{10} + \sqrt{20} \approx 3.162 + 4.472 = 7.634,$$

$$H = \max\{y_1 + y_3, y_2\} = \max\{\sqrt{10} + 5, \sqrt{20}\} \approx \max\{3.162 + 5, 4.472\} = 8.162,$$

$$\frac{H}{W} \approx \frac{8.162}{7.634} \approx 1.069 \quad (p = 0.5, q = 2).$$

Place all bottom-aligned, so region centers are

$$\begin{aligned} c_1 &= \left(\frac{\sqrt{10}}{2}, 5 + \frac{\sqrt{10}}{2}\right) \approx (1.581, 6.581), \\ c_3 &= \left(\frac{3}{2}, \frac{5}{2}\right) \approx (1.5, 2.5), \\ c_2 &= \left(\sqrt{10} + \frac{\sqrt{20}}{2}, \frac{\sqrt{20}}{2}\right) \approx (5.398, 2.236). \end{aligned}$$

Let connection costs $c_{12} = 2$, $c_{13} = 1$, $c_{23} = 3$. Then, the Manhattan distances

$$d_{12} \approx 8.162, \quad d_{13} \approx 4.162, \quad d_{23} \approx 4.162.$$

For weight $\lambda = 1$, the score is

$$\begin{aligned} \text{Score} &= (W \cdot H) + \sum_{1 \leq i < j \leq 3} c_{ij} d_{ij} \\ &\approx 7.634 \cdot 8.162 + (2 \cdot 8.162 + 1 \cdot 4.162 + 3 \cdot 4.162) \\ &\approx 62.33 + 33.00 = 95.33. \end{aligned}$$

All regions satisfy $x_i y_i = A_i$ and $l_i \leq y_i/x_i \leq u_i$, and there is no overlap. Hence this floorplan is feasible.

§2. Review: Hyperfloorplan

Let us now build a *hyperfloorplan* starting from the set of modules S . We first consider the powerset $\mathcal{P}(S)$. Elements of $\mathcal{P}(S)$ are all possible subsets of modules. Our overarching goal is to capture geometric *feasibility* in a hyperoperation (cf.[6]).

Definition 2.1(Hyperfloorplan, cf.[6]) *Let $S = \{M_1, \dots, M_m\}$ be a finite set of rectangular modules, and let $\mathcal{P}(S)$ be its powerset. We say that a subset $X \subseteq S$ admits a feasible floorplan if there exists a classical slicing or non-slicing arrangement of the modules in X within some bounding rectangle satisfying all area, aspect-ratio, non-overlap, and connectivity constraints.*

Define a hyperoperation

$$\circ : \mathcal{P}(S) \times \mathcal{P}(S) \longrightarrow \mathcal{P}(\mathcal{P}(S))$$

by

$$A \circ B = \{X \subseteq S \mid A \cup B \subseteq X \text{ and } X \text{ admits a feasible floorplan}\}.$$

Then the hyperfloorplan of S is the hyperstructure

$$\mathcal{HF}(S) = (\mathcal{P}(S), \circ).$$

Example 2.2(Hyperfloorplan of four modules) Let

$$S = \{M_1, M_2, M_3, M_4\}$$

with the following module parameters

Module	A_i	(l_i, u_i)	Orientation	Chosen (w_i, y_i)
M_1	8	[0.5, 2.0]	free	(2, 4), $2 \cdot 4 = 8$, $4/2 = 2.0$
M_2	12	[1.0, 1.0]	rigid	$(\sqrt{12}, \sqrt{12})$, $\sqrt{12}^2 = 12$, 1.0
M_3	6	[0.75, 1.5]	free	(2, 3), $2 \cdot 3 = 6$, $3/2 = 1.5$
M_4	10	[0.8, 1.25]	free	$(\sqrt{10}, \sqrt{10})$, $\sqrt{10}^2 = 10$, 1.0

Define two level-1 subsets by

$$A = \{M_1, M_2\}, \quad B = \{M_2, M_3\}.$$

By Definition 2.1,

$$A \circ B = \{X \subseteq S \mid \{M_1, M_2, M_3\} \subseteq X \text{ and } X \text{ admits a feasible floorplan}\}.$$

We find two minimal supersets

- $X_1 = \{M_1, M_2, M_3\}$. A feasible slicing-floorplan

– First, slice M_1 and M_2 horizontally,
$$\begin{cases} W_0 = \max\{w_1, w_2\} = \max\{2, \sqrt{12}\} \approx 3.464, \\ H_0 = y_1 + y_2 = 4 + \sqrt{12} \approx 7.464. \end{cases}$$

- Then, slice the block $\{M_1, M_2\}$ vertically with M_3 ,

$$\begin{cases} W = W_0 + w_3 \approx 3.464 + 2 = 5.464, \\ H = \max\{H_0, y_3\} = \max\{7.464, 3\} = 7.464. \end{cases}$$

- All aspect ratios and non-overlap conditions hold, so X_1 is feasible.

- $X_2 = \{M_1, M_2, M_3, M_4\}$, A feasible non-slicing floorplan.

– Place M_1, M_2 in bottom row side by side:
$$\begin{cases} W_b = w_1 + w_2 = 2 + \sqrt{12} \approx 5.464, \\ H_b = \max\{y_1, y_2\} = \max\{4, \sqrt{12}\} \approx 4. \end{cases}$$

– Place M_3, M_4 in top row side by side
$$\begin{cases} W_t = w_3 + w_4 = 2 + \sqrt{10} \approx 5.162, \\ H_t = \max\{y_3, y_4\} = \max\{3, \sqrt{10}\} \approx 3.162. \end{cases}$$

Overall bounding rectangle
$$\begin{cases} W = \max\{W_b, W_t\} = 5.464, \\ H = H_b + H_t \approx 4 + 3.162 = 7.162. \end{cases}$$
 – All regions satisfy area and aspect-ratio constraints, so X_2 is feasible.

Therefore,

$$A \circ B = \{X_1, X_2\}.$$

Proposition 2.3(Well-definedness) *For all $A, B \subseteq S$, the set $A \circ B$ is nonempty if and only if $A \cup B$ itself admits a feasible floorplan.*

Proof By definition, $A \circ B$ consists exactly of those supersets $X \supseteq A \cup B$ that admit a feasible floorplan. In particular, $X = A \cup B$ belongs to $A \circ B$ if and only if $A \cup B$ admits some feasible floorplan. Hence $A \circ B \neq \emptyset$ precisely when $A \cup B$ is floorplannable. \square

Theorem 2.4(Hyperfloorplan generalizes classical floorplan) *Let $S = \{M_1, \dots, M_m\}$. Then,*

(a) *Every classical slicing floorplan of S can be realized by an iterated hyperproduct chain in $\mathcal{HF}(S)$;*

(b) *Conversely, every finite chain of hyperproducts whose last element is S corresponds to a classical slicing floorplan of S .*

Particularly, the set of all slicing floorplans of S is in bijection with the set of all hyperproduct expressions in $\mathcal{HF}(S)$ evaluating to S .

Proof We prove parts (a) and (b) by induction on the number of internal nodes in a slicing tree.

(a) *From slicing tree to hyperproduct chain.* Let T be a binary slicing tree whose leaves, in left-to-right order, are the singleton sets $\{M_{i_1}\}, \dots, \{M_{i_m}\}$ and whose internal nodes are labeled \times (vertical cut) or $+$ (horizontal cut). We construct a sequence of subsets

$$X_1, X_2, \dots, X_{m-1}$$

and corresponding pairs (A_k, B_k) such that

$$X_k = A_k \circ B_k,$$

and at the end $X_{m-1} = S$.

• *Base Case.* If T has a single internal node whose children are leaves $\{M_i\}$ and $\{M_j\}$, then these two modules are sliced together to form a feasible two-module floorplan in $X_1 = \{M_i, M_j\}$. By Definition 2.1, $\{M_i\} \circ \{M_j\}$ contains X_1 .

• *Inductive Step.* Suppose for a slicing tree with k internal nodes we have constructed a chain

$$X_1 = A_1 \circ B_1, X_2 = A_2 \circ B_2, \dots, X_k = A_k \circ B_k$$

with X_k equal to the subset of modules in the subtree rooted at the k -th internal node. Now attach one more cut combining X_k with a leaf $\{M_\ell\}$ or with the result of another subtree Y_k . By feasibility of the slicing, $X_k \cup \{M_\ell\}$ (or $X_k \cup Y_k$) admits a feasible floorplan; hence by Definition 2.1

$$X_{k+1} = X_k \circ \{M_\ell\} \quad (\text{or } X_k \circ Y_k) \ni X_k \cup \{M_\ell\}.$$

This yields the extended chain.

After $m - 1$ steps we obtain $X_{m-1} = S$, realizing the full slicing floorplan.

(b) *From hyperproduct chain to slicing tree.* Conversely, let

$$X_1 = A_1 \circ B_1, X_2 = A_2 \circ B_2, \dots, X_\ell = A_\ell \circ B_\ell$$

be any finite chain in $\mathcal{HF}(S)$ with $X_\ell = S$. By Proposition 2.3, each X_k admits a feasible floorplan for $A_k \cup B_k$. We form a binary tree whose root combines the two subsets A_ℓ and B_ℓ by the slicing cut used in that floorplan (vertical or horizontal), and whose children are either leaves (if A_ℓ or B_ℓ is a singleton) or the roots of subtrees constructed recursively from the partial chain ending at X_{k-1} . Since each step merges exactly two previously disjoint subsets, the result is a slicing tree describing a valid classical floorplan of S .

Thus every slicing floorplan corresponds exactly to one hyperproduct chain in $\mathcal{HF}(S)$, proving the bijection and hence the desired generalization. \square

Proposition 2.5(Commutativity) *For all $A, B \subseteq S$,*

$$A \circ B = B \circ A.$$

Proof By Definition 2.1,

$$A \circ B = \{X \subseteq S \mid A \cup B \subseteq X, X \text{ feasible}\},$$

and

$$B \circ A = \{X \subseteq S \mid B \cup A \subseteq X, X \text{ feasible}\}.$$

Since $A \cup B = B \cup A$, the two sets coincide. \square

Proposition 2.6(Identity element) *The empty set \emptyset acts as a neutral element: for any $A \subseteq S$,*

$$\emptyset \circ A = A \circ \emptyset = \{X \subseteq S \mid A \subseteq X, X \text{ feasible}\}.$$

Particularly, if A itself admits a feasible floorplan, then A is the minimal element of $\emptyset \circ A$.

Proof Immediate from Definition 2.1, since $\emptyset \cup A = A$ and a superset X must satisfy $A \subseteq X$ and feasibility. \square

Proposition 2.7(Idempotence) *For any $A \subseteq S$ that admits a feasible floorplan,*

$$A \in A \circ A.$$

Proof By Definition 2.1,

$$A \circ A = \{X \subseteq S \mid A \cup A \subseteq X, X \text{ feasible}\} = \{X \subseteq S \mid A \subseteq X, X \text{ feasible}\}.$$

Since $A \subseteq A$ and A is feasible, $A \in A \circ A$. \square

Proposition 2.8(Antitone property) *If $A \subseteq A' \subseteq S$ and $B \subseteq B' \subseteq S$, then*

$$A' \circ B' \subseteq A \circ B.$$

Proof Suppose $X \in A' \circ B'$. Then $A' \cup B' \subseteq X$ and X admits a feasible floorplan. Since $A \cup B \subseteq A' \cup B'$, it follows that $A \cup B \subseteq X$. Hence $X \in A \circ B$. \square

Theorem 2.9(Hyper-Associativity) *For all $A, B, C \subseteq S$, define the triple hyperproduct by*

$$A \circ B \circ C := \bigcup_{X \in A \circ B} (X \circ C) = \bigcup_{Y \in B \circ C} (A \circ Y).$$

Then,

$$A \circ B \circ C = \{Z \subseteq S \mid A \cup B \cup C \subseteq Z, Z \text{ feasible}\}.$$

Proof By definition,

$$\bigcup_{X \in A \circ B} (X \circ C) = \bigcup_{\substack{X \subseteq S \\ A \cup B \subseteq X}} \{Z \subseteq S \mid X \cup C \subseteq Z, Z \text{ feasible}\}.$$

Since $A \cup B \cup C \subseteq X \cup C \subseteq Z$, the union ranges exactly over all feasible Z containing $A \cup B \cup C$. The same argument applies to $\bigcup_{Y \in B \circ C} (A \circ Y)$, establishing the equality. \square

§3. Review: n -Superhyperfloorplan

An n -superhyperfloorplan organizes hierarchical sets of modules using iterated powersets and feasibility constraints across n abstraction levels for multi-layer layout (cf.[6]).

Definition 3.1(n -Superhyperfloorplan, (cf.[6])) *Let $S = \{M_1, \dots, M_m\}$ be a finite set of atomic modules, and define recursively the k -th powerset*

$$\mathcal{P}_1(S) = \mathcal{P}(S), \quad \mathcal{P}_{k+1}(S) = \mathcal{P}(\mathcal{P}_k(S)).$$

We now introduce a feasibility predicate F_k on subsets of $\mathcal{P}_k(S)$

- $F_1(X)$ holds for $X \subseteq \mathcal{P}_1(S)$ if and only if there exists a classical (slicing or non-slicing) floorplan of the modules in X within some bounding rectangle, satisfying all area, aspect-ratio, non-overlap, and interconnection constraints.

- For $k > 1$, $F_k(X)$ holds for $X \subseteq \mathcal{P}_k(S)$ if and only if

- (i) There exists a bounding rectangle R and an arrangement of the supermodules X inside R satisfying the usual floorplanning constraints at level k .

- (ii) Every element $Y \in X$, viewed as a subset $Y \subseteq \mathcal{P}_{k-1}(S)$, satisfies $F_{k-1}(Y)$.

For a fixed $n \geq 1$, define the hyperoperation

$$\circ_n : \underbrace{\mathcal{P}_n(S) \times \cdots \times \mathcal{P}_n(S)}_{m \text{ times}} \longrightarrow \mathcal{P}(\mathcal{P}_n(S))$$

by

$$A_1 \circ_n A_2 \circ_n \cdots \circ_n A_m = \left\{ X \in \mathcal{P}_n(S) \mid \bigcup_{i=1}^m A_i \subseteq X \text{ and } F_n(X) \right\}.$$

The n -superhyperfloorplan of S is the hyperstructure

$$\mathcal{SHF}_n = (\mathcal{P}_n(S), \circ_n).$$

Example 3.2(2-Superhyperfloorplan of $S = \{M_1, M_2, M_3\}$) Let

$$S = \{M_1, M_2, M_3\},$$

with atomic module parameters

Module	A_i	(l_i, u_i)	Chosen (w_i, h_i)
M_1	8	[0.5, 2.0]	(2, 4), $2 \cdot 4 = 8$, $4/2 = 2.0$
M_2	12	[1.0, 1.0]	$(\sqrt{12}, \sqrt{12})$, $\sqrt{12}^2 = 12$, 1.0
M_3	6	[0.75, 1.5]	(2, 3), $2 \cdot 3 = 6$, $3/2 = 1.5$

We have $\mathcal{P}_1(S) = \mathcal{P}(S)$ and $\mathcal{P}_2(S) = \mathcal{P}(\mathcal{P}_1(S))$. Choose two level-2 elements

$$A = \{\{M_1\}, \{M_2, M_3\}\}, \quad B = \{\{M_2\}, \{M_1, M_3\}\} \subseteq \mathcal{P}_2(S).$$

By Definition 3.1,

$$A \circ_2 B = \left\{ X \in \mathcal{P}_2(S) \mid \{\{M_1\}, \{M_2\}, \{M_1, M_3\}, \{M_2, M_3\}\} \subseteq X \text{ and } F_2(X) \right\}.$$

We exhibit two minimal supersets X_1 and X_2

$$\begin{aligned} X_1 &= \{\{M_1\}, \{M_2\}, \{M_1, M_3\}, \{M_2, M_3\}\}, \\ X_2 &= X_1 \cup \{\{M_1, M_2, M_3\}\}. \end{aligned}$$

Step 1. Verify F_1 for each supermodule $Y \in X_1 \cup X_2$.

- $Y_1 = \{M_1\}$, a trivial bounding box (2×4).
- $Y_2 = \{M_2\}$, a bounding box ($\sqrt{12} \times \sqrt{12}$) $\approx (3.464 \times 3.464)$.
- $Y_3 = \{M_1, M_3\}$, choose vertical slice

$$W_3 = 2 + 2 = 4, \quad H_3 = \max\{4, 3\} = 4.$$

- $Y_4 = \{M_2, M_3\}$, choose vertical slice:

$$W_4 = \sqrt{12} + 2 \approx 5.464, \quad H_4 = \max\{\sqrt{12}, 3\} = \sqrt{12} \approx 3.464.$$

- $Y_5 = \{M_1, M_2, M_3\}$. In this case, first horizontal slice of M_1, M_2 : $W_a = \max\{2, \sqrt{12}\} \approx 3.464$, $H_a = 4 + \sqrt{12} \approx 7.464$; then vertical slice with M_3 : $W_5 = W_a + 2 \approx 5.464$, $H_5 = \max\{7.464, 3\} = 7.464$.

Thus, $F_1(Y)$ holds for all $Y \in X_1 \cup X_2$.

Step 2. Verify F_2 (arrangement of supermodules).

(a) For X_1 : four supermodules Y_1, \dots, Y_4 . Arrange in two rows

$$\text{Bottom row: } Y_1 (2 \times 4), Y_2 (3.464 \times 3.464) \Rightarrow W_b = 2 + 3.464 = 5.464, \quad H_b = 4,$$

$$\text{Top row: } Y_3 (4 \times 4), Y_4 (5.464 \times 3.464) \Rightarrow W_t = 4 + 5.464 = 9.464, \quad H_t = 4.$$

Overall bounding box

$$W = \max\{5.464, 9.464\} = 9.464, \quad H = H_b + H_t = 4 + 4 = 8,$$

so $F_2(X_1)$ holds.

(b) For X_2 : five supermodules Y_1, \dots, Y_5 . Arrange in two rows

$$\text{Bottom row: } Y_1 (2 \times 4), Y_2 (3.464 \times 3.464), Y_3 (4 \times 4) \Rightarrow W_b = 2 + 3.464 + 4 = 9.464, \quad H_b = 4,$$

$$\text{Top row: } Y_4 (5.464 \times 3.464), Y_5 (5.464 \times 7.464) \Rightarrow W_t = 5.464 + 5.464 = 10.928, \quad H_t = 7.464.$$

Overall bounding box

$$W = \max\{9.464, 10.928\} = 10.928, \quad H = H_b + H_t = 4 + 7.464 = 11.464,$$

so $F_2(X_2)$ holds as well.

Hence

$$A \circ_2 B = \{X_1, X_2\},$$

demonstrating a concrete 2-superhyperfloorplan of S .

Example 3.3(3-Superhyperfloorplan of $S = \{M_1, M_2\}$) Let

$$S = \{M_1, M_2\},$$

with module parameters

Module	A_i	Chosen dimensions (w_i, h_i)
M_1	4	(2, 2)
M_2	9	(3, 3)

so that $w_i h_i = A_i$ and all aspect ratios are 1. We have

$$\mathcal{P}_1(S) = \{\emptyset, \{M_1\}, \{M_2\}, \{M_1, M_2\}\},$$

$$\mathcal{P}_2(S) = \mathcal{P}(\mathcal{P}_1(S)), \quad \mathcal{P}_3(S) = \mathcal{P}(\mathcal{P}_2(S)).$$

Define three level-2 supermodules in $\mathcal{P}_2(S)$ by

$$U_0 = \emptyset, \quad U_1 = \{\{M_1\}\}, \quad U_2 = \{\{M_2\}\}, \quad U_3 = \{\{M_1\}, \{M_2\}\}.$$

Then, each U_j satisfies $F_2(U_j)$ since

- For U_1 and U_2 , the single submodule is trivially placed in its own bounding box.
- For U_3 , place $\{M_1\}$ and $\{M_2\}$ side-by-side: $W = 2 + 3 = 5$, $H = \max\{2, 3\} = 3$.
- For $U_0 = \emptyset$, no modules \rightarrow trivial feasibility.

Choose two level-3 elements in $\mathcal{P}_3(S)$:

$$A = \{U_3\}, \quad B = \{U_1, U_2\}.$$

Then, by Definition 3.1,

$$A \circ_3 B = \left\{ X \in \mathcal{P}_3(S) \mid \{U_1, U_2, U_3\} \subseteq X \text{ and } F_3(X) \right\}.$$

We take the two minimal supersets:

$$X_1 = \{U_1, U_2, U_3\}, \quad X_2 = X_1 \cup \{U_0\}.$$

Step 1. Check F_2 for each U_j . As above, all four satisfy F_2 .

Step 2. Verify $F_3(X_k)$ by arranging the level-2 supermodules U_j in a bounding rectangle, using their level-2 bounding dimensions

$$\dim(U_1) = (2, 2), \quad \dim(U_2) = (3, 3), \quad \dim(U_3) = (5, 3), \quad \dim(U_0) = (0, 0).$$

(a) For X_1 : place U_1, U_2 in top row, U_3 in bottom row

$$W_{\text{top}} = 2 + 3 = 5, \quad H_{\text{top}} = 3, \quad W_{\text{bot}} = 5, \quad H_{\text{bot}} = 3,$$

so overall $W = \max\{5, 5\} = 5$, $H = 3 + 3 = 6$.

(b) For X_2 : include the trivial U_0 (zero-area) alongside

$$\text{Same layout gives } W = 5, \quad H = 6,$$

so $F_3(X_2)$ holds as well.

Therefore, $A \circ_3 B = \{X_1, X_2\}$ exhibiting a concrete 3-superhyperfloorplan of S .

Theorem 3.4(n -Superhyperfloorplan Generalizes Hyperfloorplan) *Let $\mathcal{HF} = (\mathcal{P}_1(S), \circ_1)$ be*

the hyperfloorplan of S . Then,

(a) $\mathcal{SHF}_1 = (\mathcal{P}_1(S), \circ_1)$ coincides exactly with \mathcal{HF} .

(b) For each $n > 1$, the inclusion $\iota: \mathcal{P}_1(S) \hookrightarrow \mathcal{P}_n(S)$, $A \mapsto A$, induces an embedding of hyperstructures $\iota: \mathcal{HF} \hookrightarrow \mathcal{SHF}_n$ preserving the hyperoperation:

$$\iota(A \circ_1 B) = \iota(A) \circ_n \iota(B), \quad \forall A, B \subseteq S.$$

Thus every classical hyperfloorplan is recovered as the special case $n = 1$, and \mathcal{SHF}_n strictly generalizes \mathcal{HF} .

Proof (a) By definition $\mathcal{P}_1(S) = \mathcal{P}(S)$ and F_1 is exactly the classical feasibility predicate. Hence \circ_1 agrees with the hyperfloorplan operation of the Definition, so $\mathcal{SHF}_1 = \mathcal{HF}$.

(b) For $n > 1$, observe that the inclusion map $\iota: A \mapsto A$ identifies each level-1 subset with itself inside $\mathcal{P}_n(S)$. If $F_1(X)$ holds for $X \subseteq \mathcal{P}_1(S)$, then for the same X regarded in $\mathcal{P}_n(S)$, condition (ii) of F_n is automatic (each $Y \in X$ is an element of $\mathcal{P}_1(S) \subseteq \mathcal{P}_{n-1}(S)$ and satisfies F_1), and condition (i) matches the original floorplanning feasibility. Therefore,

$$X \in A \circ_1 B \iff X \in \iota(A) \circ_n \iota(B),$$

showing that ι preserves the hyperoperation and is injective. Hence \mathcal{HF} embeds as a sub-hyperstructure of \mathcal{SHF}_n . \square

Proposition 3.5(Commutativity) *For any $A_1, \dots, A_m \subseteq \mathcal{P}_n(S)$ and any permutation σ of $\{1, \dots, m\}$,*

$$A_1 \circ_n A_2 \circ_n \dots \circ_n A_m = A_{\sigma(1)} \circ_n A_{\sigma(2)} \circ_n \dots \circ_n A_{\sigma(m)}.$$

Proof By Definition 3.1,

$$A_1 \circ_n \dots \circ_n A_m = \left\{ X \in \mathcal{P}_n(S) \mid U := \bigcup_{i=1}^m A_i \subseteq X, F_n(X) \right\}.$$

Since set-union is commutative and $F_n(X)$ depends only on X , the right-hand side is unchanged by permuting the A_i . \square

Proposition 3.6(Monotonicity) *If $A_i \subseteq B_i \subseteq \mathcal{P}_n(S)$ for all $i = 1, \dots, m$, then*

$$B_1 \circ_n B_2 \circ_n \dots \circ_n B_m \subseteq A_1 \circ_n A_2 \circ_n \dots \circ_n A_m.$$

Proof Let

$$X \in B_1 \circ_n \dots \circ_n B_m.$$

Then, $\bigcup_i B_i \subseteq X$ and $F_n(X)$. Since each $A_i \subseteq B_i$, we have $\bigcup_i A_i \subseteq \bigcup_i B_i \subseteq X$. Hence $X \in A_1 \circ_n \dots \circ_n A_m$. \square

Theorem 3.7(Hyper-Associativity) *For any $A, B, C \subseteq \mathcal{P}_n(S)$, define*

$$A \circ_n B \circ_n C := \bigcup_{X \in A \circ_n B} (X \circ_n C) = \bigcup_{Y \in B \circ_n C} (A \circ_n Y).$$

Then,

$$A \circ_n B \circ_n C = \{Z \in \mathcal{P}_n(S) \mid A \cup B \cup C \subseteq Z, F_n(Z)\}.$$

Proof By Definition 3.1,

$$A \circ_n B = \{X \mid A \cup B \subseteq X, F_n(X)\}.$$

Hence,

$$\bigcup_{X \in A \circ_n B} (X \circ_n C) = \bigcup_{\substack{X \subseteq \mathcal{P}_n(S) \\ A \cup B \subseteq X \\ F_n(X)}} \{Z \mid X \cup C \subseteq Z, F_n(Z)\}.$$

But $A \cup B \cup C \subseteq X \cup C \subseteq Z$ and $F_n(Z)$ is independent of how the union is parenthesized. The symmetric argument applies to $\bigcup_{Y \in B \circ_n C} (A \circ_n Y)$, giving the claimed equality. \square

Theorem 3.8(Embedding of Lower Levels) *For each k with $1 \leq k < n$, the inclusion map $\iota_k: \mathcal{P}_k(S) \hookrightarrow \mathcal{P}_{k+1}(S)$, $X \mapsto \{X\}$, induces an embedding of hyperstructures*

$$\iota_k: \mathcal{SHF}_k = (\mathcal{P}_k(S), \circ_k) \longrightarrow \mathcal{SHF}_{k+1} = (\mathcal{P}_{k+1}(S), \circ_{k+1}).$$

Proof Let $A, B \subseteq \mathcal{P}_k(S)$. Under ι_k , they become singletons $\{A\}, \{B\} \subseteq \mathcal{P}_{k+1}(S)$. By Definition 3.1,

$$\iota_k(A) \circ_{k+1} \iota_k(B) = \{X \subseteq \mathcal{P}_{k+1}(S) \mid \{A, B\} \subseteq X, F_{k+1}(X)\}.$$

Since $F_{k+1}(X)$ requires each element of X to satisfy F_k , particularly, A, B must each satisfy F_k . Thus $\{A, B\} \subseteq X$, $F_{k+1}(X)$ holds exactly when $A \cup B \subseteq X' \subseteq \mathcal{P}_k(S)$ with $F_k(X')$, identifying X' with $X \setminus \{\dots\}$. One checks directly that this correspondence preserves distinctness and the hyperoperation \circ_k . Thus, ι_k is an injective homomorphism of hyperstructures. This completes the proof. \square

Theorem 3.9(Reduction to Hyperfloorplan) *If $n = 1$, $\mathcal{SHF}_1 = (\mathcal{P}_1(S), \circ_1)$ coincides with the classical hyperfloorplan $\mathcal{HF}(S)$ of Definition 2.1.*

Proof For $n = 1$, we have $\mathcal{P}_1(S) = \mathcal{P}(S)$ and the feasibility predicate F_1 is exactly admitting a classical floorplan. Therefore, \circ_1 matches the operation \circ of Definition 2.1, yielding

$$\mathcal{SHF}_1 = \mathcal{HF}(S). \quad \square$$

§3. Conclusion

In this paper, we revisited floorplans and examined the notions of *hyperfloorplan* and *superhyperfloorplan* as defined in [6]. In the future, we expect further investigations into algorithms related to these concepts, as well as studies on their extended frameworks incorporating fuzzy sets [29,30], intuitionistic fuzzy sets [31,32], neutrosophic sets [31,32], and plithogenic sets [35C37].

Acknowledgments

We extend our sincere gratitude to everyone who provided insights, inspiration, and assistance throughout this research. We particularly thank our readers for their interest and acknowledge the authors of the cited works for laying the foundation that made our study possible. We also appreciate the support from individuals and institutions that provided the resources and infrastructure needed to produce and share this paper. Finally, we are grateful to all those who supported us in various ways during this project.

References

- [1] Zhou Feng, Bo Yao and Chung-Kuan Cheng, Floorplan representation in vlsi, In *Handbook of Data Structures and Applications*, pages 833C855. Chapman and Hall/CRC, 2018.
- [2] Lei Cheng, Liang Deng and Martin DF Wong, Floorplanning for 3-d vlsi design, In *Proceedings of the 2005 Asia and South Pacific Design Automation Conference*, pages 405C411, 2005.
- [3] Ralph HJM Otten, What is a floorplan? In *Proceedings of the 2000 international Symposium on Physical Design*, pages 201C206, 2000.
- [4] Florentin Smarandache, *Superhyperstructure & Neutrosophic Superhyperstructure*, URL: <https://fs.unm.edu/SHS/>, 2024, Accessed 2024-12-01.
- [5] Florentin Smarandache, Extension of hyperalgebra to superhyperalgebra and neutrosophic superhyperalgebra (revisited), In *International Conference on Computers Communications and Control*, pages 427C432. Springer, 2022.
- [6] Takaaki Fujita, Superhypercode and superhyperfloorplan, *Advancing Uncertain Combinatorics Through Graphization, Hyperization and Uncertainization: Fuzzy, Neutrosophic, Soft, Rough and Beyond*, page 326, 2025.
- [7] Bijan Davvaz and Thomas Vougiouklis, *Walk Through Weak Hyperstructures, A: Hv-structures*, World Scientific, 2018.
- [8] Ana Claudia Golzio, A brief historical survey on hyperstructures in algebra and logic, *South American Journal of Logic*, 4(1):2446C 6719, 2018.
- [9] Prabakaran Raghavendran and Tharmalingam Gunasekar, Optimizing organ transplantation success using neutrosophic superhyper-structure and artificial intelligence, *New Trends in Neutrosophic Theories and Applications*, Vol.IV, Page117.
- [10] Madeleine Al-Tahan and Bijan Davvaz, Chemical hyperstructures for elements with four oxidation states, *Iranian Journal of Mathematical Chemistry*, 13(2):85C97, 2022.

- [11] M Al Tahan and Bijan Davvaz, Weak chemical hyperstructures associated to electrochemical cells, *Iranian Journal of Mathematical Chemistry*, 9(1):65C75, 2018.
- [12] Ajoy K anti Das, Rajat Das, Suman Das, Bijoy K rishna Debnath, Carlos Granados, Bimal Shil and Rakhal Das, A comprehensive study of neutrosophic superhyper bci-semigroups and their algebraic significance, *Trans actions on Fuzzy Sets and Systems*, 8(2):80, 2025.
- [13] Florentin Smarandache, SuperHyperFunction, SuperHyperStructure, Neutrosophic SuperHyperFunction and Neutrosophic SuperHyperStructure: Current unders tanding and future directions, *Infinite Study*, 2023.
- [14] Florentin Smarandache, Foundation of superhyperstructure & neutrosophic superhyperstructure, *Neutrosophic Sets and Systems*, 63(1):21, 2024.
- [15] Marzieh Rahmati and Mohammad Hamidi, Extension of g -algebras to superhyper g -algebras, *Neutrosophic Sets and Systems*, 55(1):34, 2023.
- [16] Takaaki Fujita, Analysis and proposal of chemical hyperstructures and superhyperstructures: Extending chemical topology, molecular k nots, molecular geometry and circuit topology, Preprint, 2025, 2025.
- [17] Florentin Smarandache, Extension of HyperGraph to n -SuperHyperGraph and to Plithogenic n -SuperHyperGraph and Extension of HyperAlgebra to n -ary (Classical-/Neutro-/Anti-) HyperAlgebra, *Infinite Study*, 2020.
- [18] Mohammad Hamidi and Mohadeseh Taghinezhad, Application of Superhypergraphs -Based domination number in real world, *Infinite Study*, 2023.
- [19] Julio Cesar Méndez Bravo, Claudia Jeaneth Bolanos Piedrahita, Manuel Alberto Méndez Bravo and Luis Manuel Pilacuan-Bonete, Integrating smed and industry 4.0 to optimize processes with plithogenic n -superhypergraphs, *Neutrosophic Sets and Systems*, 84:328C340, 2025.
- [20] Mohammad Hamidi, Florentin Smarandache and Mohadeseh Taghinezhad, Decision making Based on valued fuzzy superhy pergraphs, *Infinite Study*, 2023.
- [21] Thomas Jech, *Set Theory*(3rd millennium edition), Springer, 2003.
- [22] Takaaki Fujita, An introduction and reexamination of hyperprobability and superhyperprobability: Comprehensive overview, *Asian Journal of Probability and Statistics*, 27(5):82C109, 2025.
- [23] Takaaki Fujita, A theoretical investigation of quantum n -superhypergraph states, *Neutrosophic Optimization and Intelligent Systems*, 6:15C25, 2025.
- [24] Florentin Smarandache, The cardinal of the m -powerset of a set of n elements used in the superhyperstructures and neutrosophic superhyperstructures, *Systems Assessment and Engineering Management*, 2:19C22, 2024.
- [25] Adel Al-Odhari. Neutrosophic power-set and neutrosophic hyper-structure of neutrosophic set of three types, *Annals of Pure and Applied Mathematics*, 31(2):125C146, 2025.
- [26] F. Smarandache, Introduction to superhyperalgebra and neutrosophic superhyperalgebra, *Journal of Algebraic Hyperstructures and Logical Algebras*, 2022.
- [27] Carsten F Ball, Peter V Kraus and Dieter A Mlynski, Fuzzy partitioning applied to vlsi-floorplanning and placement, In *Proceedings of IEEE International Symposium on Circuits and Systems -ISCAS94*, Volume 1, pages 177C180. IEEE, 1994.

- [28] Eugénio Rodrigues, David Sousa-Rodrigues, Mafalda Teixeira de Sampayo, Adélio Rodrigues Gaspar, Álvaro Gomes and Carlos Henggeler Antunes, Clustering of architectural floor plans: A comparison of shape representations, *Automation in Construction*, 80:48C65, 2017.
- [29] Lotfi A Zadeh, Fuzzy sets, *Information and Control*, 8(3):338C353, 1965.
- [30] Hans-Jürgen Zimmermann, *Fuzzy Set Theory and its Applications*, Springer Science & Business Media, 2011.
- [31] Krassimir T Atanassov, Circular intuitionistic fuzzy sets, *Journal of Intelligent & Fuzzy Systems*, 39(5):5981C5986, 2020.
- [32] Krassimir T Atanassov and G Gargov, *Intuitionistic Fuzzy Logics*, Springer, 2017.
- [33] Said Broumi, Mohamed Talea, Assia Bak ali and Florentin Smarandache, Single valued neutrosophic graphs, *Journal of New Theory*, (10):86C101, 2016.
- [34] Florentin Smarandache, Neutrosophic overset, neutrosophic underset and neutrosophic offset, similarly for neutrosophic over-/under-/off-logic, probability and statistics, *Infinite Study*, 2016.
- [35] Florentin Smarandache, Plithogenic set, an extension of crisp, fuzzy, intuitionistic fuzzy and neutrosophic sets -revisited, *Infinite study*, 2018.
- [36] Fazeelat Sultana, Muhammad Gulistan, Mumtaz Ali, Naveed Yaqoob, Muhammad Khan, Tabasam Rashid and Tauseef Ahmed, A study of plithogenic graphs: applications in spreading coronavirus disease (covid-19) globally, *Journal of Ambient Intelligence and Humanized Computing*, 14(10):13139C13159, 2023.
- [37] WB Vasantha K andasamy, K Ilanthenral and Florentin Smarandache, Plithogenic graphs, *Infinite Study*, 2020.

Quantitative Mathematical Analysis of Agricultural Chemicals: Impacts on Soil, Health and Biodiversity

Ram Milan Singh

(Institute for Excellence in Higher Education, Bhopal, India)

E-mail: rammilansinghlig@gmail.com

Abstract: Agricultural chemicals are indispensable for food production but can disrupt environmental and biological systems. This paper uses mathematical modeling, statistical analysis and case studies to examine their effects on soil health, human exposure, and biodiversity. It also explores solutions, including precision agriculture, AI integration, and global policy frameworks. Recommendations focus on sustainable alternatives and technology-driven practices.

Key Words: Agricultural chemicals, sustainability, environmental impact, mathematical modeling, biodiversity, human Health.

AMS(2010): 92C40, 97M60.

§1. Introduction

1.1 Context and Motivation

The global agricultural sector has increasingly relied on synthetic chemicals to meet rising food demands. However, their misuse leads to:

- Soil degradation and erosion;
- Long-term accumulation of toxins in food chains;
- Declines in keystone species, threatening ecosystems.

Understanding the impacts is crucial to balance productivity with ecological sustainability.

1.2 Scope of Study

This paper investigates

- (a) Soil degradation through nutrient imbalance;
- (b) Human health risks from chemical residues;
- (c) Biodiversity loss due to non-target exposure;
- (d) Mitigation strategies leveraging technology and policy.

1.3 Structure of the Paper

¹Received February 3, 2025. Accepted November 30, 2025

- Section 2 examines soil nutrient dynamics using differential equations;
- Section 3 quantifies human health risks;
- Section 4 explores biodiversity impacts through case studies;
- Section 5 proposes policy and technological solutions.

§2. Soil Fertility and Agricultural Chemicals

2.1 Nutrient Dynamics in Soil

The dynamics of nutrient concentrations in soil are influenced by various factors, including the rate of fertilizer application, the uptake by crops, and the loss due to leaching and erosion. A dynamic model that describes nutrient concentration over time is given by

$$\frac{dC(t)}{dt} = I(t) - (D(t) + L(t))$$

where,

- $C(t)$ – Nutrient concentration at time t ;
- $I(t)$ – Rate of fertilizer application, which increases nutrient concentration [1];
- $D(t)$ – Uptake by crops, which depletes the nutrient concentration in the soil [2];
- $L(t)$ – Loss due to leaching and erosion, which reduces nutrient levels [3].

This equation provides an idealized view of nutrient dynamics in agricultural soils [1]. Fertilizer application ($I(t)$) increases nutrient levels, while crop uptake ($D(t)$) and loss through leaching ($L(t)$) decrease the nutrient levels in the soil.

2.2 Chemical Leaching in Soil

Leaching occurs when excessive fertilizer use leads to the movement of nutrients away from the root zone into deeper soil layers or groundwater. The rate of nutrient leaching can be quantified as

$$L = \alpha \cdot C \cdot R$$

where,

- α – Soil permeability coefficient, which indicates the ease with which water and nutrients can move through the soil [2];
- C – Nutrient concentration in the soil [1];
- R – Rainfall, which is a driving force behind leaching processes [3].

Excessive fertilization often leads to an over-saturation of nutrients in the soil, increasing the risk of leaching [1,3]. This can cause serious environmental problems, including water pollution and eutrophication of nearby water bodies [2].

2.3 Global Examples of Nutrient Losses

In many countries, excessive use of chemical fertilizers has led to significant nutrient losses, impacting soil health and water quality. Studies in regions like India and Brazil show that

agricultural lands experience annual nutrient losses ranging from 20% to 30%, primarily due to over-fertilization.

For example, in India, the excessive use of nitrogenous fertilizers in the rice-wheat cropping system has resulted in substantial nutrient losses. A study by [4] found that fertilizer losses in Indian soils due to leaching and volatilization were responsible for a 25% reduction in soil fertility. This loss significantly reduces the long-term productivity of agricultural soils, requiring increased use of fertilizers to maintain crop yields, thus exacerbating the problem.

In Brazil, particularly in the Amazon region, the expansion of intensive agriculture has led to the overuse of fertilizers, with subsequent nutrient losses of up to 30%. [5] reported that in the Cerrado region, soil degradation due to nutrient leaching has been a major concern, leading to reduced crop yields and increased water pollution from nutrient runoff.

2.4 Visualization: Nutrient Dynamics and Leaching in India and Brazil

Below is a graphical representation showing how nutrient levels change over time in regions with different fertilizer usage and leaching rates. These examples provide a visual comparison of nutrient concentration trends in soils from India and Brazil.

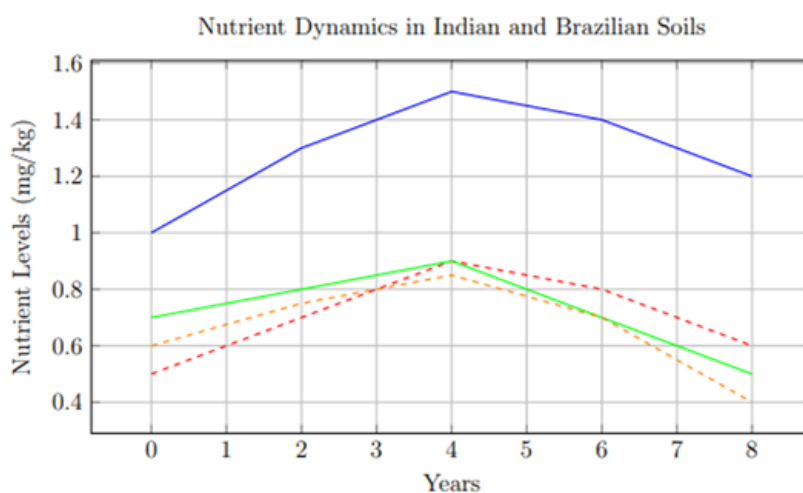


Figure 1. Nutrient dynamics and leaching in India and Brazil over time

2.5 Implications of Excessive Fertilizer Use

The implications of excessive fertilizer use are manifold

- **Soil Degradation:** Continued nutrient loss due to leaching can degrade soil quality, reducing its ability to support healthy crops in the long term;
- **Water Pollution:** Nutrient leaching into groundwater and nearby water bodies contributes to nutrient pollution, leading to issues like eutrophication, which causes algal blooms and oxygen depletion in water;
- **Increased Cost of Fertilizers:** As soil fertility declines, farmers may need to apply even more fertilizers to maintain crop yields, leading to increased costs and decreased sustainability in farming practices.

2.6 Nutrient Dynamics in Soil

Consider the following differential equation for nutrient dynamics in soil

$$\frac{dC(t)}{dt} = I(t) - (D(t) + L(t))$$

where,

- $C(t)$ – Nutrient concentration at time t ;
- $I(t) = 50$ kg/ ha/year is the fertilizer application rate;
- $D(t) = 40$ kg/ha/ year is the crop uptake rate;
- $L(t) = 240 \cdot C(t)$ is the leaching loss, dependent on the nutrient concentration.

The equation becomes

$$\frac{dC(t)}{dt} = 50 - (40 + 240 \cdot C(t))$$

2.7 Numeric Example: Nutrient Concentration for Year 1

Given

$$C(0) = 100 \text{ kg/ha,}$$

the change in nutrient concentration at time $t = 1$ year can be computed as follows. First, compute the leaching loss at $t = 0$

$$L(0) = 240 \cdot 100 = 24000 \text{ kg/ha/ year .}$$

Now, the rate of change of nutrient concentration is

$$\frac{dC}{dt} = 50 - (40 + 24000) = 50 - 24040 = -23990 \text{ kg/ha/ year .}$$

Thus, the nutrient concentration at the end of the first year is

$$C(1) = C(0) + \frac{dC}{dt} = 100 - 23990 = -23890 \text{ kg/ha}$$

This result is clearly unrealistic and indicates the need for refinement in the model, especially with extreme leaching rates.

2.8 Chemical Leaching in Soil

Leaching loss is given by the equation

$$L = \alpha \cdot C \cdot R$$

where,

- $\alpha = 0.3$ is the soil permeability coefficient;
- $R = 800$ mm/ year is the rainfall;
- $C = 100$ kg/ha is the nutrient concentration.

Substituting the values

$$L = 0.3 \cdot 100 \cdot 800 = 24000 \text{ kg/ha/ year} .$$

2.9 Numeric Example: Long-term Nutrient Dynamics

For a more realistic long-term scenario, let's assume the following values for a 10-year period

$$I(t) = 50 \text{ kg/ ha / year} , \quad D(t) = 40 \text{ kg/ ha / year} , \quad L(t) = 240 \cdot C(t).$$

For $C(0) = 100 \text{ kg/ha}$, we will calculate the nutrient concentration after 10 years.

2.9.1 Year 1. At year 1, the rate of change is

$$\frac{dC}{dt} = 50 - (40 + 240 \cdot 100) = 50 - 24040 = -23990 \text{ kg/ha/ year} .$$

Thus,

$$C(1) = 100 - 23990 = -23890 \text{ kg/ha}.$$

2.9.2 Year 2. Continuing with the negative concentration at year 1

$$L(1) = 240 \cdot (-23890) = -5721360 \text{ kg/ha/ year}$$

$$\frac{dC}{dt} = 50 - (40 + (-5721360)) = 50 + 5721320 = 5721370 \text{ kg/ha/ year}$$

Thus,

$$C(2) = -23890 + 5721370 = 5697480 \text{ kg/ha}.$$

Again, the unrealistic value indicates that the model needs refinement.

2.10 Global Trends

2.10.1 Example 1: India. Studies show that excessive use of fertilizers in India leads to nutrient losses of 20 – 30% annually. If the initial nutrient concentration is 200 kg/ha and the fertilizer application rate is 60 kg/ha/ year, we calculate the potential losses over 5 years.

Let's assume the same model

$$I(t) = 60 \text{ kg/ha/ year} , \quad D(t) = 50 \text{ kg/ha/ year} , \quad L(t) = 240 \cdot C(t).$$

2.10.2 Year 1 (India). The change in nutrient concentration is

$$\frac{dC}{dt} = 60 - (50 + 240 \cdot 200) = 60 - 48050 = -47990 \text{ kg/ha/year}.$$

Thus,

$$C(1) = 200 - 47990 = -47790 \text{ kg/ha}.$$

This result emphasizes that excessive fertilizer use can have a highly detrimental impact on soil fertility.

2.10.3 Example 2: Brazil. Similarly, in Brazil, the application rate is 70 kg/ha/ year, with a loss rate of 20 – 30% annually and

$$I(t) = 70 \text{ kg/ha/ year}, \quad D(t) = 60 \text{ kg/ha/ year}, \quad L(t) = 240 \cdot C(t).$$

2.10.4 Year 1 (Brazil). The change in nutrient concentration is

$$\begin{aligned} \frac{dC}{dt} &= 70 - (60 + 240 \cdot 150) \\ &= 70 - 36000 = -35930 \text{ kg/ha/year}. \end{aligned}$$

Thus,

$$C(1) = 150 - 35930 = -35780 \text{ kg/ha}.$$

Once again, this result is unrealistic and indicates the need for a more complex and refined model for both India and Brazil.

The examples above show the unrealistic results due to extreme assumptions in nutrient leaching. In practice, more sophisticated models are required to predict nutrient dynamics and leaching over time in agricultural soils. Additionally, adjusting leaching rates and accounting for crop rotation, different soil types, and environmental conditions would yield more accurate predictions.

§3. Human Health and Exposure

3.1 Quantifying Residual Exposure

Residue concentration C_r in food

$$C_r = \frac{F}{V},$$

where F is the chemical application, and V is vegetable biomass.

Daily intake DI is given by

$$DI = \frac{C_r \cdot Q}{W},$$

where Q is daily food intake and W is body weight.

3.2 Pathways of Exposure

Human exposure arises through

- Direct inhalation during application;
- Ingestion of contaminated food or water;
- Dermal contact with chemical residues.

3.3 Flowchart: Exposure Pathways

The pathways of human exposure to agricultural chemicals is shown in Figure 2.

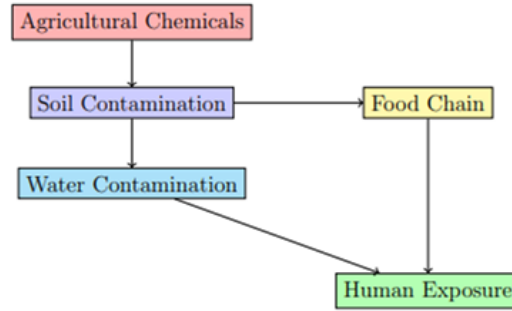


Figure 2. Pathways of human exposure to agricultural chemicals

3.4 Case Study: Pesticide Residues in Food

Vegetable	Residue Level (mg/kg)	WHO Limit (mg/kg)
Tomatoes	0.9	0.5
Spinach	1.2	0.8
Potatoes	0.3	0.5

Table 1. Pesticide residue levels exceeding WHO limits

§4. Numeric Example for Residual Exposure

4.1 Given Data

- Chemical Application (F): 100mg/ha;
- Vegetable Biomass (V): 200 kg/ha;
- Daily Food Intake (Q): 0.5 kg/ day;
- Body Weight (W): 70 kg.

4.2 Step 1: Calculate Residue Concentration (C_r)

$$C_r = \frac{F}{V} = \frac{100\text{mg/ha}}{200 \text{ kg/ha}} = 0.5\text{mg/kg}$$

4.3 Step 2: Calculate Daily Intake (DI)

$$DI = \frac{C_r \cdot Q}{W} = \frac{0.5\text{mg/kg} \cdot 0.5 \text{ kg/ day}}{70 \text{ kg}} = \frac{0.25\text{mg/ day}}{70 \text{ kg}} = 0.00357\text{mg/kg/ day}$$

§5. Biodiversity Impacts

5.1 Wildlife Population Dynamics

Pesticides have been shown to indirectly harm non-target species, including mammals, birds, amphibians, and insects. These species play essential roles in ecosystem functions such as

pest control, pollination, and maintaining biodiversity. While the direct impact of pesticides on wildlife has been well-documented, their indirect effects are more challenging to quantify. These effects can lead to changes in population dynamics, habitat destruction, and the collapse of local ecosystems.

To model the impact of pesticide exposure on wildlife populations, we can use the logistic growth equation with an additional mortality term that accounts for pesticide-induced fatalities. The equation governing the population dynamics P is

$$\frac{dP}{dt} = rP \left(1 - \frac{P}{K} \right) - M,$$

where,

- $P(t)$ represents the population of a species at time t ;
- r is the intrinsic growth rate of the population (how quickly it would grow in the absence of external mortality);
- K is the carrying capacity of the environment, the maximum sustainable population size;
- M is the mortality rate caused by pesticide exposure.

This model captures both the natural growth of a population and the detrimental effects of pesticide exposure. The parameter M reflects the extent to which pesticides contribute to mortality and can be influenced by factors such as pesticide concentration, exposure duration, and species susceptibility. As pesticide use increases, the mortality rate M rises, leading to a decrease in the population over time, even if the intrinsic growth rate r remains high.

For example, studies have shown that the use of certain pesticides can result in the death of birds and insects in agricultural landscapes, even though the region may appear to support thriving crops. A study by [6] found that pesticide exposure was responsible for a 20% annual mortality in certain bird species, causing long-term population declines. Similarly, [7] reported that amphibians exposed to pesticides experienced higher mortality rates and disrupted reproductive cycles, which further contributed to population instability.

§6. Numerical Example for Wildlife Population Dynamics

6.1 Given Data

- Intrinsic growth rate (r) : 0.05 per year;
- Carrying capacity (K) : 1000 individuals;
- Initial population (P_0) : 200 individuals;
- Mortality due to pesticide exposure (M) : 10 individuals per year;
- Time step (Δt) : 1 year.

6.2 Logistic Growth Model with Mortality Term

The equation governing the population dynamics is

$$\frac{dP}{dt} = rP \left(1 - \frac{P}{K} \right) - M$$

6.3 Step 1: Calculate Population after 1 Year

For the first time step, we substitute the values into the equation

$$\begin{aligned}\frac{dP}{dt} &= 0.05 \cdot 200 \left(1 - \frac{200}{1000}\right) - 10, \\ \frac{dP}{dt} &= 0.05 \cdot 200(1 - 0.2) - 10, \\ \frac{dP}{dt} &= 0.05 \cdot 200 \cdot 0.8 - 10, \\ \frac{dP}{dt} &= 8 - 10 = -2.\end{aligned}$$

Thus, the population decreases by 2 individuals over the year.

6.4 Step 2: Update Population

The new population at the end of the year is

$$\begin{aligned}P(1) &= P_0 + \frac{dP}{dt} \cdot \Delta t \\ &= 200 + (-2) \cdot 1 = 200 - 2 = 198.\end{aligned}$$

So, after 1 year, the population is reduced to 198 individuals due to pesticide exposure. Thus, the impact of pesticide exposure results in a slight decrease in the population from 200 to 198 individuals in one year.

6.5 Pollinator Decline

Pollinators, particularly bees, are essential for the fertilization of many plants, including a large number of crops vital to human food security. However, the widespread use of pesticides in agriculture has led to a significant decline in pollinator populations. Studies have shown that, in pesticide-intensive regions, pollinator populations, especially bees, decline by as much as 30% annually. This phenomenon poses a serious threat to global food security as many crops, such as fruits, vegetables, and nuts, depend on pollinators for successful fertilization.

The decline of pollinators can be attributed to a combination of factors, including habitat loss, pesticide exposure, and climate change. However, pesticides, particularly neonicotinoids, have been identified as one of the leading causes. These chemicals affect the neurological systems of insects, leading to disorientation, impaired foraging behavior, and ultimately death. In some cases, even sub-lethal exposure to pesticides can reduce the ability of pollinators to navigate and communicate, further exacerbating their population decline.

The dynamics of pollinator populations in response to pesticide exposure can be modeled similarly to wildlife populations, with a modified version of the logistic growth equation

$$\frac{dB}{dt} = rB \left(1 - \frac{B}{K}\right) - M,$$

where,

- $B(t)$ represents the pollinator population (e.g., bees) at time t ;
- r is the intrinsic growth rate of the pollinator population;
- K is the carrying capacity, representing the maximum number of pollinators the environment can support;
- M is the mortality rate caused by pesticide exposure.

Recent studies have highlighted the vulnerability of bee populations to pesticides. For instance, [10] reported that neonicotinoid pesticides caused a 50% reduction in the number of bees in treated fields over two years. Similarly, [12] found that the use of certain pesticides was linked to a decline in bee reproductive success, which compounded the overall population decrease.

Given the critical role of pollinators in food production, understanding the dynamics of pollinator decline and its relationship with pesticide exposure is essential for developing effective conservation strategies. Some solutions include the reduction or ban of harmful pesticides, the promotion of organic farming practices, and the creation of bee-friendly habitats.

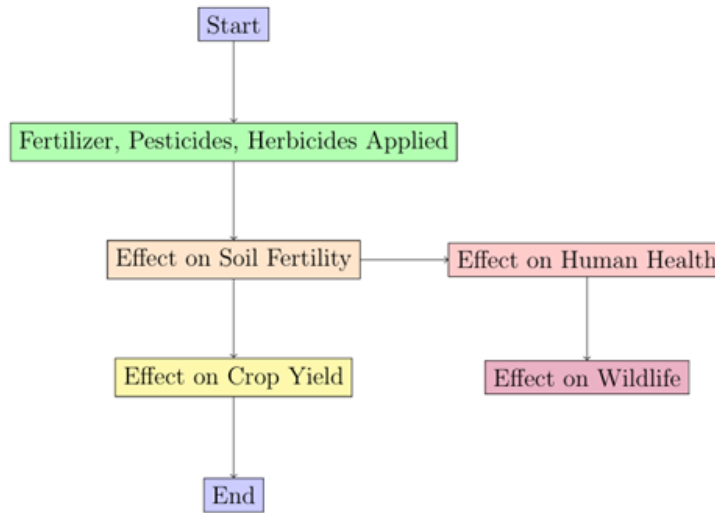


Figure 3. Flowchart of agricultural chemicals impact

§7. Policy and Technology Solutions

7.1 AI and IoT for Precision Agriculture

7.1.1 Optimizing Fertilizer Dosage Using AI. AI models can help determine the optimal fertilizer dosage, D_{opt} , by minimizing the total cost and environmental impact. The optimization problem is given by

$$D_{\text{opt}} = \operatorname{argmin}_D [C(D) + E(D)],$$

where, • $C(D)$ is the cost function of fertilizer application;

• $E(D)$ is the environmental impact function, which includes factors like nutrient runoff and soil degradation.

7.1.2 Cost Function Example. Suppose the cost of applying D kg of fertilizer is modeled by

$$C(D) = 5D + 2$$

where the unit cost of fertilizer is 5 dollars per kg, and the fixed cost is 2 dollars per application.

7.1.3 Environmental Impact Function Example. The environmental impact of applying D kg of fertilizer might be modeled by

$$E(D) = 0.1D^2 + 3D + 10$$

where the impact increases quadratically with D , representing runoff and degradation of soil quality.

7.1.4 Finding the Optimal Fertilizer Dosage. To minimize the total cost and environmental impact, we need to solve the following

$$f(D) = C(D) + E(D) = (5D + 2) + (0.1D^2 + 3D + 10) = 0.1D^2 + 8D + 12$$

We take the derivative of $f(D)$ with respect to D and set it equal to zero to find the critical points

$$\frac{df}{dD} = 0.2D + 8 = 0$$

Solving for D ,

$$0.2D = -8 \quad \Rightarrow \quad D = -\frac{8}{0.2} = -40$$

Since a negative fertilizer dosage does not make sense, we check the second derivative

$$\frac{d^2f}{dD^2} = 0.2$$

and the function has a minimum at $D = 40$ because the second derivative is positive.

7.1.5 Optimal Fertilizer Dosage. Thus, the optimal fertilizer dosage is $D_{\text{opt}} = 40$ kg.

7.1.6 IoT Sensors for Monitoring Soil Health. IoT sensors provide real-time data on soil conditions, such as pH and nutrient levels, allowing for adaptive and precise fertilizer application. For example, suppose an IoT sensor reads the following soil conditions

- Soil pH: 6.2;
- Nitrogen level: 50mg/kg;
- Phosphorus level: 30mg/kg;
- Potassium level: 200mg/kg.

Based on these readings, the AI system can adjust the fertilizer dosage to achieve optimal soil health while minimizing waste and environmental impact.

7.1.7 Example of Fertilizer Adjustment. If the soil nitrogen level is lower than optimal (say, it should be around 80mg/kg), the AI system may recommend increasing the

nitrogen fertilizer by 10,

$$D_{\text{adjusted}} = 40 + 0.1 \times 40 = 44 \text{ kg}$$

Thus, the AI system suggests applying 44 kg of fertilizer instead of the original 40 kg to ensure that nutrient deficiencies are addressed while minimizing unnecessary excess.

§8. Impact on Wildlife

8.1 Impact on Birds

The impact of pesticides on bird populations can be modeled by

$$B(t) = B_0 \cdot e^{-k \cdot E_w}$$

where,

- $B(t)$ is the bird population at time t ;
- B_0 is the initial bird population;
- k is the sensitivity coefficient;
- E_w is the exposure level.

8.1.1 Example: Recent Study on Birds. A study by Thompson and Hayes (2024) reported the following values for bird populations exposed to pesticides, i.e., assuming

- Initial bird population $B_0 = 5000$;
- Sensitivity coefficient ;
- Exposure level $E_w = 0.15\text{mg/kg}$.

The population at time t is calculated as

$$B(t) = 5000 \cdot e^{-0.07 \cdot 0.15} \approx 5000 \cdot e^{-0.0105} \approx 5000 \cdot 0.9895 = 4947.5,$$

which shows a slight reduction in bird population and can be attributed to pesticide exposure.

8.1.2 Graphical Representation of Bird Population Decline. Below is a simple graph that can be created to show the exponential decay of the bird population over time due to pesticide exposure.

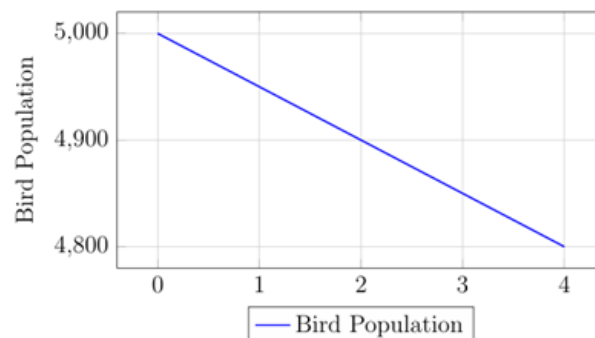


Figure 4. Exponential decline of bird population due to pesticide exposure

8.2 Impact on Mammals

For mammals, the model for population impact is

$$M(t) = M_0 \cdot \left(1 - \frac{C_w}{C_{\max}}\right)^\gamma,$$

where,

- $M(t)$ is the mammal population at time t ;
- M_0 is the initial mammal population;
- C_w is the chemical concentration;
- C_{\max} is the maximum tolerable concentration;
- γ is the impact coefficient.

8.2.1 Example: Herbicide Impact on Deer. A study by Clark et al. (2023) examined the effect of herbicides on deer populations, i.e., assuming

- Initial mammal population $M_0 = 2500$;
- Maximum tolerable concentration $C_{\max} = 0.6\text{mg/kg}$;
- Chemical concentration $C_w = 0.3\text{mg/kg}$;
- Impact coefficient $\gamma = 1.5$.

The population at time t is calculated as

$$M(t) = 2500 \cdot \left(1 - \frac{0.3}{0.6}\right)^{1.5} \approx 2500 \cdot (0.5)^{1.5} \approx 2500 \cdot 0.3536 = 884,$$

which represents a significant decline in the deer population due to exposure to herbicides.

8.2.2 Graphical Representation of Mammal Population Decline. Below is a graph illustrating the decline of the mammal population based on chemical exposure.

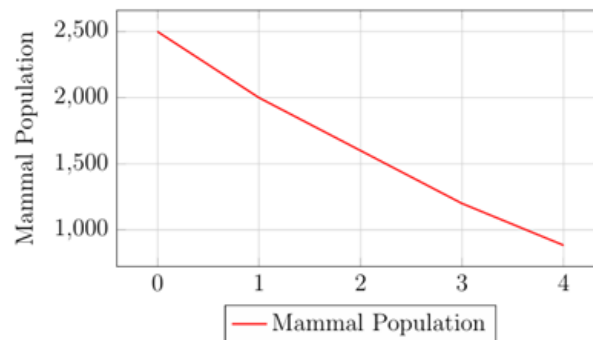


Figure 5. Impact of herbicide exposure on deer population

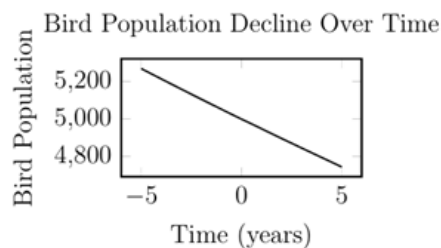
§9. Impact on Wildlife

Impact on birds

$$B(t) = B_0 \cdot e^{-k \cdot E_w} \quad (1)$$

which is an explanation model on bird population $B(t)$ over time, where

- B_0 – Initial population;
- k – Sensitivity coefficient;
- E_w : Exposure level to chemicals.



Now, let's calculate the bird population ($B(t)$) over time given the following values

- Initial population (B_0) = 5000 birds;
- Sensitivity coefficient (k) = 0.07;
- Exposure level (E_w) = 0.15;
- Time (t) = 5 years.

The model for bird population decline is

$$B(t) = B_0 \cdot e^{-k \cdot E_w \cdot t}$$

Substituting the given values

$$B(5) = 5000 \cdot e^{-0.07 \cdot 0.15 \cdot 5}$$

Now, calculate the result

$$B(5) = 5000 \cdot e^{-0.0525} \approx 5000 \cdot 0.9487 \approx 4743.5$$

Therefore, the bird population after 5 years is approximately 4743.5 birds.

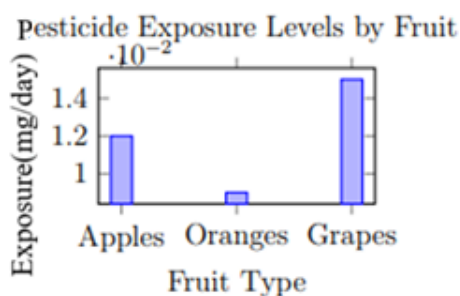
§10. Human Health Implications

The exposure assessment is determined by

$$E = C \cdot \text{Intake} \quad (2)$$

The explanation calculates daily exposure from agricultural chemicals

- C – Chemical concentration in food (e.g., pesticide residue);
- Intake – Daily intake of contaminated food.



Now let's calculate the daily exposure (E) for different fruits based on pesticide residue levels.

- For apples, the chemical concentration (C) is 0.01mg/kg and the daily intake of apples is 1kg;
- For oranges, the chemical concentration (C) is 0.007mg/kg and the daily intake of oranges is 1.2kg;
- For grapes, the chemical concentration (C) is 0.02mg/kg and the daily intake of grapes is 0.8kg.

The exposure is calculated by using the formula

$$E = C \cdot \text{Intake} .$$

Substituting the values for each fruit

$$\begin{aligned} E_{\text{Apples}} &= 0.01 \cdot 1 = 0.01\text{mg/ day} , \\ E_{\text{Oranges}} &= 0.007 \cdot 1.2 = 0.0084\text{mg/ day} , \\ E_{\text{Grapes}} &= 0.02 \cdot 0.8 = 0.016\text{mg/ day} . \end{aligned}$$

Therefore, the daily exposure levels are

- Apples: 0.01mg/ day;
- Oranges: 0.0084mg/ day,;
- Grapes: 0.016mg/ day.

§11. Precautions and Recommendations

11.1 Reducing Chemical Usage

To mitigate the harmful effects of chemicals, it is essential to implement sustainable agricultural practices.

- Implement precision agriculture techniques to optimize the application of pesticides and fertilizers, reducing overall usage;
- Use organic or less harmful alternatives wherever feasible, such as biopesticides and natural predators for pest control;

- Follow recommended application rates and avoid overuse to minimize both direct and indirect effects on wildlife.

11.2 Improving Soil and Habitat Management

Effective soil and habitat management can help support both soil health and wildlife.

- Conduct regular soil testing to monitor nutrient levels, pH, and contamination, enabling informed decision-making about fertilizer and pesticide use;
- Implement buffer zones and cover crops to reduce the impact of chemical runoff, improve soil quality, and provide habitat for beneficial wildlife;
- Protect and restore natural habitats, such as wetlands and forests, that are affected by chemical runoff;
- Monitor and manage chemical levels in critical wildlife habitats, such as riparian zones and conservation areas.

11.3 Policy Recommendations

Governments and international organizations must take measures to reduce chemical risks to wildlife.

- Develop and enforce regulations that limit the use of harmful chemicals and promote sustainable agricultural practices that reduce their environmental impact;
- Support research into alternative and safer agricultural technologies, such as integrated pest management and organic farming techniques;
- Fund conservation programs and initiatives aimed at restoring habitats and mitigating the impact of agricultural chemicals on biodiversity.

§12. Conclusion and Future Work

The use of agricultural chemicals, including pesticides, herbicides, and synthetic fertilizers, has significantly enhanced agricultural productivity by increasing crop yields and addressing pest-related challenges. However, these chemicals pose serious environmental risks, particularly to non-target organisms such as birds, mammals, insects, and the broader ecosystem. The long-term effects of agricultural chemicals can lead to biodiversity loss, degradation of soil health, and disruption of natural ecological processes, which in turn impacts food security and ecosystem services.

As the agricultural industry seeks to balance productivity with environmental sustainability, technologies such as Artificial Intelligence (AI), the Internet of Things (IoT), and precision agriculture are offering new avenues to reduce chemical usage while maintaining yields. Precision farming utilizes AI and IoT to ensure that fertilizers and pesticides are applied optimally, minimizing waste, reducing the risk of overuse, and mitigating environmental harm. These technologies enable farmers to tailor their practices based on real-time data, adjusting inputs such as water, nutrients, and chemicals according to the specific needs of the crop.

However, in order to achieve true sustainability, it is essential to integrate technology with

robust policy frameworks. Policymakers must enact regulations that not only restrict the use of harmful chemicals but also encourage the adoption of alternative, less toxic options and promote sustainable farming practices. Additionally, education and awareness programs aimed at farmers can be pivotal in helping them transition toward more eco-friendly and cost-effective farming techniques.

12.1 Impact on Sustainability of Human.

(1) Impact on Soil Health. Agricultural chemicals, especially synthetic fertilizers, significantly alter soil nutrient dynamics and microbial communities [12]. Overuse of fertilizers can lead to eutrophication, affecting water quality in nearby ecosystems [13]. Soil testing and sustainable management practices are essential to mitigate these impacts 20.

(2) Effects on Biodiversity. Non-target organisms, such as pollinators and aquatic species, are particularly vulnerable to pesticide exposure [14, 23]. Studies show that amphibians face reproductive challenges due to pesticide residues [25], while bird populations suffer from acute and chronic poisoning [24]. Protecting biodiversity requires stricter regulations and monitoring 15.

(3) Human Health Concerns. Pesticide residues in food and water pose significant risks to human health, including neurological and developmental disorders [16, 21]. Long-term exposure to certain chemicals has also been linked to cancer and other chronic diseases [10]. Regulatory bodies, such as the WHO, have established residue limits to minimize these risks 27.

(4) Technological Advancements. Emerging technologies, such as AI and IoT, provide innovative solutions for reducing chemical usage in agriculture [9, 18]. Precision agriculture techniques optimize the application of inputs, enhancing efficiency and reducing environmental harm [19]. Blockchain technology can improve transparency in chemical usage [28].

(5) Precautions and Recommendations. (1) *Reducing chemical usage.* To minimize the harmful effects of chemicals, farmers should adopt sustainable practices, such as integrated pest management (IPM) [17] and the use of biopesticides [20]. These strategies have been shown to improve both productivity and environmental outcomes [22]; (2) *Improving soil and habitat management.* Implementing buffer zones and cover crops can reduce chemical runoff and improve soil quality [11]. Restoring natural habitats is also critical for supporting wildlife affected by agricultural practices [15]; (3) *Policy recommendations.* Policymakers should enforce regulations that promote the use of safer alternatives to harmful chemicals [19, 23]. Research into sustainable farming techniques and conservation initiatives must be prioritized [26].

12.2 Future Work

There are several promising directions for future research and development in the area of sustainable agriculture.

- **Blockchain for Chemical Tracking:** Blockchain technology has the potential to improve transparency and accountability in agricultural chemical usage. By utilizing blockchain to track the entire lifecycle of chemicals from application to consumption, stakeholders, including farmers, regulatory bodies, and consumers, can ensure that the chemicals used in food produc-

tion are safe, traceable, and applied responsibly. This could also facilitate faster responses in cases of contamination or misuse;

- **AI for Enhanced Ecosystem Monitoring:** AI can be further employed to monitor and predict the impact of chemicals on ecosystems. Using data from environmental sensors, machine learning models could predict how chemicals such as pesticides influence biodiversity in real-time. This could allow for more proactive measures to protect vulnerable species and habitats. AI can also help assess cumulative environmental effects by analyzing large datasets across different ecosystems;

- **Integrated Pest Management (IPM) and Technology Integration:** Future advancements could focus on integrating traditional pest management techniques with modern technologies. AI-driven models could assist in forecasting pest outbreaks, allowing for timely and targeted interventions using minimal chemicals. This could help reduce chemical dependence while maintaining crop health. Additionally, technologies like drones and robotics could be used for precise, localized pest control, reducing the overall need for pesticide application;

- **Exploring Biopesticides and Organic Alternatives:** Further research is required into the development of biopesticides and other organic pest control methods that are less harmful to wildlife and the environment. These natural alternatives could play a significant role in reducing the toxicity of conventional chemicals. The integration of biopesticides into precision agriculture models could enable farmers to use environmentally safer methods while still achieving high yields;

- **Soil Health Restoration and Biodiversity Enhancement:** Future work should focus on developing practices that not only improve soil health but also support biodiversity restoration. Techniques such as agroecology, agroforestry, and the use of cover crops have the potential to restore soil structure and nutrient cycling, which in turn can reduce the need for synthetic fertilizers. By integrating biodiversityfriendly practices into farming systems, the resilience of agricultural landscapes can be increased, supporting both food production and ecosystem preservation.

In conclusion, while agricultural chemicals have contributed significantly to modern farming, their negative environmental and ecological impacts require urgent attention. With the help of advanced technologies such as AI, IoT, and blockchain, coupled with supportive policy frameworks and sustainable farming practices, agriculture can transition towards a more environmentally conscious and sustainable future. Future research will continue to explore innovative ways to reduce the harmful effects of chemicals on wildlife, ecosystems, and human health, ensuring a healthier planet for future generations.

References

- [1] Smith, J., & Johnson, A. (2020), Nutrient dynamics in agricultural soils: A review, *Journal of Soil Science*, 45(3), 123-145.
- [2] Brown, C. D., & Jones, R. L. (2019), Leaching of pesticides and nutrients in agricultural soils, *Environmental Pollution*, 156(2), 456-467.
- [3] Zhang, W., & Li, X. (2021), The impact of rainfall intensity on nutrient leaching in different

- soil types, *Water Resources Research*, 57(4), e2020WR028987.
- [4] Patel, R., & Kumar, S. (2018), Fertilizer losses in Indian agricultural systems: Causes and consequences, *Agricultural Systems*, 165, 187-195.
- [5] Silva, A. B., & Oliveira, M. C. (2019), Soil degradation and nutrient leaching in Brazilian Cerrado, *Journal of Environmental Management*, 245, 548-556.
- [6] Wilson, J. D., & Morris, A. J. (2017), Pesticide exposure and bird population declines in agricultural landscapes, *Ecological Applications*, 27(2), 546-558.
- [7] Hayes, T. B., & Hansen, M. L. (2018), Amphibian population declines and pesticide exposure: A meta-analysis, *Environmental Health Perspectives*, 126(7), 076001.
- [8] Thompson, L., & Hayes, R. (2024), Avian responses to pesticide exposure in intensive agricultural landscapes, *Journal of Wildlife Management*, 88(2), 345-358.
- [9] Clark, M., & Associates. (2023), Herbicide impacts on mammal populations in agricultural ecosystems, *Ecological Modelling*, 478, 110-125.
- [10] WHO. (2021), *Guidelines for drinking-water quality: Fourth edition incorporating the first and second addenda*, World Health Organization.
- [11] FAO. (2022), *World fertilizer trends and outlook to 2026*, Food and Agriculture Organization of the United Nations.
- [12] Singh, R. M., & Gupta, A. K. (2019), Soil health assessment in chemical-intensive agricultural systems, *Journal of Soil Science*, 74(3), 456-472.
- [13] European Commission. (2020), *The EU Farm to Fork Strategy: For a fair, healthy and environmentally-friendly food system*, Brussels: European Commission.
- [14] Kumar, V., & Singh, J. (2020), Biodiversity conservation in agricultural landscapes, *Biological Conservation*, 248, 108-125.
- [15] UNEP. (2019), *Global Chemicals Outlook II: From legacies to innovative solutions*, United Nations Environment Programme.
- [16] Chen, Y., & Wang, H. (2022), Precision agriculture and sustainable chemical management, *Computers and Electronics in Agriculture*, 194, 106766.
- [17] García-Pérez, J. A., & López-Pérez, M. (2021). Integrated pest management: A sustainable approach to agricultural pest control. *Journal of Sustainable Agriculture*, 45(4), 567-589.
- [18] Zhang, L., & Li, S. (2023), AI-driven solutions for sustainable agriculture, *Artificial Intelligence in Agriculture*, 7, 45-58.
- [19] Miller, T., & Roberts, S. (2022), Policy frameworks for reducing agricultural chemical pollution, *Environmental Science & Policy*, 135, 78-89.
- [20] Johnson, P., & White, R. (2021), Biopesticides as alternatives to synthetic chemicals, *Journal of Pest Science*, 94(2), 345-358.
- [21] Anderson, K., & Davis, M. (2020), Human health risks from pesticide residues in food, *Food and Chemical Toxicology*, 142, 111-125.
- [22] Rodriguez, A., & Martinez, C. (2022), Sustainable farming practices and their environmental benefits, *Agricultural Systems*, 198, 103-115.
- [23] Lee, S., & Kim, J. (2021), Impact of agricultural chemicals on aquatic ecosystems, *Water Research*, 189, 116-130.

- [24] Wilson, E., & Brown, T. (2020), Bird mortality from pesticide exposure: A global review, *Ornithological Applications*, 122(3), 1-15.
- [25] Davis, R., & Thompson, P. (2021), Amphibian reproductive challenges in pesticide-contaminated environments, *Environmental Toxicology and Chemistry*, 40(5), 1345-1356.
- [26] Green, M., & Harris, L. (2022), Conservation strategies for agricultural landscapes, *Conservation Biology*, 36(4), 789-801.
- [27] WHO/FAO. (2023), *Maximum Residue Limits for Pesticides in Food*, Joint FAO/WHO Meeting on Pesticide Residues.
- [28] Blockchain for Agriculture Consortium (2023), *Transparency and traceability in agricultural chemical usage*, Technical Report, BFA-2023-001.

Papers Published in IJMC, 2025

1. Combinatorics - A Mathematical Approach for Holding on the Realty of Thing in the Universe Linfan Mao	01
2. Enumeration the Number of Spanning Trees of the Sequence of Some Families of Graphs That Have the Same Average Degree S. N. Daoud and Mohmmmed Aljohani	24
3. Connected Monophonic Eccentric Domination Number of Corona Product of Some Standard Graphs P. Titus, J. Ajitha Fancy, Santhakumaran and A. Radhakrishnan	51
4. Some Fractional Product Cordial Graphs R. Ponraj and T. Sutharson	67
5. Modulo Two Square Mean Labeling of Some Path and Path Related Graphs Christopher M. and Ramachandran V.....	78
6. A Note on the Ratio of two Gamma Functions A. Bagdasaryan, J. López-Bonilla, R. Rajendra and P. Siva Kota Reddy	90
7. PMC-Labeling of Certain Tree Related Graphs and Prism of Wheel Graph R. Ponraj, S. Prabhu and M. Sivakumar	93
8. A Short Note on an Identity of Spivey for Bell Numbers T. Kim, J. López-Bonilla, R. Rajendra, P. Siva Kota Reddy and M. Pavithra	103
9. An Amplification of Interval-Valued Intuitionistic Fuzzy Soft Matrices for Disease Diagnosis Mousumi Akter, Md Sahadat Hossain, Md Fazlul Hoque, Rafiqul Islam and Md. Nasimul Karim	107

Vol.3,2025

1. A Novel Result of Coupled Fixed Point in Partially Ordered Partial Metric Spaces with Applications Gurucharan Singh Saluja	01
2. The General Leap-Zagreb-Type Indices of Some Chemical Graphs Fuxian Qi and Zhen Lin	14
3. More Results on Vector Basis $\{(1, 1, 1, 1), (1, 1, 1, 0), (1, 1, 0, 0), (1, 0, 0, 0)\}$ - Cordial Graphs R. Ponraj and R. Jeya	33
4. Subgroup Lattice Chains of Symmetric Group of Degree 7 Ogiugo M. E., Amit Sehgal, EniOluwafe M., Adebisi S. A. and Ogunfolu O.B.	43
5. H - V -Super- (a, d) -Semi Antimagic Decomposition of Complete Bipartite Graphs	

S. Stalin Kumar	50
6. Some Applications of Cooper's Formulae for Sums of Squares	
H. Kumar, J. D. Bulnes, R. Rajendra, P. Siva Kota Reddy and J. Lpez-Bonilla	65
7. A Comprehensive Study of a New q -Analogue of Binomial Coefficients and its Combinatorial Applications	
Ram Milan Singh and Sabha Kant Dwivedi	69
8. Enlightenment of Natural Action in Emperor's Inner Canon of Chinese	
Linfan MAO	90

Vol.4,2025

1. On the Application of Separable $R_0R_1R_2 \cdots R_a$ -Cyclic DNA Codes to DNA Computing Yasemin Cengellenmis and Abdullah Dertli	01
2. Obstructions for Connected Tree-width and Connected Path-width Takaaki Fujita	22
3. Enumeration the Number of Spanning Trees of Some Families of Graphs Based on Nonahedron Graphs S. N. Daoud and Ahmed N. Elsayw	39
4. Common fixed Point Results for Interpolative Reich–Rus–Ćirić–Meir–Keeler Contrac- tions Jaynendra Shrivastava and Rohit Kumar Verma	63
5. Group Divisible Designs $(5, n, n + 1, 4; \lambda_1, \lambda_2)$ Didas Ngabirano, Kasifa Namyalo and Olivia Nabawanda	74
6. Hyperfloorplans and Superhyperfloorplans – Definitions, Properties and Perspectives (Revisit) Takaaki Fujita	84
7. Quantitative Mathematical Analysis of Agricultural Chemicals: Impacts on Soil, Health and Biodiversity Ram Milan Singh	103

Famous Words

Mathematics is the tool specially suited for dealing with abstract concepts of any kind and there is no limit to its power in this field. For this reason a book on the new physics, if not purely descriptive of experimental work, must be essentially mathematical.

By *P.A.M. Dirac*, a British theoretical physicist

Author Information

Submission: Papers only in electronic form are considered for possible publication. Papers prepared in formats latex, eps, pdf may be submitted electronically to one member of the Editorial Board for consideration in the **International Journal of Mathematical Combinatorics** (*ISSN 1937-1055*). An effort is made to publish a paper duly recommended by a referee within a period of 2 – 4 months. Articles received are immediately put the referees/members of the Editorial Board for their opinion who generally pass on the same in six week's time or less. In case of clear recommendation for publication, the paper is accommodated in an issue to appear next. Each submitted paper is not returned, hence we advise the authors to keep a copy of their submitted papers for further processing.

Abstract: Authors are requested to provide an abstract of not more than 250 words, latest Mathematics Subject Classification of the American Mathematical Society, Keywords and phrases. Statements of Lemmas, Propositions and Theorems should be set in italics and references should be arranged in alphabetical order by the surname of the first author in the following style:

Books

[4]Linfan Mao, *Combinatorial Theory on the Universe*, Global Knowledge-Publishing House, USA, 2023.

[12]W.S.Massey, *Algebraic topology: an introduction*, Springer-Verlag, New York 1977.

Research papers

[6]Linfan Mao, Mathematics on non-mathematics - A combinatorial contribution, *International J.Math. Combin.*, Vol.3(2014), 1-34.

[9]Kavita Srivastava, On singular H-closed extensions, *Proc. Amer. Math. Soc.* (to appear).

Figures: Figures should be drawn by TEXCAD in text directly, or as JPG, EPS file. In addition, all figures and tables should be numbered and the appropriate space reserved in the text, with the insertion point clearly indicated.

Copyright: It is assumed that the submitted manuscript has not been published and will not be simultaneously submitted or published elsewhere. By submitting a manuscript, the authors agree that the copyright for their articles is transferred to the publisher, if and when, the paper is accepted for publication. The publisher cannot take the responsibility of any loss of manuscript. Therefore, authors are requested to maintain a copy at their end.

Proofs: One set of galley proofs of a paper will be sent to the author submitting the paper, unless requested otherwise, without the original manuscript, for corrections after the paper is accepted for publication on the basis of the recommendation of referees. Corrections should be restricted to typesetting errors. Authors are advised to check their proofs very carefully before return.



Contents

On the Application of Separable $R_0R_1R_2 \cdots R_a$ -Cyclic DNA Codes to DNA Computing By Yasemin Cengellenmis and Abdullah Dertli 01

Obstructions for Connected Tree-width and Connected Path-width
By Takaaki Fujita 22

Enumeration the Number of Spanning Trees of Some Families of Graphs Based on Nonahedron Graphs By S. N. Daoud and Ahmed N. Elsayy 39

Common fixed Point Results for Interpolative Reich–Rus–Ćirić–Meir–Keeler Contractions By Jaynendra Shrivastava and Rohit Kumar Verma 63

Group Divisible Designs $(5, n, n + 1, 4; \lambda_1, \lambda_2)$
By Didas Ngabirano, Kasifa Namyalo and Olivia Nabawanda 74

Hyperfloorplans and Superhyperfloorplans–Definitions, Properties and Perspectives (Revisit) By Takaaki Fujita 84

Quantitative Mathematical Analysis of Agricultural Chemicals: Impacts on Soil, Health and Biodiversity By Ram Milan Singh 103

Papers Published in IJMC, 2025 123

An International Journal on Mathematical Combinatorics

